AD NUMBER

ADB282057

NEW LIMITATION CHANGE

TO

Approved for public release, distribution unlimited

FROM

Distribution authorized to U.S. Gov't. agencies only; Proprietary Information; Oct 2001. Other requests shall be referred to US Army Medical Research and Materiel Command, 504 Scott Street, Fort Detrick, MD 21702

AUTHORITY

USAMRMC ltr, 8 Jan 2003

AD_____

Award Number: DAMD17-97-1-7320

TITLE: Identification of Genetic Markers of the Invasive Phenotype in Human Breast Cancer

PRINCIPAL INVESTIGATOR: Dr. Peter Watson

CONTRACTING ORGANIZATION: University of Manitoba
Winnipeg, Manitoba, R3E-0W3 Canada

REPORT DATE: October 2001

TYPE OF REPORT: Final

PREPARED FOR: U.S. Army Medical Research and Materiel Command
Fort Detrick, Maryland 21702-5012

NOTICE

USING GOVERNMENT DRAWINGS, SPECIFICATIONS, OR OTHER DATA INCLUDED IN THIS DOCUMENT FOR ANY PURPOSE OTHER THAN GOVERNMENT PROCUREMENT DOES NOT IN ANY WAY OBLIGATE THE U.S. GOVERNMENT. THE FACT THAT THE GOVERNMENT FORMULATED OR SUPPLIED THE DRAWINGS, SPECIFICATIONS, OR OTHER DATA DOES NOT LICENSE THE HOLDER OR ANY OTHER PERSON OR CORPORATION; OR CONVEY ANY RIGHTS OR PERMISSION TO MANUFACTURE, USE, OR SELL ANY PATENTED INVENTION THAT MAY RELATE TO THEM.

LIMITED RIGHTS LEGEND

Award Number: DAMD17-97-1-7320
Organization: University of Manitoba

Those portions of the technical data contained in this report marked as limited rights data shall not, without the written permission of the above contractor, be (a) released or disclosed outside the government, (b) used by the Government for manufacture or, in the case of computer software documentation, for preparing the same or similar computer software, or (c) used by a party other than the Government, except that the Government may release or disclose technical data to persons outside the Government, or permit the use of technical data by such persons, if (i) such release, disclosure, or use is necessary for emergency repair or overhaul or (ii) is a release or disclosure of technical data (other than detailed manufacturing or process data) to, or use of such data by, a foreign government that is in the interest of the Government and is required for evaluational or informational purposes, provided in either case that such release, disclosure or use is made subject to a prohibition that the person to whom the data is released or disclosed may not further use, release or disclose such data, and the contractor or subcontractor or subcontractor asserting the restriction is notified of such release, disclosure or use. This legend, together with the indications of the portions of this data which are subject to such limitations, shall be included on any reproduction hereof which includes any part of the portions subject to such limitations.

THIS TECHNICAL REPORT HAS BEEN REVIEWED AND IS APPROVED FOR PUBLICATION.

Earl Grant Jr LTC, MS
31 July 02

_____

_____

_____

REPORT DOCUMENTATION PAGE

Form Approved
OMB No. 074-0188

1. AGENCY USE ONLY (Leave blank)	2. REPORT DATE	3. REPORT TYPE AND DATES COVERED
	October 2001	Final (1 Sep 97 - 1 Sep 01)

4. TITLE AND SUBTITLE
Identification of Genetic Markers of the Invasive Phenotype in Human Breast Cancer

5. FUNDING NUMBERS
DAMD17-97-1-7320

6. AUTHOR(S)
Dr. Peter Watson

7. PERFORMING ORGANIZATION NAME(S) AND ADDRESS(ES)
University of Manitoba
Winnipeg, Manitoba, R3E-0W3 Canada

E-mail: pwatson@cc.umanitoba.ca

8. PERFORMING ORGANIZATION REPORT NUMBER

9. SPONSORING / MONITORING AGENCY NAME(S) AND ADDRESS(ES)
U.S. Army Medical Research and Materiel Command
Fort Detrick, Maryland 21702-5012

10. SPONSORING / MONITORING AGENCY REPORT NUMBER

11. SUPPLEMENTARY NOTES

12a. DISTRIBUTION / AVAILABILITY STATEMENT
Distribution authorized to U.S. Government agencies only (proprietary information, Oct 01). Other requests for this document shall be referred to U.S. Army Medical Research and Materiel Command, 504 Scott Street, Fort Detrick, Maryland 21702-5012.

12b. DISTRIBUTION CODE

13. Abstract ***(Maximum 200 Words)*** *(abstract should contain no proprietary or confidential information)*

Invasion is a crucial component of the complex process of metastasis that marks the transition of breast cancer from local to life threatening disease. The approach we have taken to identify the molecular pathology underlying the onset of invasion, is to apply a combined microdissection and molecular approaches to a unique tissue bank resource. This enables us to isolate mRNA and directly compare gene expression profiles from pathologically defined regions of DCIS and early invasive tumor cells.

We have microdissected and identified a number of genes that show differential expression between DCIS and invasive components (in 5 tumors by subtraction hybridization and 8 tumors by membrane filter cDNA array techniques), as well as between low and high grade DCIS. We have also pursued 3 specific genes, previously unexplored in relation to breast cancer, that show patterns of differential expression consistent with a role in the process of invasion - Psoriasin (S100A7), Lumican, (a small leucine-rich proteoglycan) and Angio-Associated Migratory Protein (AAMP).

We conclude that our approach is productive in identifying novel genes that are previously unexplored in relation to early breast tumor progression and believe that these may provide markers of progression to invasive disease

14. SUBJECT TERMS	15. NUMBER OF PAGES
Breast Cancer	82
	16. PRICE CODE

17. SECURITY CLASSIFICATION OF REPORT	18. SECURITY CLASSIFICATION OF THIS PAGE	19. SECURITY CLASSIFICATION OF ABSTRACT	20. LIMITATION OF ABSTRACT
Unclassified	Unclassified	Unclassified	Unlimited

TABLE OF CONTENTS

"Identification of markers of the invasive phenotype in human breast cancer"

Dr Peter H. Watson

INTRODUCTION.

The acquisition of the ability to invade is the single most important aspect of breast tumor progression, as it is a crucial component of the process of metastasis and marks the transition from local to life threatening disease. Assessment of risk of progression to invasive breast cancer has recently become an increasingly recognizable and defined problem in clinical management [1]. This is partly due to the increasing number of patients who present with pre-invasive ductal carcinoma in-situ, (DCIS). More recently, the demonstration that breast cancer can be delayed or inhibited by tamoxifen therapy in women at high risk as defined in the NSABP trial has also provided a new focus and impetus to improve the accuracy of risk determination.

The management of Ductal Carcinoma in-situ (DCIS) depends on the estimation of the risk or likelihood of recurrence as in-situ or invasive disease[2]. Recent morphological studies have provided useful potential improvements to older classifications of pre-invasive disease with more accurate prognostic significance, however there is clearly a need for better predicators of biological potential[2]. To address this critical issue we and others have begun to search for molecular changes that may serve as such predictors. Our specific hypothesis is that alteration of gene expression is responsible for the progression of DCIS to invasive breast cancer and the acquisition of the invasive phenotype. Our method has been to use an approach that can directly identify genes and alterations that occur in-vivo and that may contribute to the invasive phenotype, through microdissection of histologically defined components within single breast tumor sections[3] and application of molecular techniques[4] to compare gene expression. The approach is made feasible by the unique design of our tumor bank resource[5].

BODY OF REPORT

The original grant contract was for 3 years from Sept 1997. However due to unforeseen changes in personel an extension of one additional year was requested and granted to complete the project. The accomplishments over the entire period of this award from Sept 1997 to Sept 2001 are detailed below in the context of the 2 major tasks defined in the statement of work.

Prior to the start of this project we had conducted an initial review of 388 invasive ductal carcinomas in the Manitoba Breast Tumor Bank[3] and found that 32% contained an identifiable in-situ component but less than 5% were suitable for microdissection. These cases comprised early invasive cancer with >50% in-situ and associated invasive components, microdissectable within a single tissue block and with similar cytology and stromal backgrounds. In preliminary experiments prior to this grant we had also developed microdissection techniques capable of isolating high quality mRNA from histologically defined regions within breast tumor sections[4] and a modified subtraction hybridization technique to accommodate approximately 1ug mRNA as input material[5], and completed analysis of one case (tumor $^{dcis/inv}$ #1) and identified one gene, psoriasin S100A7, as differentially expressed between in-situ and invasive component[6].

ORIGINAL TECHNICAL OBJECTIVE 1 / AIM 1

- 1 - 12, microdissect 12 tumors,

- 3 - 15 complete 12 subtraction experiments (12 screens to detect genes showing loss of expression in DCIS relative to invasive components and 12 to detect genes with gain of expression),

- 6 - 18 clone, sequence, and initiate screening of 100+ candidate genes by ISH and RT-PCR to confirm expression patterns,

Year 1. In the first year of the project we applied our proven approach of microdissection, subtractive hybridization, cDNA cloning and analysis to complete a second case (tumor $^{dcis/inv}$ #2), and identified cDNA's corresponding to 15 known genes, 5 ribosomal genes, and 4 unknown expressed sequences apparently overexpressed in either DCIS or invasive components. To rapidly determine the potential of this approach we initially focused on 6 known cDNAs (identified in other systems) from the two cases analyzed. We confirmed amongst these, real differential expression (3 cDNA's, see below), differential expression attributable to differences in local regional composition (Ets-like cDNA expressed in the denser vascular endothelium of invasive component in the sentinel case) and false positives (2 cDNA's, tra-1 and OCP2) by in-situ hybridization and RT-PCR. Consideration of the patterns of expression amongst the 3 differentially expressed cDNA's encouraged us to pursue the potential role of psoriasin, lumican and mammaglobin genes in invasion (see Aim 2).

Year 2. At this stage in the project and after microdissection of 3 additional tumors, we identified a technical problem with the magnetic bead subtraction assay (attributable to changes in the properties of the beads) that introduced contamination and discouraged us from further experiments with this assay. So we began to assess alternative molecular assays for analysis of differentially expressed mRNA. We next tested an RT-RDA protocol with small amounts (5-10ug) of cell line RNA and tested this on breast cell lines and confirmed by dot blot that 8/36 potentially differentially expressed cDNAs showed differential expression in the original sample. We concluded that RT-RDA was an acceptable assay as a first step to screen for differentially expressed genes in tumor samples, even though it produced a large number of 'false-positive' cDNA's. However, after 5 experiments on 4 microdissected tumors we concluded that it was not practical to obtain sufficient quantities of RNA from subregions within typical tumor sections for the RT-RDA assay. Nevertheless, the advent of microarray technology with many advantages for over our previous methodologies, and the commercial availability of microarray membranes and analysis software, led us instead to select the Research Genetics GeneFilters system for future

experiments. This was based on preliminary experiments to confirm that we could obtain adequate signals from labeled probes from 1 ug of microdissected total RNA.

Years 3&4. At this stage, given the dramatically improved capacity offered by lazer microdissection and microarray methodologies to analyse cases, we were now able to progress with our original aims to identify patterns of genetic alterations that correlate with the onset of the invasive phenotype and to expand the scope to analyze differential gene expression between low and high risk DCIS as well as between DCIS and invasive components of selected tumors.

- To identify molecular alterations occurring between low risk and high risk DCIS we have selected, microdissected, and compared gene expression within a cohort of 10 cases of DCIS (4 low-grade DCIS without necrosis and 6 high and intermediate-grade DCIS with necrosis). While the maturation and scale of the Manitoba Breast Tumor Bank[3] allowed us to select several DCIS cases that were amenable to manual microdissection using our standard protocol, the acquisition of lazer microdissection capability also enabled us to select and microdissect additional DCIS cases where more accurate (but labor intensive) microdissection was required. For the purpose of analysis, the six DCIS tumors with high or intermediate grade nuclear morphology and necrosis were grouped together and compared with each of the four low-grade tumors giving 24 pairs of comparisons. After masking those transcripts showing expression levels lower than 10x background, we were left with approximately 1,500 cDNAs for our comparison analysis. To exclude those transcripts that might be differentially expressed due to individual differences between the tumors or due to variations in hybridization conditions between each experiment, we restricted our final list of differentially expressed transcripts to only those that were differentially expressed in at least 9 pairs of comparison, ensuring the inclusion of transcripts that were differentially expressed in at least three different high-grade/intermediate-grade DCIS compared with the low-grade DCIS samples. Using this selection criterion, 14 transcripts (7 named genes and 7 ESTs) were overexpressed in the low-grade DCIS compared with high-grade/intermediate grade DCIS, whereas 28 transcripts (18 named genes and 10 ESTs) were overexpressed in high-

grade/intermediate-grade DCIS compared with the low-grade DCIS lesions. The value of these selection criteria was shown by a two-way pairwise average linkage cluster analysis to cluster the 10 DCIS cases on the basis of the expression profile of these 42 cDNAs, where apart from one high-grade tumor, all the high- and intermediate-grade DCIS were more closely related to each other than they were to the low- grade DCIS lesions, which in turn were more related to a normal breast sample.

- To continue to work to identify molecular alterations occurring between DCIS and invasive components we also microdissected 8 new tumors and subjected these to microarray analysis to identify a number of cDNA's (total 593 ; mean 74; sd 3) that appeared to be differentially expressed between adjacent in-situ DCIS and invasive elements within the same tumor. Further assessment to identify patterns of highly and/or consistently differentially expressed cDNA's (ie those overexpressed in 3 or more DCIS/invasive tumor pairs) has found that 36 cDNAs are consistently differentially overexpressed in the DCIS versus invasive component. These 36 candidate cDNAs emerged from out of approximately 5000 ESTs and known genes included on the filter array (amongst which approximately 1500 were considered to be expressed above background level). Additional analysis has also found the following; a) the number of cDNAs overexpressed in DCIS vs invasive elements is higher in cases where there is necrosis in the DCIS component (mean # cDNAs = 135 in necrosis+ve DCIS versus 70 in necrosis –ve DCIS, p=0.0325 t-test) and b) the number of cDNAs is also higher in cases where the invasive component is high nuclear grade (mean #cDNAs = 112 where the invasive component is high nuclear grade versus 51 in low/intermediate nuclear grade, p=0.0104, t-test). Work is still in progress to confirm differential expression of these 36 candidates by other techniques including in-situ hybridization and RT-PCR.

ORIGINAL TECHNICAL OBJECTIVE 2 / AIM 2

- 18 - 24, determine expression patterns and relation to 'invasiveness' of a subset of genes isolated in tasks 1 to 3 in panels of pre-neoplastic, pre-invasive, invasive and metastatic breast lesions

- 24 - 30, clone full-length cDNA's of a limited number of candidate invasion genes identified in task 4 and construct expression vectors

- 30 - 36, create cell line models with overexpression of specific genes by stable transfection for future testing of the influence on invasion in in-vitro assay and nude mouse models

Psoriasin (S100A7)

- We have continued to study the psoriasin (S100A7) gene that we have previously identified as differentially expressed between in-situ (DCIS) and invasive carcinoma [6]. We developed an anti-psoriasin polyclonal antibody to distinguish S100A7 from other S100 proteins and completed investigation of the role of persistent expression in invasive disease. Persistence of psoriasin expression in invasive tumors was significantly associated with poor prognostic markers including ER and PR negative ($n=57$, $p<0.0001$, $p=0.0003$) and lymph node positive status ($p=0.035$). Psoriasin protein expression was also associated with inflammatory infiltrates (all tumors excluding medullary subtypes where inflammation is a diagnostic criteria, $p=0.0022$). These results suggest that psoriasin may be a marker of aggressive behaviour in invasive tumors and are also consistent with a function as a chemotactic factor [7].
- We have examined the effect of psoriasin on invasive breast tumor cells in-vitro. On the basis of our initial hypothesis in which we took the view that loss of psoriasin might facilitate invasiveness in the neoplastic breast cell, we transfected a CMV-psoriasin construct into a subline of MDA-MB-231 breast cells that do not express psoriasin and that are known to be invasive , tumorigenic and metastatic in an in-vivo metastasis model. We isolated 2 MDA-

231psoriasin clones that demonstrate high and low mRNA and protein expression. However, assessment of these cells by in-vitro growth and in-vitro Boyden chamber invasion assays showed no significant effect on the growth or invasiveness of this already invasive breast tumor cell line. We next transfected CMV-psoriasin into a non-invasive breast cell, the MCF-10AT3B cell (using zeocin as a marker since they have previously been transfected with ras-neo) and have obtained a single clone with overexpression detected by northern and western blot. We plan to repeat transfection to obtain further clones prior to in-vitro assessment of growth and invasiveness and in-vivo study of the effect of psoriasin on early tumorigenesis and progression.

- We have also pursued the cell biology of psoriasin in breast. In-situ hybridization consistently shows that psoriasin mRNA expression is restricted to epithelial cells in breast tumors as well as in hyperplastic epidermis in the skin. Psoriasin protein, studied by immunohistochemistry is also localized predominantly but not exclusively to epithelial cells in both sites, but with both cytoplasmic and nuclear staining (the latter most prominent in breast tumor cells). Therefore to pursue the possible intracellular interactions of psoriasin we used the yeast 2-hybrid assay to screen a normal breast cell library to identify interacting proteins, and identified the apparently centrosome associated protein, RanBPM as a possible binding partner. We next conducted co-immunoprecipitation of psoriasin and RanBPM, which was achieved by cloning by PCR each cDNA into T7 promoter expression vectors and by subsequent in-vitro transcription-translation of ^{35}S-Met labelled proteins and detection using anti-HisG and anti-psoriasin antibody to confirm an interaction in-vitro. Co-localization of psoriasin to the centrosome in breast cells in-vivo was also done using the two different human mammary epithelial cell lines that had been stably transfected with psoriasin (MCF10AT and MDA-MB-231). Psoriasin protein was detected and colocalized with the peri-centrosomal protein pericentrin using confocal microscopy. Psoriasin protein was not observed in non-transfected cells [8]. We have however very recently become aware of a new publication concerning RanBPM from the original group that had identified it, that suggests that a) RanBPM is a larger protein than originally described and b) RanBPM localizes to the

nucleus, as well as to the peri-nuclear and peri-centrosomal regions. Nevertheless, the protein-protein interaction observed in yeast between the C-terminal portion of RanBPM and psoriasin is supported by our co-immunoprecipitation and co-localization studies. However this new publication does impact on our work over the last year to develop cell models as we had already cloned the original RanBPM sequence into a CMV expression vector and were in the process of screening several neomycin resistant MCF7 clones for expression of the RanBPM transgene. We have therefore begun to reconstruct our vectors with the full length RanBPM cDNA in preparation for a new round of cell transfection.

Lumican

- We identified lumican as a gene that is differentially overexpressed in the in-situ versus the invasive component of an initial microdissection case (tumor $^{dcis/inv}$ #2). Subsequent in-situ hybridization study confirmed this finding and showed that as anticipated, lumican is expressed by stromal cells that had been incorporated into the samples (despite our best efforts at microdissection) and had emerged from our assay because of the differences in expression in fibroblast-like cells immediately adjacent to in-situ and invasive epithelial tumor cells [9].
- We then went on to study lumican in the context of other small leucine rich proteoglycans (SLRPs) and showed that lumican and decorin are the most abundant of the SLRPs and are expressed by similar fibroblast-like cells, while biglycan and fibromodulin are only detected occasionally and at low levels in breast tissues. However, while lumican mRNA expression was significantly increased in tumors ($n=34$, $p<0.0001$), decorin mRNA was decreased ($p=0.0002$) in neoplastic relative to adjacent normal stroma. This was accompanied by similar changes in both lumican ($p=0.0122$) and decorin (similar trend but p=ns) proteins. Alteration of lumican expression in breast tumor stroma may also be manifested by discordance between mRNA and protein localization in some tumors, where in some areas it is possible to demonstrate mRNA expression by in-situ hybridization but no detectable protein is present in

parallel sections assessed both by immunohistochemistry or by western blot performed on microdissected material [10].

- We have now gone on to examine the prognostic significance of lumican and decorin, focusing first on a cohort of 140 early invasive breast carcinomas. All cases selected were axillary lymph node negative and treated by adjuvant endocrine therapy, as these represent early stage invasive disease and it is also in this subset of breast cancers that EGFR expression has been shown to be predictive of outcome. The latter criteria is significant as it is believed that decorin is a natural ligand for EGFR and related growth factor receptors. Lumican and decorin expression analysed by western blot was highly correlated ($r=0.45$, $p<0.0001$) in these invasive tumors. Low levels of lumican were associated with higher grade, large size, negative estrogen receptor and progesterone receptor status and increased host inflammatory response (all $p<0.05$) while decorin levels did not show significance with any factor. However, using univariate analysis both were predictive of short recurrence free survival (lumican $p=0.0013$, decorin $p=0.026$) and poor overall survival (lumican $p=0.001$, decorin $p=0.0076$). Multivariate Cox analysis is currently being performed. These results suggest that higher levels of SLRPs in breast tumors are associated with a worse prognosis in a selected series of invasive breast carcinoma patients and support the notion that they may play a role in invasion [11].

Mammaglobin

- This gene had been identified by others as a mammary specific gene expressed by approximately 2/3 of invasive breast tumors. Mammaglobin is considered to be a member of the uteroglobin gene family and also maps to a region, 11q13 that is frequently associated with alterations in breast tumorigenesis. However the cellular origin of expression of mammaglobin and the relationship between expression and tumor progression has not been previously determined. We identified mammaglobin as a gene that is differentially overexpressed in the in-situ versus the invasive component of an initial microdissection case

(tumor $^{dcis/inv}$ #2). However, our subsequent results showed that the pattern of mammaglobin expression within breast tissues and tumor components is more complex. In-situ hybridization analysis of 13 primary tumors containing normal, in-situ, invasive elements revealed that mammaglobin expression occurs in all compartments and can overexpressed in either the in-situ or invasive component. However, it is restricted to epithelial cells, and persists in axillary lymph node metastases. Reverse transcription-PCR analysis of 20 tumors and matched lymph nodes showed a direct correlation between mammaglobin mRNA expression and histological detection of nodal metastases. So while this data suggested that mammaglobin is unlikely to be relevant to invasion and we have not studied it further, our results indicated that mammaglobin could be a marker of axillary lymph node breast metastases, and this concept continues to be explored by others [12].

Angio-Associated Migratory Protein (AAMP)

- Amongst the 42 candidate cDNAs identified in the most recent DCIS cohort analysed, the angio-associated migratory protein (AAMP) was identified as a gene that is consistently higher in high grade versus low grade DCIS and that is also induced by hypoxia in the T47D breast cancer cell line. AAMP was differentially overexpressed in 11 pairs of tumor comparisons (mean 2.1 fold across two high-grade DCIS and one intermediate-grade DCIS compared with the low-grade DCIS lesions). Differential expression was confirmed by in situ hybridization and quantitative reverse transcriptase polymerase chain reaction (RT-PCR) analysis of the original cases of DCIS and a second non-microdissected set of 28 cases. AAMP expression detected by ISH showed some relationship to grade and necrosis (borderline significance at p=0.05). However by RT-PCR AAMP mRNA was associated with high and intermediate-grade DCIS (p=0.0095) in the original cohort and total AAMP expression within the tumor section tended to be associated with higher grade and necrosis but did not reach statistical significance (P=0.08, Mann Whitney) in the non-microdissected second cohort. However, no relationship was observed between AAMP and angiogenesis, and its functional role in tumorigenesis and breast cancer progression remains to be determined [13].

KEY RESEARCH ACCOMPLISHMENTS

- Microdissection and molecular analysis of the patterns of gene expression at the transition between DCIS and invasive cancer components within 13 invasive breast tumor cases
- Microdissection and molecular analysis of the patterns of gene expression between low and high risk DCIS within 10 pre-invasive DCIS breast tumor cases.
- Identification of several potentially important genes including psoriasin (S100A7), lumican, mammaglobin, angio-associated migratory protein, as genes not previously known to be overexpressed in DCIS or differentially expressed between DCIS and invasive components.
- Establishing that psoriasin expression correlates with poor prognostic features in invasive tumors and that an interaction occurs between psoriasin and a novel nuclear and peri-nuclear protein, RanBPM.
- Establishing that lumican and decorin are the most abundant among the small leucine rich proteoglycan (SLRP) genes in breast tissues, that their expression is altered in breast tumors, and that low levels of these extracellular proteins may be predictive of outcome in node negative invasive breast cancer.
- Establishing that the Angio-Associated Migratory Protein is hypoxia regulated and that the altered expression of AAMP occurs between low and high grade DCIS.

REPORTABLE OUTCOMES

PAPERS

1. Leygue E, Snell L, Dotzlaw H, Hole K, Hiller-Hitchcock T, Roughley PJ, Watson PH, Murphy LC. Expression of lumican in human breast carcinoma. **Cancer Research** 58:1348-1352, 1998.
2. Leygue E, Snell L, Dotzlaw H, Hole K, Troup S., Hiller T, Murphy L, Watson PH, "Mammaglobin, a potential marker of breast cancer nodal metastasis" **J Pathology** 189: 28-33, 1999
3. Al-Haddad S, Zhang Z, Leygue E, Snell L, Huang A, Niu Y, Hiller T, Hone K, Murphy LC, Watson PH. The role of psoriasin (S100A7) in invasive breast cancer. **Am J Pathology**. 155(6):2057-66. 1999
4. Leygue E, Snell L, Dotzlaw H, Hole K, Hiller-Hitchcock T, Murphy LC, Roughley PJ, Watson PH. Lumican and decorin are differentially expressed in human breast carcinoma. **J Pathology**. Nov;192(3):313-20. 2000

PAPERS – submitted

- Adewale Adeyinka, Ethan Emberley, Yulian Niu, Linda Snell, Leigh C. Murphy, Heidi Sowter, Charlie Wykoff, Adrian Harris, and Peter H. Watson Angio-Associated Migratory Cell Protein (AAMP) mRNA is a hypoxia-regulated protein associated with necrosis and is differentially expressed between High-grade and Low-grade Ductal Carcinoma In Situ (DCIS) of the Breast. Submitted to **Am J Path**

CHAPTERS

1. Watson PH, Leygue E, Murphy LC. "Psoriasin (S100A7)" Int J Biochem Cell Biol. 30(5): 567-571. 1998
2. Watson PH, Hiller T, Snell LS, Murphy LC, Leygue E, Dotzlaw H, Kossakowska A, Kulakowski A. "Update to : microdissection RT-PCR analysis of gene expression in

pathologically defined frozen tissue sections" in "the PCR technique: RT-PCR, editor Paul Siebert, Eaton Publishing, p28-29, 1998.

3. Watson PH, Hiller T, Snell LS, Murphy LC, Leygue E, Dotzlaw H, "microdissection RT-PCR analysis of gene expression" in "Expression Genetics: Differential Display". Editors Arthur and Michael McClelland Eaton Publishing. 1999.

PAPERS – in preparation

- Sandra Troup, Cal Roskelley, Shukti Chakravarti, Peter J. Roughley, Leigh C. Murphy, Peter H. Watson. Reduced expression of the small leucine-rich proteoglycans, Lumican and Decorin, is associated with poor outcome in node negative invasive breast cancer. Manuscript in preparation.
- Ethan D. Emberley, A. Kate Hole, R. Daniel Gietz, Leigh C. Murphy and Peter H. Watson. Interaction of the Differentially Expressed S100A7 Gene With RanBPM. Manuscript in preparation.

ABSTRACTS & PRESENTATIONS

4. Leygue E, Snell L, Dotzlaw, Hole, Hiller T, Watson P, Murphy L. "Differential expression of mammaglobin mRNA during breast tumorigeneisis". 20th Breast Cancer Symposium, San Antonio, Texas, Dec 1997
5. Leygue E, Snell L, Dotzlaw H, Hole K, Hiller-Hitchcock T, Murphy LC, Roughley PJ, Watson P,. "Lumican and decorin are differentially expressed in human breast carcinoma" submitted 21st Breast Cancer Symposium, San Antonio, Texas, Dec 1998
6. Al-Haddad S, Zhang Z, Leygue E, Snell L, Huang A, Niu Y, Hiller T, Hone K, Murphy LC, Watson PH. "The role of psoriasin (S100A7) in invasive breast cancer." AACR Philadelphia, April 1999.
7. Hiller-Hitchcock T., Leygue E., Hole K., Snell L., Troup S., Emberley E., Dotzlaw H., Murphy L.C.., Watson P.H.. "Dissecting genes involved in the invasive phenotype of human

breast cancer". CBCRI. Reasons for Hope, Toronto, June 1999

8. Emberley E., Al-Haddad S., Hole K., Snell L., Pind M., Hiller-Hitchcock T., Zhang Z.,Leygue E., Dotzlaw H., Gietz RD., Murphy LC.,Watson PH. "Psoriasin (S100A7) And Progression of Breast Cancer?" CBCRI. Reasons for Hope, Toronto, June 1999
9. Peter H. Watson, Leigh C. Murphy, Etienne Leygue, Tamara Hiller-Hitchcock, Kate Hole, Sahar Al-Haddad, Zi Zhang, Linda Snell. Identification of markers of the invasive phenotype in human breast cancer. USAMRMC Era of Hope. Atlanta, June 2000.
10. Ethan D. Emberley, A. Kate Hole, R. Daniel Gietz, Leigh C. Murphy and Peter H. Watson. Interaction of the Differentially Expressed S100A7 Gene With Centrosomal Proteins., San Antonio Dec 2000.
11. Adeyinka A, Emberley E, Murphy LC, Watson PH. Differential Gene Expression Analysis of Microdissected Ductal Carcinoma In Situ of The Breast. AACR April 2001
12. Adeyinka A, Emberley E, Murphy LC, Watson PH. Differential Gene Expression Analysis of Microdissected Ductal Carcinoma In Situ of The Breast. CBCRI reasons for hope. May 2001
13. Emberley E, Murphy LC, Geitz RD, Watson PH. Role of RanBPM in breast cancer. CBCRI Reasons for Hope, May 2001

EXTERNAL INVITED PRESENTATIONS, MEETINGS, SYMPOSIA

- BC Cancer Agency, Vancouver "Dissecting the mechanism of invasion in human breast cancer', June 1998
- Dept of Pathology, Cross Cancer Center, Edmonton ""Dissecting the mechanism of invasion in human breast cancer', July 1998
- 17th UICC International Cancer Congress, "Biological/Tissue based risk factors of invasive breast cancer UICC, Rio de Janeiro, August 1998
- 2nd Affiliated Medical University, Wuhan, China " Tissue markers of invasion in breast disease", April 1999

- Canadian Assocation of Pathologists, Molecular Oncology Symposium, Calgary. "Tissue markers of invasion in breast disease" June 1999
- Institute of Molecular Medicine, John Radcliffe Hospital, University of Oxford, UK. "Microdissecting elements of progression in breast cancer" Nov 1999
- Cancer Care Manitoba, "Invasive phenotype in breast cancer", Winnipeg, Feb 2000
- USAMRMC Era of Hope Breast Cancer conference, "Identification of markers of the invasive phenotype", Atlanta June 2000
- FASEB 2001, "Microdissecting breast cancer tumor banks" Orlando Florida, March 2001
- CBCRI Reasons for Hope conference, "Invasion genes in DCIS, - the real McCoy", Quebec City, May 2001

Funding

New Operating Grants awarded based in part on data generated through this project:

a. National Cancer Institute of Canada/Canadian Breast Cancer Research Initiative (NCIC/CBCRI), "The role of Psoriasin in progression of early breast cancer", $109,000 pa, 2000-2003
b. Canadian Institutes of Health Research (CIHR/MRC), "The role of the small leucine rich proteoglycan in human breast cancer", $120,000pa, 2000-2003
c. NCIC/CBCRI Streams of Excellence, group grant, "The role of extracellular matrix in mediating risk of breast cancer", $60,000 pa, 2000-2003

New Personnel Awards awarded based in part on data generated through this project:

a. US Army studentship award to Ethan Emberley. "Role of the RanBPM-Psoriasin (S100A7) Interaction in Human Breast Cancer". 2000-2003

CONCLUSION

Elucidation of the molecular changes involved in the development of the invasive phenotype is a critical clinical question. The lethal effects of distant metastasis can only occur after the onset of invasive capability and the ability to assess these genetic alterations may offer markers of risk of invasive disease in pre-invasive lesions. We have identified several genes that are differentially expressed in association with the pathology of transition to the invasive disease, and some of which are potentially involved in breast cancer cell invasion. Psoriasin (S100A7), a member of the S100 calcium binding protein family, demonstrates an overall pattern of expression and intracellular interaction, as well as a known capability to influence cell motility that is compatible with the hypothesis that altered expression may be functionally involved with and a marker of invasiveness. Lumican, a small leucine-rich proteoglycan, also shows a distinct regional distribution within tumors in concert with its relative decorin, and an expression pattern that relates to outcome in early invasive tumors. Although not previously studied in tumor progression, the known role of these genes in cross linking of collagen supports the hypothesis that changes in lumican and decorin expression may also influence invasiveness. Angio-associated migratory protein (AAMP) also shows a pattern of expression within DCIS that together with its known role in cell migration and angiogenesis warrants further study. Further studies to examine the role of these genes in invasion through manipulation of cell models are in progress to understand their possible functional contributions to progression. However these genes, in particular psoriasin, have potential as biological markers that are directly relevant to early progression to invasive disease, and again particularly in the case of psoriasin, offer targets for new strategies to improve on current treatments for early invasive disease.

REFERENCES

1. A) Norton L, Rosen PP, Rosen N. Refining the origins of breast cancer. Editorial Nature Medicine, 1: 1250-51 B) N.I.H. Consensus Development Conference Statement: early stage breast cancer: June 18-21,1990. C) Ernster VL, Barclay J, Kerlikowske K, Grady D, Henderson IC. Incidence of and treatment for ductal carcinoma in-situ of the breast. JAMA 275: 913-918,1996
2. A) Silverstein ML Lagios MD Craig PH, Waisman JR Lewinsky BS Colburn WJ Poller DN A prognostic index for ductal carcinoma in situ of the breast. Cancer 77: 2267-74 1996. B) Schnitt SJ, Harris JR, Smith BL Developing a prognostic index for ductal carcinoma in situ of the breast. Are we there yet? Editorial, Cancer 77: 2189-92, 1996, C) Morrow M. The natural history of ductal carcinoma in-situ , Implications for clinical decision making. Editorial Cancer76: 1113-1115, 1995. D) Kerlikowske K, Barclay J, Grady D, Sickles EA, Ernster V J Comparison of risk factors for ductal carcinoma in situ and invasive breast cancer. Natl Cancer Inst Jan 1;89(1):76-82 1997; E) Allred DC, O'Connell P, Fuqua SAW.Biomarkers in early breast neoplasia. J Cell Biochem 17G: 125,1993
3. A) Watson P, Snell L, Parisien M. "The Role of a Tumor Bank in Translational Research" Canadian Medical Association Journal, 155, 281-283, 1996 B) Watson P.H. "Tumor tissue and clinical databanks – a review of the importance, role and future of tumor banks". Cancer Strategy 6:1-6, 1999
4. Hiller, T., L. Snell, Watson P. "Microdissection RT-PCR analysis of gene expression in pathologically defined frozen tissue sections." Biotechniques 21(1): 38-44, 1996.
5. Leygue, E. R., Watson,PH, Murphy LC. "Identification of differentially expressed genes using minute amounts of RNA." Biotechniques 21(6): 1008-12,1996.
6. Leygue E, Snell L, Hiller T, Dotzlaw H, Hole K, Murphy LC, Watson PH. Differential expression of psoriasin messenger RNA between in situ and invasive human breast carcinoma Cancer Research 56:4606-4609, 1996.

7. Al-Haddad S, Zhang Z, Leygue E, Snell L, Huang A, Niu Y, Hiller T, Hone K, Murphy LC, Watson PH. The role of psoriasin (S100A7) in invasive breast cancer. **Am J Pathology**. 155(6):2057-66. 1999

8. Ethan D. Emberley, A. Kate Hole, R. Daniel Gietz, Leigh C. Murphy and Peter H. Watson. Interaction of the Differentially Expressed S100A7 Gene With RanBPM. Manuscript in preparation.

9. Leygue E, Snell L, Dotzlaw H, Hole K, Hiller-Hitchcock T, Roughley PJ, Watson PH, Murphy LC. Expression of lumican in human breast carcinoma. **Cancer Research** 58:1348-1352, 1998.

10. Leygue E, Snell L, Dotzlaw H, Hole K, Hiller-Hitchcock T, Murphy LC, Roughley PJ, Watson PH. Lumican and decorin are differentially expressed in human breast carcinoma. **J Pathology**. Nov;192(3):313-20. 2000

11. Sandra Troup, Cal Roskelley, Shukti Chakravarti, Peter J. Roughley, Leigh C. Murphy, Peter H. Watson. Reduced expression of the small leucine-rich proteoglycans, Lumican and Decorin, is associated with poor outcome in node negative invasive breast cancer. In preparation.

12. Leygue E, Snell L, Dotzlaw H, Hole K, Troup S., Hiller T, Murphy L, Watson PH, "Mammaglobin, a potential marker of breast cancer nodal metastasis" **J Pathology** 189: 28-33, 1999

13. Adewale Adeyinka, Ethan Emberley, Yulian Niu, Linda Snell, Leigh C. Murphy, Heidi Sowter, Charlie Wykoff, Adrian Harris, and Peter H. Watson Angio-Associated Migratory Cell Protein (AAMP) mRNA is a hypoxia-regulated protein associated with necrosis and is differentially expressed between High-grade and Low-grade Ductal Carcinoma In Situ (DCIS) of the Breast. Submitted to **Am J Pathology**

APPENDIX

1. List of Personnel receiving pay from the research effort

2. Publications arising from this work;

i. Leygue E, Snell L, Dotzlaw H, Hole K, Hiller-Hitchcock T, Roughley PJ, Watson PH, Murphy LC. Expression of lumican in human breast carcinoma. **Cancer Research** 58:1348-1352, 1998.

ii. Leygue E, Snell L, Dotzlaw H, Hole K, Troup S., Hiller T, Murphy L, Watson PH, "Mammaglobin, a potential marker of breast cancer nodal metastasis" **J Pathology** 189: 28-33, 1999

iii. Al-Haddad S, Zhang Z, Leygue E, Snell L, Huang A, Niu Y, Hiller T, Hone K, Murphy LC, Watson PH. The role of psoriasin (S100A7) in invasive breast cancer. **Am J Pathology**. 155(6):2057-66. 1999

iv. Leygue E, Snell L, Dotzlaw H, Hole K, Hiller-Hitchcock T, Murphy LC, Roughley PJ, Watson PH. Lumican and decorin are differentially expressed in human breast carcinoma. **J Pathology**. Nov;192(3):313-20. 2000

v. Adewale Adeyinka, Ethan Emberley, Yulian Niu, Linda Snell, Leigh C. Murphy, Heidi Sowter, Charlie Wykoff, Adrian Harris, and Peter H. Watson Angio-Associated Migratory Cell Protein (AAMP) mRNA is a hypoxia-regulated protein associated with necrosis and is differentially expressed between High-grade and Low-grade Ductal Carcinoma In Situ (DCIS) of the Breast. Submitted to **Am J Path**

vi. Watson PH, Leygue E, Murphy LC. "Psoriasin (S100A7)" Int J Biochem Cell Biol. 30(5): 567-571. 1998

vii. Watson PH, Hiller T, Snell LS, Murphy LC, Leygue E, Dotzlaw H, Kossakowska A, Kulakowski A. "Update to : microdissection RT-PCR analysis of gene expression in pathologically defined frozen tissue sections" in "the PCR technique: RT-PCR, editor Paul Siebert, Eaton Publishing, p28-29, 1998.

viii. Watson PH, Hiller T, Snell LS, Murphy LC, Leygue E, Dotzlaw H, "microdissection RT-PCR analysis of gene expression" in "Expression Genetics: Differential Display". Editors Arthur and Michael McClelland Eaton Publishing. 1999.

PERSONNEL RECEIVING PAY FROM THE RESEARCH EFFORT

Hole, Kate (Research Associate)

Pind, Molly (Research Associate)

Snell, Linda (Technologist)

Hitchcock, Tamara (Graduate Student)

Emberley, Ethan (Graduate Student)

[CANCER RESEARCH 58, 1348–1352, April 1, 1998]

Advances in Brief

Expression of Lumican in Human Breast Carcinoma[1]

Etienne Leygue,[2] Linda Snell, Helmut Dotzlaw, Kate Hole, Tamara Hiller-Hitchcock, Peter J. Roughley, Peter H. Watson, and Leigh C. Murphy

Departments of Biochemistry and Molecular Biology [E. L., H. D., L. C. M.] and Pathology [L. S., K. H., T. H-H., P. H. W.], University of Manitoba, Faculty of Medicine, Winnipeg, Manitoba, Canada, R3E OW3; and Genetic Unit, Shriners Hospital for Children, Montreal, Quebec, Canada, H3G 1A6 [P. J. R.]

Abstract

Lumican mRNA has been identified as being differentially expressed between different regions of the same human breast tumor. *In situ* hybridization study of 26 independent breast tumors confirmed the presence of lumican mRNA in fibroblast-like cells within stroma and showed a significant increase of its expression in tumor compared to adjacent normal stroma ($P < 0.001$). Higher lumican expression was associated with higher tumor grade, lower estrogen receptor levels in the tumor, and younger age of the patients ($P < 0.05$). Reverse transcription-PCR analysis of total RNA extracted from 19 independent breast tissues exhibiting lesions that are thought to parallel tumor progression also suggests that this proteoglycan is differentially expressed during tumor progression.

Introduction

The molecular mechanisms underlying the transition of normal breast tissue to invasive breast tumor *in vivo* are still poorly understood. It is believed that sequential genetic alterations that contribute to the development of phenotypic changes, such as deregulated proliferation and the cytological appearance of malignancy, accumulate in epithelial cells. Paralleling these changes in epithelial cells, changes in expression of genes within fibroblasts surrounding tumor lesions have been described (1–4) and are believed to signal complex interactions between transformed epithelial cells and adjacent host stromal cells that also contribute to the progression of the tumor (3). Knowledge of the mechanisms underlying these interactions and identification of genes differentially expressed during tumor progression would allow a better understanding of tumorigenesis and might provide targets for new therapies (5). To address this issue, we have undertaken a study to identify genes differentially expressed during tumorigenesis (6). Using a recently described subtractive hybridization technique (7), we have here identified lumican mRNA as being differentially expressed between two regions of the same tumor biopsy sample. The expression of lumican has then been investigated by *in situ* hybridization and RT-PCR[3] in independent breast tissue specimens.

Materials and Methods

Human Breast Tissues and Cell Lines. All breast tumor cases used for this study were selected from the National Cancer Institute of Canada-Manitoba Breast Tumor Bank (Winnipeg, Manitoba, Canada). As described previously (8), tissues from all cases are rapidly collected and processed to create formalin-fixed and paraffin-embedded tissue blocks and mirror-image frozen tissue blocks. The precise histological detail, interpreted in H&E-stained sections from the former block, was used as a guide to microdissection of the frozen block. Four groups of tissues or cell lines were used in this study, as detailed below.

For initial microdissection, a single tumor case with extensive *in situ* and limited (<25%) invasive components was selected from the Manitoba Breast Tumor Bank. Both components were present within a single frozen tissue block. For the *in situ* hybridization studies, 26 tumors were selected to allow comparison of normal ducts/lobules and *in situ* and invasive tumor elements within a single section in each case. For subsequent statistical analyses, cases were divided into groups of lower-grade [Nottingham (9) scores of 4–6; $n = 12$] and higher-grade (Nottingham scores of 7–9; $n = 14$) tumors; younger ($n = 14$) and older ($n = 12$) than the mean patient age (54 years old); higher ER (ER > 20 fmol/mg protein; $n = 10$) and lower ER (ER < 20 fmol/mg protein; $n = 16$) status tumors, as determined by ligand-binding assay; higher PR (PR > 15 fmol/mg protein; $n = 14$) and lower PR (PR < 15 fmol/mg protein; $n = 12$) status, as determined by ligand-binding assay; or axillary node-positive ($n = 15$) and -negative ($n = 11$) tumors.

For RT-PCR analysis of lumican expression in breast lesions that are thought to parallel the development of breast cancer, a second panel of 19 breast tissue samples, corresponding to 19 different patients, was selected. This panel consisted of five cases with normal breast tissue, four cases with proliferative disease without atypia, five cases with ductal carcinoma *in situ*, and five cases of invasive ductal carcinoma. In all cases, the histology of the frozen tissue block that was used was determined by direct comparison with an adjacent H&E-stained section from a mirror-image paraffin block.

For study of cell lines, both ER-positive and -negative breast cancer cells (T47-D, T47-D5, MCF-7, BT20, MDA-MB-231, and MDA-MB-468) were grown as described previously (10).

Microdissection, RNA Extraction, and Subtractive Hybridization Analysis. A single tumor case was microdissected as described previously (8), and RNA was extracted from histologically defined regions of *in situ* and invasive tumor using a small-scale RNA extraction protocol (Tri-reagent; MRCI, Cincinnati, OH). The subtractive hybridization was performed as described previously, using the *in situ* and invasive component as the tester and the driver respectively (7). Total RNA was similarly extracted from frozen sections of other breast samples or cell lines.

***In Situ* Hybridization.** Paraffin-embedded 5-μm breast tumor sections corresponding to tumor specimens were analyzed by *in situ* hybridization according to a previously described protocol (6). The plasmid Lumi-398 which consisted of PCRII plasmid (Invitrogen, San Diego, CA) containing a 398-bp insert of lumican cDNA between bases 1332 and 1729 (11), was used as a template to generate [^{35}S]UPT-labeled sense and antisense riboprobes using Riboprobe Systems (Promega, Madison, WI), according to the manufacturer's instructions. Sections were then developed and counterstained with H&E after 7–21 days. Levels of lumican expression were assessed in normal and tumor regions within each section by brightfield microscopic examination at low-power magnification and with reference to a positive control tumor section and a control normal tissue section. This was done by scoring the estimated average signal intensity (on a scale of 0–3) and the proportion of stromal cells showing a positive signal (0, none; 0.1, less than 1/10; 0.5, less than 1/2; 1.0, greater than 1/2). The intensity and proportion scores were then multiplied to give an overall score. Regions with a score lower than 1.0 were deemed negative or weakly positive.

Received 12/22/97; accepted 2/16/98.

The costs of publication of this article were defrayed in part by the payment of page charges. This article must therefore be hereby marked *advertisement* in accordance with 18 U.S.C. Section 1734 solely to indicate this fact.

[1] This work was supported by grants from the Canadian Breast Cancer Research Initiative (CBCRI) and the United States Army Medical Research and Materiel Command (USAMRMC). The Manitoba Breast Tumor Bank is supported by funding from the National Cancer Institute of Canada (NCIC). P. H. W. is a Medical Research Council of Canada (MRC) Clinician Scientist, and L. C. M. is a MRC Scientist. E. L. is a recipient of a USAMRMC Postdoctoral Fellowship.

[2] To whom requests for reprints should be addressed. Phone: (204) 789-3812; Fax: (204) 789-3900; E-mail: eleygue@cc.umanitoba.ca.

[3] The abbreviations used are: RT-PCR, reverse transcription-PCR; ER, estrogen receptor; PR, progesterone receptor; GAPDH, glyceraldehyde-3-phosphate dehydrogenase.

SDS-PAGE and Immunoblotting. Total proteins were extracted from frozen tissue sections corresponding to three tumors expressing lumican mRNA (as shown by *in situ* hybridization) using 4 M guanidinium chloride in the presence of proteinase inhibitors, as described previously (11). Proteins present in the extracts were analyzed by SDS-PAGE and immunoblotting, using antipeptide antibodies specific for the COOH-terminal regions of lumi- 11, 12). Prior to analysis, extracts were dialyzed into 10 mM sodium ...ate and treated with chondroitinase ABC. In some cases, the samples were also treated with keratanase II or endo-β-galactosidase, which are capable of degrading sulfated and nonsulfated polylactosamine chains, respectively.

RT-PCR Analysis. One μg of total RNA was reverse-transcribed in a final volume of 15 μl, and 1 μl of the reaction mixture was subsequently amplified by PCR, as described previously (6). Primers used corresponded to lumican (sense, 5′-TAAACCACAACAACCTGACA-3′, located in lumican sequence between bases 448 and 467; and antisense 5′-AGAAAAACATAACCATA-AAA-3′, located in lumican sequence between bases 1118 and 1138; Ref. 11) and to the ubiquitously expressed *GAPDH* gene (sense, 5′-ACCCACTCCTC-...CTTTG-3′; and antisense, 5′-CTCTTGTGCTCTTGCTGGG-3′). To am-... cDNA corresponding to lumican, 30 cycles (1 min at 94°C, 1 min at 52°C, and 2 min at 72°C) of PCR were used. For amplification of *GAPDH* cDNA, PCR consisted of 30 cycles (30 s at 94°C, 30 s at 52°C, and 30 s at 72°C). Ten μl of lumican PCR and *GAPDH* PCR were mixed before migration on 2% agarose gels and staining with ethidium bromide (15 μg/ml). Identity of the 691-bp-long fragment corresponding to lumican was confirmed after subcloning and sequencing.

Results

Identification of Lumican mRNA in Breast Cancer. To identify genes differentially expressed during tumor progression, a "microdissection case" containing high-grade lobular carcinoma *in situ* associated with invasive lobular carcinoma was selected. Two regions, one rich in *in situ* and the other rich in invasive components, were microdissected, and corresponding total RNA was extracted to provide the substrate for a recently described subtractive hybridization technique (7). Upon completion of subtractive hybridization, a 398-bp-long fragment was isolated as corresponding to a gene being overexpressed in the *in situ* compartment of this single microdissection case (data not shown). Sequencing of this fragment identified nucleotides 1332–1729 of the sequence encoding the core protein of the keratan sulfate proteoglycan lumican (11).

***In Situ* Hybridization Analysis of the Pattern of Lumican mRNA Expression within Tumors and Adjacent Normal Tissue.** To establish the cellular origin of expression and to examine the distribution of lumican expression between different tumor components in other tumors, 26 invasive tumors were studied by *in situ* hybridization (Fig. 1). For each case, an adjacent H&E-stained section was used to facilitate the pathophysiological interpretation of the frozen section (Fig. 1*A*). In almost all cases, a similar pattern was evident, with prominent mRNA expression, detected using an antisense probe, in stromal fibroblast like cells within the tumor and immediately adjacent to *in situ* and invasive tumor cells (Fig. 1*B*). No signal was observed in any case using a lumican sense probe (Fig. 1*C*). In 24 of these cases, regions of normal tissue, *in situ* tumor, and invasive tumor were present within the single section studied, therefore allowing comparison of lumican expression within the stromal elements associated with these epithelial components. Expression of lumican was evaluated within normal and tumor compartments using a semiquantitative approach as detailed in "Materials and Methods" (Table 1). Lumican was found to be expressed at very low levels (<1) within the collagenous stromal tissues associated with normal ducts and lobules in all but 1 of the 24 cases, whereas expression was evident at higher levels (≥ 1) in stromal fibroblast-like cells within the collagenous stroma of 23 of 26 invasive tumors ($P < 0.001$; Fisher's exact test). Furthermore, a marked difference between stromal expression within adjacent matched regions of normal and invasive tumor (*i.e.*, difference between tumor and normal scores higher than 1) was present in 16 of 24 cases in which this could be directly compared (see Fig. 1*D*). In 16 of 23 cases in which lumican expression was high in the invasive tumor, the ductal or lobular carcinoma *in situ* components of the tumor were associated with equivalent or higher levels of lumican expression in the immediately adjacent periductal or perilobular stroma (see Fig. 1, *B* and *D*).

The relationship between lumican expression and prognostic factors was conducted by Fisher's exact test analysis. For this purpose, tumors were divided into two subgroups with high (>1; $n = 17$) or low (≤ 1; $n = 9$) levels of lumican expression and with different tumor characteristics (high or low tumor grade, younger and older patients, high or low ER status, high or low PR status, and presence or absence

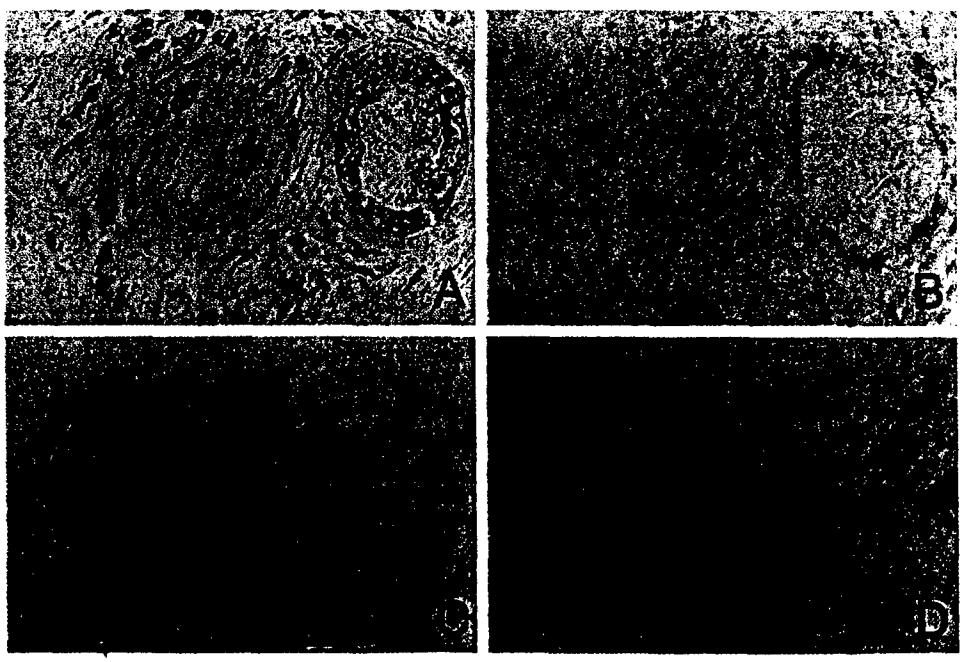

Fig. 1. Expression of lumican mRNA in breast tumors studied by *in situ* hybridization. Consecutive sections from a single breast tumor show H&E-stained paraffin section with collagenous stromal reaction surrounding ductal carcinoma *in situ* (*right*) and invasive (*left*) components (*A*), lumican expression in stroma detected using an antisense probe (*B*), and lumican sense probe (*C*). *D*, lumican expression detected within a different tumor, illustrating a gradient in the level of expression between regions of *in situ* (*top left*) and invasive ductal carcinoma (*middle*) and normal tissue ... Original magnifications, ×100 (*A–C*) and ...(*D*).

Table 1 *Clinical and pathological features of breast tumors studied for lumican mRNA expression by* in situ *hybridization*[a]

	Lumican score		Tumor characteristic				
No.	Normal	Tumor	Nottingham grade	Age (yr)	ER status	PR status	NS
1	0.1 (0.1 × 1.0)	0.1 (0.1 × 1.0)	5	48	−	−	+
2	0.0 (0.0 × 0.1)	0.2 (0.1 × 2.0)	6	56	+	−	+
3	0.1 (0.1 × 1.0)	0.3 (0.1 × 3.0)	7	80	−	−	+
4	0.0 (0.0 × 0.0)	1.0 (1.0 × 1.0)	5	66	+	−	+
5	0.5 (0.5 × 1.0)	1.0 (0.5 × 2.0)	5	71	+	+	−
6	0.0 (0.0 × 0.0)	1.0 (0.5 × 2.0)	6	61	+	+	−
7	0.1 (0.1 × 1.0)	1.0 (0.5 × 2.0)	6	58	+	+	+
8	0.1 (0.1 × 1.0)	1.0 (0.5 × 2.0)	9	46	−	−	+
9	0.1 (0.1 × 1.0)	1.0 (0.5 × 2.0)	5	75	+	+	−
10	0.0 (0.0 × 0.0)	1.5 (0.5 × 3.0)	9	38	−	−	−
11	0.1 (0.1 × 1.0)	2.0 (1.0 × 2.0)	8	72	+	+	−
12	2.0 (1.0 × 2.0)	2.0 (1.0 × 2.0)	8	45	−	+	−
13	0.1 (0.1 × 1.0)	2.0 (1.0 × 2.0)	4	57	−	+	−
14	—	2.0 (1.0 × 2.0)	7	32	−	+	+
15	0.1 (0.1 × 1.0)	2.0 (1.0 × 2.0)	8	48	−	−	+
16	0.1 (0.1 × 1.0)	2.0 (1.0 × 2.0)	7	36	+	+	+
17	—	2.0 (1.0 × 2.0)	8	34	−	−	+
18	0.1 (0.1 × 1.0)	3.0 (1.0 × 3.0)	6	72	+	+	−
19	0.1 (0.1 × 1.0)	3.0 (1.0 × 3.0)	4	44	−	−	−
20	0.1 (0.1 × 1.0)	3.0 (1.0 × 3.0)	7	63	−	−	+
21	0.1 (0.1 × 1.0)	3.0 (1.0 × 3.0)	5	51	−	+	+
22	0.5 (0.5 × 1.0)	3.0 (1.0 × 3.0)	8	37	−	+	+
23	0.1 (0.1 × 1.0)	3.0 (1.0 × 3.0)	9	51	−	−	−
24	0.0 (0.0 × 0.0)	3.0 (1.0 × 3.0)	8	66	+	−	−
25	0.1 (0.1 × 1.0)	3.0 (1.0 × 3.0)	7	45	−	+	+
26	0.1 (0.1 × 1.0)	3.0 (1.0 × 3.0)	6	44	−	+	+

[a] For each case, lumican score (proportion of positive cells × estimated average intensity), determined as indicated in "Materials and Methods," is given for normal and tumor components. —, compartment not present within studied section; NS, axillary nodal status.

of axillary nodes, as specified in "Materials and Methods"). Increased lumican expression was associated with higher tumor grade ($P < 0.04$), younger patient age ($P < 0.04$), and ER status ($P < 0.05$). No correlation was observed between lumican expression and PR levels or nodal status. The conclusion that lumican expression is restricted to stromal cells was further supported by RT-PCR analysis of RNA extracted from several epithelial breast cancer cell lines (T47-D, T47-D5, MCF-7, MDA-MB-231, MDA-MB-468, and BT20) that did not show detectable levels of lumican mRNA (data not shown).

Analysis of Lumican mRNA Expression in Relation to Breast Tumorigenesis. To determine the relationship between the increased expression of lumican mRNA and breast lesions associated with increasing risk of invasive cancer, a range of tissues containing normal breast tissue, benign proliferative lesions, preinvasive ductal carcinoma *in situ*, and invasive carcinoma were studied by RT-PCR assay. This was performed on 1 mg of total RNA, extracted from histologically defined frozen sections. Three independent PCR experiments were performed that gave similar results as presented in Fig. 2. A lumican-corresponding band was observed in all of the invasive tumor samples but was undetectable or present only at low levels in all of the normal samples, consistent with the results from *in situ* hybridization, as detailed above. Between these two extremes, a very faint band or no band was detectable in proliferative disease without atypia lesions, but high levels comparable with those seen in invasive tumors were present in most pure ductal carcinoma *in situ* samples. The differences observed were not attributable to differences in input cDNAs, as shown by the intensity of *GAPDH* signals in each samples.

SDS-PAGE Detection of Lumican Protein in Breast Tumors. To characterize the lumican protein in breast tumor tissue, total proteins were extracted from three cases expressing lumican mRNA, as assessed by *in situ* hybridization. Western blot analysis of these proteins using an antilumican serum revealed that lumican protein is effectively expressed in breast tumor tissue (Fig. 3). Because several forms of lumican have been described (11), which differ by their glycosylated chains by sizes ranging from M_r 65 to 150,000, the effect of keratanase II and endo-β-galactosidase, which are capable of degradating sulfated and nonsulfated polylactosamine chains, respectively, was also investigated (Fig. 3). Keratanase II treatment had little, if any, effect on the size of tumor-derived lumican, whereas the endo-β-galactosidase reduced the size of the lumican to a relatively homogeneous component of M_r 55,000. This corresponds in size to the protein core of lumican observed in adult articular cartilage, which is devoid of keratan sulfate or polylactosamine chains (11). Thus, the tumor lumican appears to possess nonsulfated or poorly sulfated polylactosamine chains rather than the more highly sulfated keratan sulfate. Furthermore, there is no evidence of proteolytic degradation of lumican occurring in the tumor because the protein core size corresponds to that expected for the intact molecule following endo-β-galactosidase treatment.

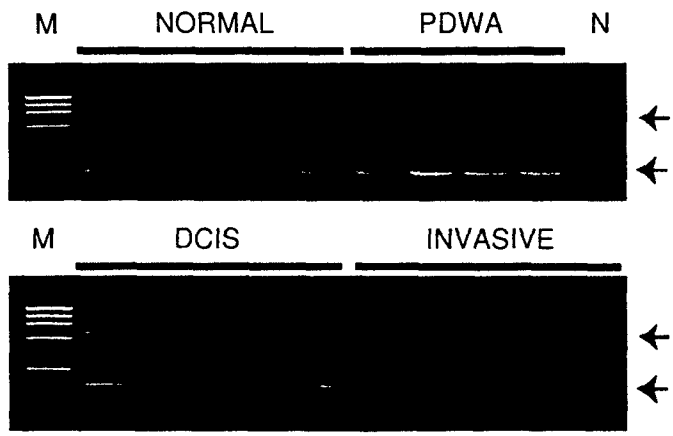

Fig. 2. RT-PCR analysis of lumican and GAPDH mRNA expression in normal samples from reduction mammoplasties (*NORMAL*) and samples from proliferative disease without atypia (*PDWA*; *top*), ductal carcinoma *in situ* (*DCIS*), and invasive ductal carcinoma (*INVASIVE*; *bottom*). PCR products were mixed before separation on 2% agarose gels and staining with ethidium bromide. *Black arrow*, product corresponding to lumican; *gray arrow*, product corresponding to *GAPDH*. *Lanes M*, molecular weight marker (ϕ×174 RF DNA/*Hae*III fragments; Life Technologies, Inc., Grand Island, NY). *Lane N*, negative control, no cDNA added during the PCR.

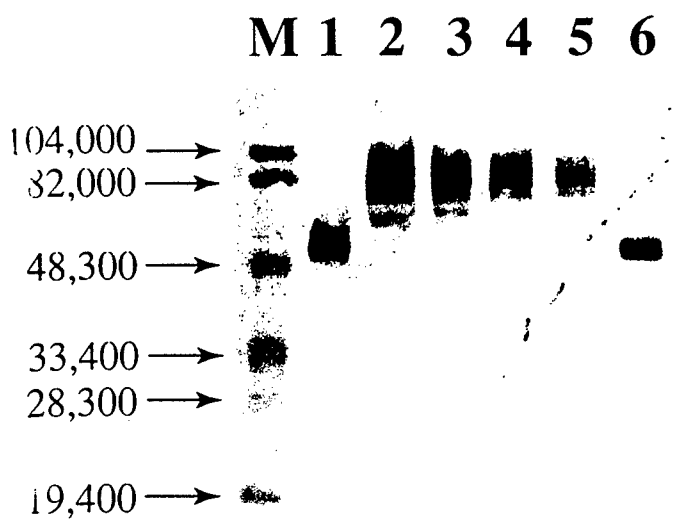

Fig. 3. Immunoblotting analysis of lumican. Proteins were extracted from three human breast tumors and lumican present in the extracts was analyzed by SDS-PAGE and immunoblotting as described in "Materials and Methods." An adult cartilage extract (*Lane 1*) and three breast tumor extracts (*Lanes 2–4*) were analyzed directly. One breast tumor extract was analyzed following treatment with keratanase II (*Lane 5*) and endo-β-galactosidase (*Lane 6*). *Left*, migration position of molecular weight markers.

Discussion

The data presented here demonstrate the presence and increased expression of lumican mRNA in human breast tumors relative to normal breast tissue. Lumican is a major constituent of the corneal stroma that is thought to participate in the acquisition of corneal transparency by regulating collagen fibril diameter and interfibrillar spacing (13, 14). Lumican expression has already been described in several other human tissues, including skin, articular cartilage, heart, placenta, skeletal muscle, kidney, and pancreas (11). This is, however, to our knowledge, the first observation of lumican expression in breast tissue, as well as its possible deregulation in tumorigenesis. Lumican belongs to the family of small interstitial leucine-rich proteoglycan proteins. Like other members of this family (decorin, biglycan, and fibromodulin), the lumican core protein contains a central region of leucine-rich repeats flanked at either side by a disulfide-bonded domain. The central region of the molecule possesses four asparagine residues capable of participating in *N*-linked glycosylation. Modification of *N*-linked glycosaccharides by sulfation of their polylactosamine units led to the classification of lumican as a keratan sulfate proteoglycan. Small keratan sulfate proteoglycans have been shown to organize collagen fibrils in extracellular matrix and may, therefore, be involved in the maintenance of tissue stromal structure (15, 16). However, other potential functions include the ability to influence cell adhesion or cell growth through interactions with growth factors (17, 18). Modifications of extracellular matrix components during tumor progression have been extensively reported, and the potential importance of proteoglycans in particular has also been underlined in both colon and breast cancer (19–24). In colon cancer, increased stromal expression of both large and small proteoglycans has been observed in tumor stroma, whereas ectopic expression of decorin in a colon tumor cell line reduced growth and tumorigenic potential. In breast cancer, different proteoglycans are distinct in their pattern of expression (21). The large proteoglycan versican has been shown to be prominent in the fibrous stroma within invasive tumor, as compared to surrounding normal tissue stroma (24). This contrasts with the pattern of expression of small leucine-rich chondroitin and dermatan sulfate proteoglycans, which were predominantly localized by immunocytochemistry to surrounding normal tissues and were absent from the invasive tumor stroma (24).

Our results suggest that increased expression of lumican can occur in tumor stroma in a similar pattern to that of versican. We have also found, albeit in a small cohort, an association between increased lumican mRNA expression and high tumor grade, younger patient age, and low ER levels, all of which are factors that are associated with increased tumor aggressiveness. Further study is needed to confirm this in a larger cohort and to distinguish whether this reflects a cause or an effect of increased tumor progression.

Here, we show that lumican protein is present in breast tumors mainly in its nonsulfated polylactosamine form. Such a nonsulfated form of lumican has already been described in noncorneal tissues, including articular cartilage and aorta (11, 25). The putative functions of lumican in noncorneal tissues, as well as the possible influences of its glycosylation state, remain to be established. In cornea, a conversion from nonsulfated polylactosamine chains to keratan sulfate chains, concurrent with eye opening, is suspected to contribute directly to corneal transparency (13, 26). Conversely, poorly sulfated chains replace highly sulfated ones during pathological conditions of the cornea including stromal inflammation and scarring (27, 28). Funderburgh *et al.* (28) recently demonstrated that, in contrast to the highly sulfated form of lumican, the nonsulfated form of the protein promotes macrophage attachment and spreading. This action is thought to be mediated through a high-affinity receptor for lumican, expressed in a constitutive manner by macrophages and different from the already described scavenger receptor or from receptors for other extracellular matrix molecules. This receptor recognizes the lumican protein both in glycosylated and deglycosylated forms through structures that can be masked by keratan sulfate chains. Poorly sulfated lumican could, therefore, act to localize macrophages in regions of inflammation. One could speculate that increased expression of lumican in its nonsulfated state in breast cancer may be a mechanism that encourages macrophage adhesion and localization within the tumor. This increased macrophage concentration could in turn influence angiogenesis and prognosis through the production of tumor-associated macrophage cytokine production (29, 30).

In conclusion, the detection of lumican in the stromal reaction within breast carcinoma suggests than this proteoglycan may have a role in breast tumorigenesis and progression. Further studies are needed to determine the exact function of lumican in breast tissues and how changes in its expression and in its glycosylation pattern modify properties of the extracellular matrix or the adjacent tumor cells.

Acknowledgments

We thank Helen Bergen and Caroline Cumins-Leygue for their assistance with cell culture.

References

1. Basset, P., Bellocq, J. P., Wolf, C., Stoll, I., Limacher, J. M., Podhajcer, O. L., Chenard, M. P., Rio, M. C., and Chambon, P. A novel metalloproteinase gene specifically expressed in stromal cells of breast carcinoma. Nature (Lond.), *348:* 699–704, 1990.
2. Iozzo, R. V. Tumor stroma as a regulator of neoplastic behavior. Lab. Invest., *73:* 157–160, 1995.
3. Wernert, N. The multiple role of tumor stroma. Virchows Arch., *430:* 433–443, 1997.
4. Peyrol, S., Raccurt, M., Gerard, F., Gleyzal, C., Grimaud, J. A., and Sommer, P. Lysyl oxidase gene expression in the stromal reaction to *in situ* and invasive ductal breast carcinoma. Am. J. Pathol., *150:* 497–507, 1997.
5. Kohn, E. C., and Liotta, L. A. Molecular insights into cancer invasion: strategies for prevention and intervention. Cancer Res., *5:* 1856–1862, 1995.
6. Leygue, E., Snell, L., Hiller, T., Dotzlaw, H., Hole, K., Murphy, L. C., and Watson, P. H. Differential expression of psoriasin mRNA between *in situ* and invasive human breast carcinoma. Cancer Res., *56:* 4606–4609, 1996.
7. Leygue, E., Watson, P. H., and Murphy, L. C. Identification of differentially expressed genes using minute amount of RNA. BioTechniques, *21:* 1008–1012, 1996.
8. Hiller, T., Snell, L., and Watson, P. Microdissection/RT-PCR analysis of gene expression. BioTechniques, *21:* 38–44, 1996.

9. Elston, C. W., and Ellis, I. O. Pathological prognostic factors in breast cancer. Histopathology (Oxford), *19:* 403–410, 1991.
10. Murphy, L. C., and Dotzlaw, H. Regulation of transforming growth factor α and transforming growth factor β messenger ribonucleic acid abundance in T-47D human breast cancer cells. Mol. Endocrinol., *3:* 611–617, 1989.
11. Grover, J., Chen, X. N., Korenberg, J. R., and Roughley, P. J. The human lumican gene: organization, chromosomal location, and expression in articular cartilage. J. Biol. Chem., *270:* 21942–21949, 1995.
12. Cs-Szabo, G., Melching, L. I., Roughley, P. J., and Glant, T. T. Changes in messenger RNA and protein levels of proteoglycans and link protein in human osteoarthritic cartilage samples. Arthritis Rheum., *40:* 1037–1045, 1997.
13. Cornuet, P. K., Blochberger, T. C., and Hassell, J. R. Molecular polymorphism of lumican during corneal development. Invest. Ophthalmol., *35:* 870–877, 1994.
14. Rada, J. A., Cornuet, P. K., and Hassell, J. R. Regulation of corneal collagen fibrillogenesis *in vitro* by corneal proteoglycan (lumican and decorin) core proteins. Exp. Eye Res., *56:* 635–648, 1993.
15. Scott, J. E. Supramolecular organization of extracellular matrix glycosaminoglycans, *in vitro* and in the tissues. FASEB J., *6:* 2639–2645, 1992.
16. Scott, J. E. Proteodermatan and proteokeratan sulfate (decorin, lumican/fibromodulin) proteins are horseshoe shaped. Implications for their interactions with collagen. Biochemistry, *35:* 8795–8798, 1996.
17. Hildebrand, A., Romaris, M., Rasmussen, L., Heinegard, D., Twardzik, D. R., Border, W. A., and Ruoslahti, E. Interaction of the small interstitial proteoglycans biglycan, decorin and fibromodulin with transforming growth factor β. Biochem. J., *302:* 527–534, 1994.
18. Delehedde, M., Deudon, E., Boilly, B., and Hondermarck, H. Production of sulfated proteoglycans by two human breast cancer cell lines. Binding to fibroblast growth factor-2. Exp. Cell Res., *229:* 398–406, 1996.
19. Heino, J. Biology of tumor cell invasion. Interplay of cell adhesion and matrix degradation. Int. J. Cancer, *65:* 717–722, 1996.
20. Hauptmann, S., Zardi, L., Siri, A., Carnemolla, B., Borsi, L., Castellucci, M., Klosterhalfen, B., Hartung, P., Weis, J., Stocker, G., Haubeck, H. D., and Kirkpatrick, C. J. Extracellular matrix proteins in colorectal carcinomas. Lab. Invest., *73:* 172–182, 1995.
21. Delehedde, M., Deudon, E., Boilly, B., and Hondermarck, H. Protéoglycannes et cancer du sein. Pathol. Biol., *45:* 305–311, 1997.
22. Losa, G. A., and Alini, M. Sulfated proteoglycans in extracellular matrix of human breast tissues with infiltrating carcinoma. Int. J. Cancer, *54:* 552–557, 1993.
23. Alini, M., and Losa, G. Partial characterization of proteoglycans isolated from neoplastic and nonneoplastic human breast tissues. Cancer Res., *51:* 1443–1447, 1991.
24. Nara, Y., Kato, K., Torii, Y., Tsui, Y., Nakagaki, S., Goto, S., Isobe, H., Nakashima, N., and Takeuchi, J. Immunohistochemical localization of extracellular matrix components in human breast tumours with special reference to PG-M/Versican. Histochem. J., *29:* 21–30, 1997.
25. Funderburgh, J. L., Funderburgh, M. L., Mann, M. M., and Conrad, G. W. Arterial lumican. Properties of a corneal-type keratan sulfate proteoglycan from bovine aorta. J. Biol. Chem., *266:* 24773–24777, 1991.
26. Ying, S., Shiraishi, A., Kao, C. W., Converse, R. L., Funderburgh, J. L., Swiergiel, J., Roth, M. R., Conrad, G. W., and Kao, W. W. Characterization and expression of the mouse lumican gene. J. Biol. Chem., *272:* 30306–30313, 1997.
27. Funderburgh, J. L., Funderburgh, M. L., Rodriguez, M. M., Krachmer, J. H., and Conrad, G. W. Altered antigenicity of keratan sulfate proteoglycan in selected corneal diseases. Invest. Ophthalmol. Vis. Sci., *31:* 419–428, 1990.
28. Funderburgh, J. L., Mitschler, R. R., Fundenburgh, M. L., Roth, M. R., Chapes, S. K., and Conrad, G. W. Macrophage receptors for lumican. A corneal keratan sulfate proteoglycan. Invest. Ophthalmol. Vis. Sci., *38:* 1159–1167, 1997.
29. Lewis, C. E., Leek, R., Harris, A., and McGee, J. O. Cytokine regulation of angiogenesis in breast cancer: the role of tumor-associated macrophages. J. Leukocyte Biol., *57:* 747–751, 1995.
30. Leek, R. D., Lewis, C. E., Whitehouse, R., Greenall, M., Clarke, J., and Harris, A. L. Association of macrophage infiltration with angiogenesis and prognosis in invasive breast carcinoma. Cancer Res., *56:* 4625–4629, 1996.

JOURNAL OF PATHOLOGY
J. Pathol. **189**: 28–33 (1999)

MAMMAGLOBIN, A POTENTIAL MARKER OF BREAST CANCER NODAL METASTASIS

ETIENNE LEYGUE[1]*, LINDA SNELL[2], HELMUT DOTZLAW[1], KATE HOLE[2], SANDY TROUP[2], TAMARA HILLER-HITCHCOCK[2], LEIGH C. MURPHY[1] AND PETER H. WATSON[2]

[1]*Department of Biochemistry and Molecular Biology, University of Manitoba, Faculty of Medicine, Winnipeg, Manitoba R3E 0W3, Canada*
[2]*Department of Pathology, University of Manitoba, Faculty of Medicine, Winnipeg, Manitoba R3E 0W3, Canada*

SUMMARY

The *Mammaglobin* gene, a breast-specific member of the uteroglobin gene family, has been previously identified as being overexpressed in some breast tumours, but the cellular origin and relationship to tumour progression are unknown. Using a subtractive hybridization approach, *mammaglobin* mRNA has also been found to be overexpressed in the *in situ* compared to the invasive element within an individual breast tumour. Further study by *in situ* hybridization performed in 13 breast tumours, selected to include normal, *in situ*, and invasive primary tumour elements, and in most cases axillary lymph node metastases, revealed that *mammaglobin* expression occurs in all elements, is restricted to epithelial cells, and is significantly increased in tumour cells compared with normal cells ($p<0{\cdot}04$). Analysis of *mammaglobin* expression within 20 independent primary breast tumours and their corresponding axillary lymph nodes revealed that all 13 lymph nodes positive and none of the seven nodes negative for metastatic breast carcinoma by histology were mammaglobin-positive by reverse transcription-polymerase chain reaction (RT-PCR) ($p=0{\cdot}0001$). These results suggest that *mammaglobin* could be a marker of axillary lymph node breast metastases. Copyright © 1999 John Wiley & Sons, Ltd.

KEY WORDS—**breast cancer; tumour progression; *mammaglobin*; uteroglobin; metastasis; marker; lymph node; subtractive hybridization**

INTRODUCTION

The detection of breast cancer metastases and micrometastases based on specific genetic markers may provide useful information to guide early therapeutic decisions.[1] Various biological markers have been proposed for the detection of breast cancer cells, including *Keratin*-19 and *Muc*-1,[2] but the frequency of expression of these markers is often related to tumour differentiation and is not always confined to breast tissue.[3] This relates in part to the fact that most potential markers are derived initially from the study of other tissues and systems.

In order better to understand the molecular alterations that are specifically involved in breast tumour progression and that might provide molecular targets for detection, we and others have undertaken direct studies of human breast tumours. These studies aim to identify genes differentially expressed between normal and neoplastic tissue, or between different components of the same human breast tumour.[4–6] *Mammaglobin*, a member of the uteroglobin gene family, has recently been identified by this approach as a gene that is overexpressed in breast tumours.[7] In this study, we have also identified *mammaglobin* mRNA as being differentially expressed between the non-invasive *in situ* and invasive components of a single breast tumour. We have gone on to investigate the cellular origin *in vivo* and the pattern of expression of *mammaglobin* mRNA in relation to tumour progession within primary tumours and their nodal metastases by *in situ* hybridization and reverse transcription-polymerase chain reaction (RT-PCR).

MATERIALS AND METHODS

Human breast tissues

All breast tumour cases were selected from the NCIC-Manitoba Breast Tumour Bank (Winnipeg, Manitoba, Canada). As previously described, all cases in the bank have been processed to create formalin-fixed and paraffin-embedded tissue blocks and mirror-image frozen tissue blocks.[8] Histopathological analysis has been performed on haematoxylin and eosin (H&E) stained paraffin sections from the former block in each case to determine the tumour type, tumour grade (Nottingham system),[9] and the distinction between *in situ* and invasive elements. Steroid receptor status has been determined for all cases by ligand binding assay performed on an adjacent portion of tumour tissue. Tumours with oestrogen and progesterone receptor levels below 3 and 10 fmol/mg of total protein, respectively, were considered ER- or PR-negative. Three groups of cases were used in this study as detailed below.

The initial 'microdissection case' consisted of a single tumour (tumour No. 2, Table I) with extensive *in situ* lobular and limited (<25 per cent) invasive lobular components.

*Correspondence to: Etienne Leygue, PhD, Department of Biochemistry and Molecular Biology, University of Manitoba, 770 Bannatyne Avenue, Winnipeg, MB R3E 0W3, Canada.
E-mail: eleygue@cc.umanitoba.ca

Contract/grant sponsor: Canadian Breast Cancer Research Initiative (CBCRI).

Contract/grant sponsor: U.S. Army Medical Research and Matériel Command (USAMRMC).

CCC 0022–3417/99/100028–06$17.50

Received 2 July 1998
Revised 1 December 1998
Accepted 14 April 1999

Table I—Clinical and pathological features of the breast tumours studied for *mammaglobin* mRNA expression by *in situ* hybridization*

	Mammaglobin score				Tumour characteristics					
No.	Normal ducts/lobules	*In situ* carcinoma	Invasive carcinoma	Nodal metastasis	Tumour type	Age (years)	Grade	ER	PR	NS
1	**0·0** (0·0 × 0·0)	**0·1** (1·0 × 0·1)	**0·0** (0·0 × 0·0)	**0·1** (1·0 × 0·1)	Ductal NOS	56	II	47	4·9	+
2	**0·2** (2·0 × 0·1)	**1·5** (3·0 × 0·5)	**0·0** (0·0 × 0·0)	**1·0** (2·0 × 0·5)	Lobular	45	II	3·5	28	+
3	**0·1** (1·0 × 0·1)	**0·2** (2·0 × 0·1)	**0·0** (0·0 × 0·0)	**na**	Lobular	75	I	7·4	9·1	−
4	**0·1** (1·0 × 0·1)	**0·5** (1·0 × 0·5)	**0·1** (1·0 × 0·1)	**0·2** (2·0 × 0·1)	Ductal NOS	48	III	0·6	2·2	+
5	**0·2** (2·0 × 0·1)	**2·0** (2·0 × 1·0)	**1·0** (1·0 × 1·0)	**2·0** (2·0 × 1·0)	Lobular	58	II	37	15·9	+
6	**0·1** (1·0 × 0·1)	**0·1** (1·0 × 0·1)	**1·0** (2·0 × 0·5)	**1·5** (3·0 × 0·5)	Ductal NOS	63	II	1·8	12·2	+
7	**0·2** (2·0 × 0·1)	**0·2** (2·0 × 0·1)	**2·0** (2·0 × 1·0)	**na**	Lobular	70	I	9·2	53	−
8	**0·0** (1·0 × 0·0)	**2·0** (2·0 × 1·0)	**3·0** (3·0 × 1·0)	**3·0** (3·0 × 1·0)	Lobular	48	I	10·3	7·2	+
9	**0·0** (0·0 × 0·1)	**2·0** (2·0 × 1·0)	**3·0** (3·0 × 1·0)	**na**	Ductal NOS	72	III	32	46	−
10	**0·1** (1·0 × 0·1)	**0·1** (1·0 × 0·1)	**3·0** (3·0 × 1·0)	**2·0** (2·0 × 1·0)	Duct–Lob mix	44	II	0·6	27	+
11	**0·0** (0·0 × 0·0)	**0·0** (0·0 × 0·0)	**0·0** (0·0 × 0·0)	**0·0** (0·0 × 0·0)	Ductal NOS	80	II	1	8·5	+
12	**0·5** (1·0 × 0·5)	**0·0** (0·0 × 0·0)	**0·0** (0·0 × 0·0)	**0·0** (0·0 × 0·0)	Ductal NOS	36	II	22	42	+
13	**0·2** (2·0 × 0·1)	**0·0** (0·0 × 0·0)	**0·0** (0·0 × 0·0)	**na**	Ductal NOS	32	II	5·8	41	+

*No=case number. The level of *mammaglobin* expression within normal ducts and lobules, *in situ* tumour, invasive tumour, and nodal metastasis components in each case is indicated by an overall score (shown in bold) derived from the product of the average signal intensity × the proportion of positive epithelial cells in each region (shown in parentheses) as described in the Materials and Methods section. Tumour type: ductal NOS=invasive ductal carcinoma; lobular=invasive lobular carcinoma; duct–lob mix=mixed invasive ductal and invasive lobular carcinoma. Grade: Nottingham grade score. ER/PR: oestrogen and progesterone receptor levels in fmol/mg total protein. na: not available. NS: axillary nodal status, +=node-positive; −=node-negative.

For the *in situ* hybridization studies, a series of 13 tumours was selected that contained normal ducts and lobules, and *in situ* and invasive tumour components, within a single section. For nine of these cases, axillary lymph node metastases were also available and these tissue blocks were analysed simultaneously. The histological features are summarized in Table I. These cases, which included the initial microdissection case, comprised invasive ductal ($n=7$), invasive lobular ($n=5$), and invasive mixed duct and lobular ($n=1$) carcinoma types. The tumour grades ranged from high (grade III, $n=2$), through intermediate (grade II, $n=8$), to low (grade I, $n=3$), and the steroid receptor status included both ER-positive ($n=9$) and ER-negative cases ($n=4$).

For the RT-PCR analysis studies of *mammaglobin* expression, a second panel of 20 primary breast tumours and their corresponding axillary nodes was selected. This panel included 13 node-positive tumours and seven node-negative tumours and in each case, the nodal status (i.e. absence, lymph node-negative; or presence, lymph node-positive) of the frozen tissue lymph node block that was used for this analysis was determined by histological analysis of H&E-stained sections from the adjacent mirror-image formalin-fixed and paraffin-embedded block. In this series, 18 cases were invasive ductal and two were invasive lobular carcinomas and the majority were high ($n=7$) or intermediate ($n=11$) grade, and ER-positive ($n=16$).

Subtractive hybridization analysis

The microdissection of the initial single tumour case was performed as previously described.[8] After extraction of total RNA, the subtractive hybridization was performed as previously described, using the *in situ* and the invasive component of the initial microdissection case as the tester and the driver, respectively.[4]

In situ *hybridization*

Paraffin-embedded 5 μm breast tumour sections were analysed by *in situ* hybridization according to a previously described protocol.[5] The plasmid Mam-503, which consisted of PCR™II plasmid (Invitrogen, San Diego, CA, U.S.A.), containing a 503 bp insert of *mammaglobin* cDNA between bases 1 and 503,[7] was used as a template to generate [^{35}S] UTP-labelled sense and antisense riboprobes using Riboprobe® Systems (Promega, Madison, WI, U.S.A.) according to the manufacturer's instructions. Sections were then developed and counterstained with H&E after 15 days. Levels of *mammaglobin* expression were assessed in normal, *in situ*, invasive, and, when possible, nodal metastatic regions by bright-field microscopic examination at low magnification and using a previously described semiquantitative approach.[10] Scores were obtained for each component by estimating the average signal intensity (on a scale of 0–3) and the proportion of epithelial cells showing a positive signal (0, none; 0·1, less than one-tenth; 0·5, less than one-half; 1·0 greater than one-half). The intensity and proportion scores were then multiplied to give an overall score. Statistical comparisons between matched compartments were performed using the two-tailed Wilcoxon signed rank test. The correlation between *mammaglobin* expression within the invasive component and the corresponding nodal metastasis was established

by calculation of the Spearman rank correlation coefficient.

RT-PCR analysis

One microgram of total RNA was reverse-transcribed in a final volume of 20 μl and 1 μl of the reaction mixture subsequently amplified by PCR as previously described.[5] The primers used corresponded to *mammaglobin* (sense, exon 1, 5′-CCGACAGCAGCAGCC TCAC-3′, located in the *mammaglobin* sequence between bases 41 and 59[7] and antisense, exon 3, 5′-TCCGT AGTTGGTTTCTCAC-3′, located in the *mammaglobin* sequence between bases 401 and 383[7]) and to the ubiquitously expressed glyceraldehyde-3-phosphate dehydrogenase (*GAPDH*) gene (sense 5′-ACCCACTCCTC CACCTTTG-3′ and antisense 5′-CTCTTGTGCTCTT GCTGGG-3′). To amplify cDNA corresponding to *mammaglobin* and *GAPDH*, 30 cycles (30 s at 94°C, 30 s at 55°C, and 30 s at 72°C) of PCR were used. Ten microlitres of *mammaglobin* PCR and *GAPDH* PCR were mixed and analysed by electrophoresis on prestained (ethidium bromide, 15 μg/ml) 2 per cent agarose gels. The identity of the expected 361 bp long fragment corresponding to *mammaglobin* was confirmed by sequencing. Association between *mammaglobin* expression within nodal metastasis and histopathological determination of nodal status was tested using Fisher's exact test.

RESULTS

Identification of mammaglobin *mRNA in breast cancer*

A 'microdissection case' that contained lobular carcinoma *in situ* associated with invasive carcinoma was selected and frozen tissue blocks were subjected to microdissection to obtain material for extraction of total RNA corresponding to both regions.[8] This RNA provided the substrate for a recently described subtractive hybridization technique.[4] Upon completion of subtraction, a 503 bp long fragment was isolated as corresponding to a gene overexpressed in the *in situ* compartment (data not shown). Sequencing of this fragment identified nucleotides 1–503 of the sequence encoding *mammaglobin*, a recently described putative member of the uteroglobin family.[7]

Assessment of mammaglobin *mRNA expression in normal breast tissue,* in situ *and invasive tumour elements and corresponding axillary lymph nodes*

To establish which cells express *mammaglobin* mRNA within breast tumour tissues and to examine the distribution of the expression of this mRNA within different breast tumour components, 13 cases that included both lobular and ductal tumours were selected from the NCIC-Manitoba Breast Tumour Bank. For each case, the age of the patient and clinical characteristics of the tumour [i.e. Nottingham grade, oestrogen receptor (ER), progesterone receptor (PR) levels, as determined by ligand binding assay, and nodal status] are given in Table I. Paraffin tissue sections containing normal ducts/lobules, *in situ* and invasive elements were studied by *in situ* hybridization, together (when available) with corresponding axillary lymph node paraffin sections (Fig. 1). No signal was detectable when a sense probe was used (Fig. 1A). In contrast, a signal varying in intensity was observed in epithelial cells when an antisense probe was used (Figs 1B–1D). *Mammaglobin* mRNA was not detected in stromal or inflammatory cells in any of the sections studied. Expression of *mammaglobin* was quantified in each component using a semi-quantitative approach described in the Materials and Methods section (Table I). Although *mammaglobin* mRNA was found to be overexpressed in the *in situ* tumour cells compared with normal adjacent epithelial cells in 7/13 cases, this difference did not reach statistical significance (Wilcoxon signed rank test, $n=9$, $p>0{\cdot}05$). Similarly, even though *mammaglobin* expression appeared higher within the invasive component compared with normal adjacent elements in 6/13 cases, this difference was not statistically significant (Wilcoxon signed rank test, $n=10$, $p>0{\cdot}05$). However, when both *in situ* and invasive elements were combined, *mammaglobin* expression observed in tumour was higher than that seen in normal adjacent cells (Wilcoxon signed rank test, $n=12$, $p<0{\cdot}02$). This suggests that although *mammaglobin* mRNA is predominantly overexpressed in cancer cells within the primary tumour, the exact stage at which this increase in expression occurs varies between tumours and the nature of the alteration is complex. For example, when comparing matched *in situ* and invasive components, the *mammaglobin* mRNA level was found to be increased within *in situ* elements in 5/13 (40 per cent) cases (Table I, cases 1–5) but was increased within invasive elements in 5/13 (40 per cent) cases (Table I, cases 6–10) and was similar and low in 3/13 (20 per cent) cases (Table I, cases 11–13).

In nine cases, a paraffin tissue block from a synchronous nodal metastasis was also available for study. *Mammaglobin* expression was detectable within metastatic tumour cells in 7/9 cases and was undetectable only in the two cases where *mammaglobin* expression was absent in the primary tumour (Table I). This detection was possible in both early metastasis within the subcapsular sinus (Fig. 1C) and established metastasis (Fig. 1D). Evaluation of the level of *mammaglobin* mRNA expression within these lymph node metastases revealed a significantly (Wilcoxon signed rank test, $n=8$, $p<0{\cdot}04$) higher level than that detected in matched normal breast tissue. The level of expression of *mammaglobin* mRNA within axillary lymph node metastatic cells was also found to correlate closely with the level observed within matched invasive elements (Spearman $r=0.89$, $p<0{\cdot}002$).

Mammaglobin mRNA expression within the primary invasive tumour component appeared to be unrelated to several pathological indicators of tumour differentiation and prognosis. Expression was observed in both invasive ductal and lobular tumour types and increased expression showed no relation to tumour grade, the level of steroid receptors, or the presence or absence of nodal

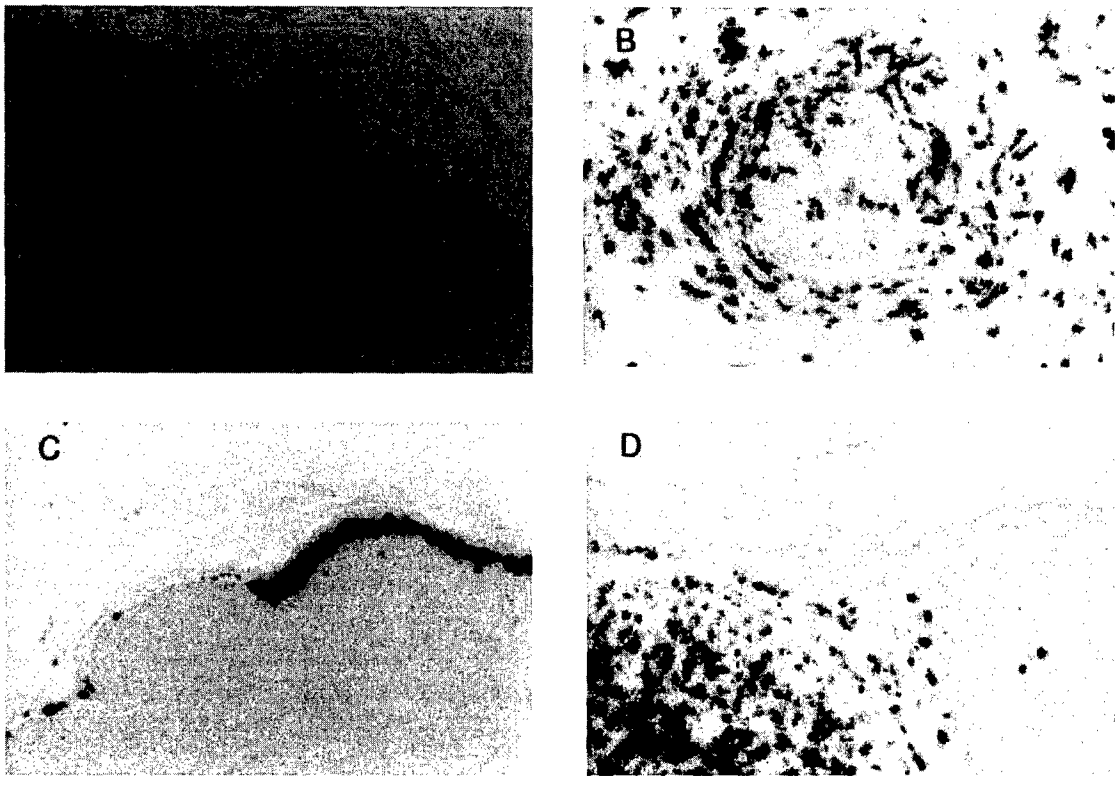

Fig. 1—Expression of *mammaglobin* mRNA in a primary breast tumour and concurrent nodal metastases (case 10, Table I) studied by *in situ* hybridization. Plates A and B illustrate consecutive sections from the primary tumour showing a normal lobular unit (in the middle) surrounded by invasive lobular carcinoma. Plate C shows a focus of early metastatic tumour confined to the subcapsular lymph node sinus. Plate D shows established nodal metastasis in an adjacent lymph node. (A) sense probe; (B, C, D) antisense probe

metastasis. Similarly, cases which showed an apparent reduction in the level of expression between *in situ* and invasive elements of the primary tumour showed no distinguishing features from those which showed the opposite changes.

Detection of mammaglobin *mRNA expression in axillary nodal metastases*

Because it was possible to detect *mammaglobin* mRNA in axillary lymph node metastases in seven out of nine metastases by *in situ* hybridization, and because this mRNA had previously been described as being absent from normal lymph node tissue,[7] we investigated the possibility that *mammaglobin* could be a marker of axillary lymph node metastases. Twenty independent cases were selected, 13 axillary lymph node-positive and seven node-negative. Total RNA was extracted from frozen primary tumour sections and frozen node sections of corresponding axillary lymph nodes. The histological status of all tissues was confirmed in paraffin sections cut from adjacent mirror-image paraffin tissue blocks that had been processed in parallel to the frozen blocks.[8] Total RNA was reverse-transcribed and analysed by RT-PCR using primers recognizing specifically *mammaglobin* cDNA and chosen to span intronic regions. PCRs were performed in triplicate with reproducible results. The identity of the PCR product obtained was confirmed by sequencing. As shown in Fig. 2, no *mammaglobin* expression was detected in lymph nodes from cases without histologically detectable tumour cells (0/7 cases). In contrast, all lymph nodes previously identified to contain metastatic breast tumour cells following histopathological assessment had detectable *mammaglobin* expression (13/13 cases). The RT-PCR detection of *mammaglobin* mRNA in axillary lymph nodes appeared, therefore, strongly associated (Fisher's exact test, $p<0{\cdot}0001$) with the histopathological detection of lymph node metastases.

Consideration of the frequency of *mammaglobin* mRNA expression detectable by RT-PCR in this series (as opposed to *in situ* hybridization as performed in the first series) shows that 16/20 primary tumours were positive overall. The absence of signal in four cases could not be attributed to degraded RNA and/or cDNA, as shown by the amplification of the ubiquitously expressed *GAPDH* cDNA in the same cDNA samples. These *mammaglobin*-negative cases included ductal ($n=3$) and lobular ($n=1$) tumour types, both high ($n=3$) and intermediate grade ($n=1$) and ER-positive ($n=2$) and -negative ($n=2$) tumours. *Mammaglobin* was detected at a higher frequency in primary tumours that were node-positive (12/13 cases, 90 per cent) than in primary tumours that were node-negative (4/7 cases, 60

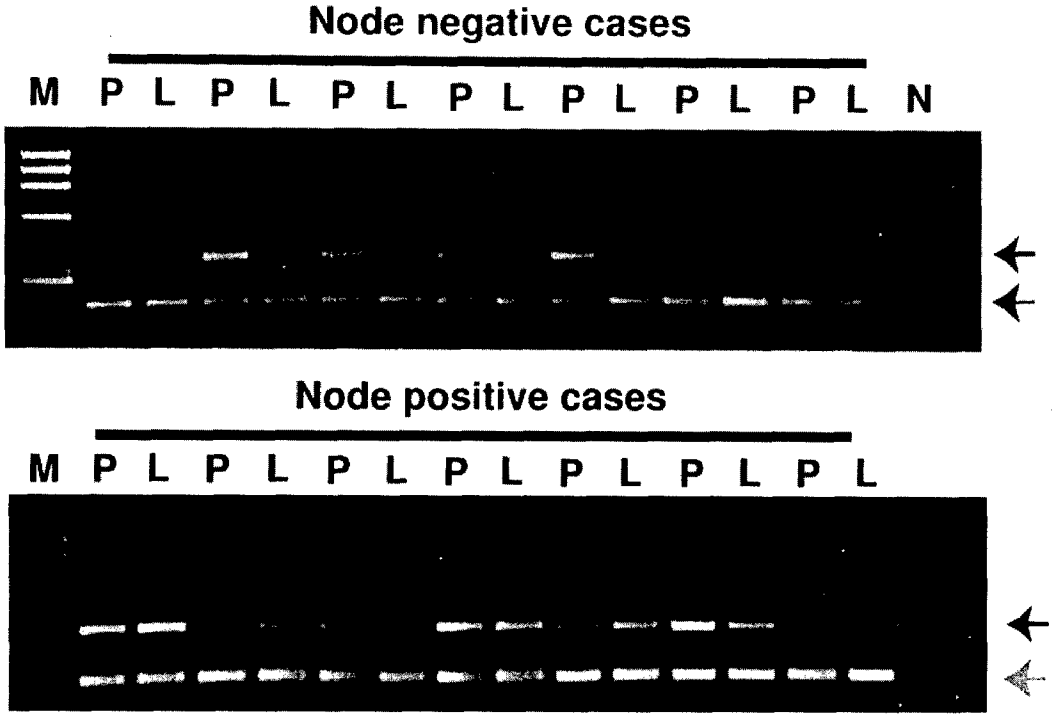

Fig. 2—RT-PCR analysis of *mammaglobin* and *GAPDH* mRNA expression in primary breast tumours (P) and their corresponding axillary lymph nodes (N) histologically shown to contain (node-positive) or not to contain (node-negative) metastases. PCR products were mixed before separation on 2 per cent agarose gels prestained with ethidium bromide. Black arrow: product corresponding to *mammaglobin*; grey arrow: product corresponding to *GAPDH*. M: Molecular weight marker (φx174 RF DNA/Hae III fragments; Gibco BRL, Grand Island, NY, U.S.A.). N: Negative control; no cDNA added during the PCR

per cent), although a similar trend was not seen in the initial series studied by *in situ* hybridization.

DISCUSSION

Mammaglobin has recently been identified as a breast-specific gene overexpressed by approximately 23 per cent of primary breast tumours.[7] *Mammaglobin* is considered to be a member of the uteroglobin gene family and also maps to a region,[11] 11q13, that is frequently associated with alterations in breast tumourigenesis,[12–18] but the cellular origin of expression of *mammaglobin* and the relationship between expression and tumour progression has not been previously determined. Our results show that the pattern of *mammaglobin* expression within breast tissues and tumour components is complex. Expression, is however, restricted to mammary epithelial cells, and in those tumours that show overexpression of *mammaglobin* in the invasive primary tumour, this expression appears invariably conserved in the concurrent axillary nodal metastases.

Mammaglobin was identified in the present study through detailed analysis of a single breast tumour to distinguish genes differentially expressed at early stages of tumour progression. The initial observation suggested that *mammaglobin* might be more highly expressed in the pre-invasive *in situ* than in the invasive elements of breast tumours. This is a pattern of expression that would be consistent with data which suggest that expression of the uteroglobin can influence the invasiveness of epithelial tumour cells in other tissues.[19,20] However, subsequent analysis revealed a more complex pattern of expression. In some cases ($\approx$20 per cent), expression was undetectable by *in situ* hybridization at all stages; in some ($\approx$40 per cent), the expression changed little, or even declined with progression from *in situ* to invasive disease; and in others ($\approx$40 per cent), the expression increased. We also found that *mammaglobin* mRNA expression, measured by either *in situ* hybridization or RT-PCR in the primary tumours, was unrelated to tumour type, grade, or steroid receptor levels, as has been previously reported.[7,11]

This complexity in expression may be related to the fact that the *mammaglobin* gene is localized to a chromosomal region, 11q13, that has been previously shown to be commonly modified during breast tumourigenesis. Alterations at this locus include loss of heterozygosity at markers adjacent to and on either side of the *mammaglobin* gene (*Pygm* and *Int*-2) occurring at increasing frequencies (from 9 per cent up to 67 per cent of informative cases) in association with progression from atypical ductal hyperplastic breast lesions, through lobular and ductal *in situ* neoplastic lesions, to invasive breast cancer.[12,13,18] Amplification of the 11q13 region that includes several known genes such as *int*-2, *cyclin* D1 and *ems*-1 has also been observed in up to 15 per cent of invasive breast carcinomas,[14–17] although the

amplified region may not directly involve the *mammaglobin* gene. The possible role of 11q13 modifications in the differential expression of the *mammaglobin* gene between normal and malignant breast tissue thus remains to be addressed.

In the course of our own molecular studies, even though based on the careful microdissection of regions containing a majority of epithelial cells, we have identified genes expressed only by epithelial cells,[5] only by fibroblastic cells,[10] or by both tumour and stromal cell types (our unpublished data). Therefore, the determination of the epithelial cellular origin and range of tumour components that express a particular gene *in vivo*, as opposed to within established cell lines, is of crucial importance if we are to understand the molecular functions of encoded proteins and their potential applications as tumour cell markers.

Given the previous suggestion that *mammaglobin* expression is restricted to breast tissues,[7] we have examined the potential of this gene to be a marker of breast metastasis within axillary lymph nodes. Using RT-PCR, it was possible to detect *mammaglobin* in 13 out of 13 sections from axillary lymph nodes shown by histopathological examination of adjacent paraffin sections to contain metastatic cells and in none of seven nodes that were negative. The increased frequency of detection of *mammaglobin* in breast tumour cells using RT-PCR (primary 16/20 cases, 80 per cent; metastasis 13/13 cases, 100 per cent), compared with *in situ* hybridization (primary 10/13 cases, 77 per cent; metastasis 7/9 cases, 77 per cent) or northern blot (primary 23 per cent) as used by others,[7] is most likely due to differences in sensitivity between assays.

The physiological role of *mammaglobin* in breast tissue is unknown, as is its possible involvement in breast tumourigenesis. Our data suggest, however, that *mammaglobin* gene expression is modified during breast tumourigenesis and that it may be a good candidate marker for the detection and characterization of breast cancer metastasis.

ACKNOWLEDGEMENTS

This work was supported by grants from the Canadian Breast Cancer Research Initiative (CBCRI) and the U.S. Army Medical Research and Matériel Command (USAMRMC). The Manitoba Breast Tumour Bank is supported by funding from the National Cancer Institute of Canada (NCIC). PHW is a Medical Research Council of Canada (MRC) Clinician-Scientist; LCM is an MRC Scientist; EL is a recipient of a USAMRMC Postdoctoral Fellowship; and TH-H is a recipient of an MRC studentship.

REFERENCES

1. Mori M, Mimori K, Inoue H, *et al.* Detection of micrometastases in lymph nodes by reverse transcriptase-polymerase chain reaction. *Cancer Res* 1995; **55:** 3417–3420.
2. Noguchi S, Aihara T, Motomura K, Imaoka S, Koyama H. Detection of breast cancer micrometastases in axillary lymph nodes by means of reverse transcription-polymerase chain reaction. Comparison between *Muc*-1 mRNA and *Keratin*-19 mRNA amplification. *Am J Pathol* 1996; **148:** 649–656.
3. Dingemans AM, Brakenhoff RH, Postmus PE, Giaccone G. Detection of cytokeratin-19 transcripts by reverse transcription-polymerase chain reaction in lung cancer cell lines and blood lung cancer patients. *Lab Invest* 1997; **77:** 213–220.
4. Leygue E, Watson PH, Murphy LC. Identification of differentially expressed genes using minute amount of RNA. *Biotechniques* 1996; **21:** 1008–1012.
5. Leygue E, Snell L, Hiller T, *et al.* Differential expression of psoriasin mRNA between *in situ* and invasive human breast carcinoma. *Cancer Res* 1996; **56:** 4606–4609.
6. Watson MA, Flemming TP. Isolation of differentially expressed sequence tags from human breast cancer. *Cancer Res* 1994; **54:** 4598–4602.
7. Watson MA, Fleming TP. Mammaglobin, a mammary-specific member of the uteroglobin gene family, is overexpressed in human breast cancer. *Cancer Res* 1996; **56:** 860–865.
8. Hiller T, Snell L, Watson PH. Microdissection/RT-PCR analysis of gene expression. *Biotechniques* 1996; **21:** 38–44.
9. Elston CW, Ellis IO. Pathological prognostic factors in breast cancer. *Histopathology* 1991; **19:** 403–410.
10. Leygue E, Snell L, Hiller T, *et al.* Expression of lumican in human breast carcinoma. *Cancer Res* 1998; **58:** 1348–1352.
11. Watson MA, Darrow C, Zimonjic DB, Popescu NC, Fleming TP. Structure and transcriptional regulation of the human mammaglobin gene, a breast cancer associated member of the uteroglobin gene family localized to chromosome 11q13. *Oncogene* 1998; **16:** 817–824.
12. Chuaqui RF, Zhuang Z, Emmert-Buck MR, Liotta LA, Merino MJ. Analysis of loss of heterozygosity on chromosome 11q13 in atypical ductal hyperplasia and *in situ* carcinoma of the breast. *Am J Pathol* 1997; **150:** 297–303.
13. Nayar R, Zhuang Z, Merino MJ, Silverberg SG. Loss of heterozygosity on chromosome 11q13 in lobular lesions of the breast using microdissection and polymerase chain reaction. *Hum Pathol* 1997; **28:** 277–282.
14. Fantl V, Richards MA, Smith R, *et al.* Gene amplification on chromosome 11q13 and estrogen receptor status in breast cancer. *Eur J Cancer* 1990; **26:** 423–429.
15. Bieche I, Lidereau R. Genetic alterations in breast cancer. *Genes Chromosome Cancer* 1995; **14:** 227–251.
16. Courjal F, Cuny M, Simony-Lafontaine J, *et al.* Mapping of DNA amplifications at 15 chromosomal localizations in 1875 breast tumours: definition of phenotypic groups. *Cancer Res* 1997; **57:** 4360–4367.
17. Driouch K, Champeme MH, Beuzelin M, Bieche I, Lidereau R. Classical gene amplifications in human breast cancer are not associated with distant solid metastases. *Br J Cancer* 1997; **76:** 784–787.
18. Kerangueven F, Noguchi T, Coulier F, *et al.* Genome-wide search for loss of heterozygosity shows extensive genetic diversity of human breast carcinomas. *Cancer Res* 1997; **57:** 5469–5774.
19. Kundu GC, Mantile G, Miele L, Cordella-Miele E, Mukherjee AB. Recombinant human uteroglobin suppresses cellular invasiveness via a novel class of high-affinity cell surface binding site. *Proc Natl Acad Sci USA* 1996; **93:** 2915–2919.
20. Leyton J, Manyak MJ, Mukherjee AB, Miele L, Mantile G, Patierno SR. Recombinant human uteroglobin inhibits the *in vitro* invasiveness of human metastatic prostate tumour cells and the release of arachidonic acid stimulated by fibroblast-conditioned medium. *Cancer Res* 1994; **54:** 3696–3699.

American Journal of Pathology, Vol. 155, No. 6, December 1999

Psoriasin (S100A7) Expression and Invasive Breast Cancer

Sahar Al-Haddad,* Zi Zhang,* Etienne Leygue,† Linda Snell,* Aihua Huang,* Yulian Niu,* Tamara Hiller-Hitchcock,* Kate Hole,* Leigh C. Murphy,† and Peter H. Watson*

Departments of Pathology and Biochemistry and Molecular Biology,† University of Manitoba, Faculty of Medicine, Winnipeg, Manitoba, Canada*

Alteration of psoriasin (S100A7) expression has previously been identified in association with the transition from preinvasive to invasive breast cancer. In this study we have examined persistence of psoriasin mRNA and protein expression in relation to prognostic factors in a cohort of 57 invasive breast tumors, comprising 34 invasive ductal carcinomas and 23 other invasive tumor types (lobular, mucinous, medullary, tubular). We first developed an IgY polyclonal chicken antibody and confirmed specificity for psoriasin by Western blot in transfected cells and tumors. The protein was localized by immunohistochemistry predominantly to epithelial cells, with both nuclear and cytoplasmic staining, as well as occasional stromal cells in psoriatic skin and breast tumors; however, *in situ* hybridization showed that psoriasin mRNA expression was restricted to epithelial cells. In breast tumors, higher levels of psoriasin measured by reverse transcriptase-polymerase chain reaction and Western blot (93% concordance) were significantly associated with estrogen and progesterone receptor-negative status ($P < 0.0001$, $P = 0.0003$), and with nodal metastasis in invasive ductal tumors ($P = 0.035$), but not with tumor type or grade. Psoriasin expression also correlated with inflammatory infiltrates (all tumors excluding medullary, $P = 0.0022$). These results suggest that psoriasin may be a marker of aggressive behavior in invasive tumors and are consistent with a function as a chemotactic factor. *(Am J Pathol 1999, 155:2057–2066)*

Earlier diagnosis of breast cancer has increased the need for the identification of molecular alterations that might serve as tissue markers to predict the risk of progression to metastatic disease. Among the most important of these alterations are likely to be those associated with the development of the invasive phenotype and the transition from preinvasive to invasive cancer with the capability for subsequent metastasis.

We have recently identified psoriasin (S100A7) as a gene that is frequently overexpressed in preinvasive ductal carcinoma *in situ* (DCIS) relative to adjacent invasive carcinoma, suggesting a role in breast tumor progression.[1] Other members of the S100 gene family of calcium-binding proteins have been implicated in a range of biological processes, including tumor metastasis.[2] In particular, S100A2 has been shown to be down-regulated in breast tumor cells relative to their normal epithelial cell counterparts,[3] whereas up-regulation of S100A4 has been strongly implicated in breast tumor metastasis.[4–6] In the latter case this may reflect the ability of S100A4 to influence cell motility,[7] the cytoskeleton[6,8,9] or cell adhesion molecules.[10] Psoriasin was initially identified as a highly abundant protein belonging to the S100 gene family,[11] expressed by abnormally proliferating keratinocytes in psoriatic epidermis.[12,13] It has subsequently been shown to be a secreted protein that can exert an effect as a chemotactic factor for inflammatory cells.[14,15] However, the function of psoriasin in breast cancer remains to be determined.[16] In this study we have developed a psoriasin-specific antibody and evaluated the persistence of psoriasin expression in invasive breast tumors with different invasive and metastatic potential as well as host inflammatory response.

Materials and Methods

Human Breast Tissues and Cell Lines

All breast tumor cases used for this study were selected from the NCIC–Manitoba Breast Tumor Bank (Winnipeg, Manitoba, Canada). As has previously been described,[17] tissues accrue to the Bank from cases at multiple centers within Manitoba and are rapidly collected and processed to create matched formalin-fixed embedded and frozen tissue blocks for each case, with mirror-image surfaces

Supported by grants from the Medical Research Council of Canada (MRC) and the U.S. Army Medical Research and Materiel Command (USAMRMC). The Manitoba Breast Tumor Bank is supported by funding from the National Cancer Institute of Canada (NCIC). P. H. W. is an MRC Clinician-Scientist; L. C. M. is an MRC Scientist; E. L. is a recipient of a USAMRMC Postdoctoral Fellowship. T. H.-H. is a recipient of an MRC studentship award.

Accepted for publication August 24, 1999.

Address reprint requests to Dr. Peter Watson, Department of Pathology, D212-770 Bannatyne Ave., University of Manitoba, Winnipeg, MB R3E OW3, Canada. E-mail: pwatson@cc.umanitoba.ca.

oriented by colored inks. The histology of every sample in the Bank is uniformly interpreted in hematoxylin/eosin (H&E)-stained sections from the face of the paraffin tissue block by a pathologist. This information is available in a computerized database along with relevant pathological and clinical information and was used as a guide for the selection of specific paraffin and frozen blocks from cases for this study. For each case interpretations included an estimate of the cellular composition (including the percentage of invasive epithelial tumor cells, collagenous stroma, and fatty stroma), tumor type, and tumor grade for ductal tumors (Nottingham score).[18,19] The inflammatory host response was scored semiquantitatively on a scale of 1 (low) to 5 (high). Steroid receptor status was determined for all cases by ligand binding assay performed on an adjacent portion of tumor tissue. Tumors with estrogen and progesterone receptor levels above 20 fmol/mg and 15 fmol/mg of total protein, respectively, were considered ER- or PR-positive.

Two cohorts of tumors were selected. The first cohort comprised 35 invasive ductal carcinomas selected to include six subgroups differing with respect to estrogen receptor status (ER-positive and ER-negative) and tumor grade (low, intermediate, high). Additional selection criteria also included high tissue quality, presence of invasive tumor within >35% of the cross section of the frozen block for invasive ductal cases, and minimal (<5%) normal or *in situ* epithelial components. The second cohort comprised 23 invasive tumors selected to include four subgroups of different tumor types[18] that vary in differentiation and metastatic potential, including invasive lobular (six), medullary (five), tubular (six), and colloid (six). Similar secondary criteria were also used for this cohort.

For analysis of antibody specificity and for positive controls for tumor assays, MCF7 human breast cancer cells obtained from the American Type Culture Collection (Manassas, VA) were used. MCF7 cells were grown as previously described under normal conditions in the presence of 5% fetal bovine serum, to provide a negative control.[20] Alternatively MCF7 cells were subjected to estrogen-deprived conditions in the presence of charcoal-stripped serum before stimulation by estradiol (10^{-8} mol/L) for 48 hours before harvesting to induce psoriasin expression and provide a positive control. As an additional positive control MDA-MB-231 human breast cancer cells were transfected with a plasmid containing the cytomegalovirus (CMV) promotor adjacent to the psoriasin cDNA (Hiller-Hitchcock T, Leygue E, Cummins-Leygue C, Murphy LC, Watson PH, manuscript in preparation), and stable transfectants (CL7FD3 cell clone) expressing psoriasin mRNA were also used.

Antibody Reagents

A psoriasin-specific chicken IgY polyclonal antibody was generated by immunization of chickens with a 14-amino acid peptide corresponding to the carboxy terminus of psoriasin (KQSHGAAPCSGGSQ; Bionostics, Toronto, and Aves Labs). A >90% pure IgY fraction from chicken egg yolk was obtained in phosphate-buffered saline (PBS) and then further purified by passing it over a psoriasin peptide affinity column made by binding the synthetic peptide to N-hydroxy-succinimide-activated Sepharose 4B (Pharmacia Biotech), according to the manufacturer's instructions. The bound IgY was then eluted with 5.0 mol/L sodium thiocyanate, followed by dialysis against PBS. Additional antibodies used included a commercial anti-S100 antibody (Sigma, St. Louis, MO) as well as a rabbit polyclonal antibody, raised against the recombinant protein (kindly provided by Prof J. Celis, University of Aarhus, Aarhus, Denmark).

Western Blot Analysis

For tumors, multiple sections (10–20 × 20 μm) were cut from the face of frozen tissue blocks immediately adjacent to the face of the matching paraffin block.[17] For cell lines, trypsinized cell pellets were obtained from breast cancer cell lines (grown to ~80% confluence). Total protein lysates were extracted from both the cell line pellets and frozen tissue sections, using Tri-reagent (Sigma), as described by the manufacturer. The recovered protein was dissolved in SDS isolation buffer (50 mmol/L Tris, pH 6.8, 20 mmol/L EDTA, 5% sodium dodecyl sulfate (SDS), 5 mmol/L β-glycerophosphate) and a cocktail of protease inhibitors (Boehringer Mannheim, Laval, PQ). Protein concentrations were determined using the Micro-BCA protein assay kit (Pierce, Rockford, IL). Sixty micrograms of total protein lysates were run on a 16.5% sodium dodecyl sulfate-polyacrylamide gel electrophoresis (SDS-PAGE) mini gel, using Tricine SDS-PAGE to separate the proteins,[21] and then transferred to 0.2-μm Nitrocellulose (Bio-Rad, Mississauga, ON). After blocking in 10% skimmed milk powder in Tris-buffered saline-0.05% Tween (TBST buffer), blots were incubated with chicken IgY anti-psoriasin antibody (~15 μg/ml in TBST), followed by incubation with secondary antibody, rabbit IgG anti-chicken IgY conjugated to horseradish peroxidase (1:5000 dilution in TBST; Jackson ImmunoResearch Laboratories), and visualization by incubation with Supersignal (Pierce), per the manufacturer's instructions. Exposed x-ray films were photographed, and the band intensities were determined by video image analysis, using MCID M4 software (Imaging Research, ST. Catherine's, ON). All signals were adjusted with reference to the psoriasin-transfected MDA-MB-231 cell control (CL7FD3), run on each blot.

Immunohistochemistry

Immunohistochemistry was performed on 5-μm paraffin-embedded breast tumor tissue sections from tissue blocks fixed in 10% neutral buffered formalin for 18–24 hours. After deparaffinizing, clearing, and hydrating to PBS buffer (pH 7.4) containing 0.05% Tween 20 (Mallinckrodt), the sections were pretreated with hydrogen peroxide (3%) for 10 minutes to remove endogenous peroxidases, and nonspecific binding was blocked with normal rabbit serum (1:50; Sigma). Primary chicken IgY

anti-psoriasin antibody (1:500 dilution in PBS) was applied for 1 hour at 37°C followed by washing and incubation with the secondary antibody, peroxidase-conjugated affinity purified rabbit anti-chicken (1:200 dilution), for 1 hour at room temperature. Detection was performed with 3,3′-diaminobenzidine tetrahydrochloride peroxidase substrate (Sigma) and counterstaining with methyl green (2%), followed by dehydration, clearing, and mounting. A positive tissue control and a negative reagent control (normal rabbit serum only/no primary antibody) were run in parallel in all experiments. Immunostaining was scored semiquantitatively by assessing the average signal intensity (on a scale of 0 to 3) and the proportion of tumor cells showing a positive nuclear signal (0, none; 0.1, less than one-tenth; 0.5, less than one-half; 1.0 greater than one-half). The intensity and proportion scores were then multiplied to give an overall score, and tumors with a score equal to or higher than 1.0 were deemed positive.

In Situ *Hybridization*

In situ hybridization was performed on paraffin sections (5 μm) according to a previously described protocol.[1] Linearized psoriasin plasmid cDNA (1.0 μg/μl) was used to generate UTP^{S35}-labeled sense and antisense RNA probes with the Riboprobe System (Promega, Madison, WI) according to the manufacturer's instructions. Sense and antisense probes were equalized by diluting 1×10^6 cpm/μl in hybridization solution. These were then applied to paraffin sections (approximately 30 μl of probe per section) that had undergone postfixation with 4% paraformaldehyde (pH 7.4) in PBS and further pretreatments with triethanolamine/acetic anhydride and proteinase K before hybridization. Sections were then coverslipped, sealed, and incubated overnight in a humid chamber at 42°C. After coverslip removal, sections underwent incubation in posthybridization solution and buffered RNase A (20 μg/ul), followed by several washes in descending dilutions of standard saline citrate buffer to remove weakly bound nonspecific label. After dehydration in ethanol containing 300 mmol/L ammonium acetate, the sections were coated in NTB-2 Kodak emulsion, subsequently developed after various time intervals from 2 to 5 weeks, and counterstained with Lee's methylene blue and basic fuchsin. Psoriasin expression was assessed by bright-field microscopic examination at low power (10× objective) magnification with reference to the negative sense and positive control tumor sections run with each batch. Levels were scored semiquantitatively as previously described[22] by assessing the average signal intensity (on a scale of 0 to 3) and the proportion of tumor cells showing a positive signal (0, none; 0.1, less than one-tenth; 0.5, less than one-half; 1.0 greater than one-half). The intensity and proportion scores were then multiplied to give an overall score, and tumors with a score equal to or higher than 1.0 were deemed positive.

Reverse Transcriptase-Polymerase Chain Reaction Analysis

Reverse transcriptase-polymerase chain reaction (RT-PCR) was performed based on extracted RNA (600 ng) that was reverse transcribed in a total volume of 20 μl as described previously.[1] Briefly, reverse transcription was completed with the following reaction mixture: for each sample, 200 ng (2 μl of 0.1 μg/μl) of total RNA was added to 16 μl of RT mix (4 μl of 5× RT buffer; 1 μl of each of dATP, dCTP, dGTP, and dTTP, all at 2.5 mmol/L; 2 μl of 0.1% bovine serum albumin; 2 μl of 0.1 mol/L dithiothreitol; 1 μl of 0.25 mol/L random hexamer primer; 2 μl of dimethyl sulfoxide (DMSO), and 1 μl of 200 units/μl of Moloney murine leukemia virus reverse transcriptase) and incubated at 37°C for 1.5 hours. Each PCR was performed in 50-μl volume, using 1 μl of the completed RT reaction (cDNA); 30.8 μl of sterile water; 5 μl of 10× PCR buffer; 5 μl of 25 mmol/L $MgCl_2$; 200 mmol/L each of dATP, dCTP, dGTP, and dTTP; 1 μl of DMSO; 1 unit of Taq DNA polymerase; and 0.5 μl of 50 mmol/L PCR primers. The psoriasin primers were sense (5′-AAG AAA GAT GAG CAA CAC-3′) and antisense (5′-CCA GCA AGG ACA GAA ACT-3′) corresponding to the cDNA sequence,[13] or alternatively, PCR was performed with GAPDH primers, sense (5′-ACC CAC TCC TCC ACC TTT G-3′) and antisense (5′-CTC TTG TGC TCT TGC TGG G-3′).[23] For PCR amplification the reaction comprised an initial step of 5 minutes at 94°C, and then 45 cycles (30 seconds at 94°C, 30 seconds at 56°C, 30 seconds at 72°C) for psoriasin or 35 cycles (45 seconds at 93°C, 45 seconds at 58°C, 30 seconds at 72°C) for GAPDH. PCR products of the two genes amplified from the same RT reaction were loaded into the same wells onto a 1.5% agarose gel before electrophoresis and ethidium bromide staining to visualize psoriasin (246 bp) and GAPDH (198 bp) cDNAs under UV illumination.

Preliminary experiments were performed with cell line and tumor RNA samples to establish the appropriate RNA input and PCR cycle number conditions to achieve amplification with both psoriasin and GAPDH primers in the linear range in a typical sample. Tumors from each cohort were processed as a batch, from frozen sectioning to RNA extraction, reverse transcription in triplicate, and then duplicate PCRs from each RT reaction. For each batch controls included RT-negative and RNA-negative controls and both psoriasin-positive (estradiol-stimulated MCF7) and psoriasin-negative (untransfected, wild-type MDA-MB-231 cells) RNA controls. All primary tumor PCR signals were assessed in gels and autoradiographs by video image capture and with a MCID-M4 image analysis program. Psoriasin expression was standardized to GAPDH expression assessed from the same RT reaction in separate PCR reactions and run in parallel on the same gel, and the mean of each duplicate PCR was then expressed relative to the levels in the MCF7 cell line standard. The invasive tumor component within each section was also assessed in the adjacent mirror image paraffin section, and the percentage area occupied by tumor was

used to correct for differences in epithelial cell content of the tumor sections used for RNA extraction.

Statistical Analysis

For analysis of associations, standardized psoriasin mRNA levels were used either as a continuous variable or transformed into low- or high-expression categories, using a level of one relative density unit. This cutpoint was selected to correspond to the lowest level at which protein could be detected by Western blot. Correlations with estrogen (ER) and progesterone (PR) receptor levels and inflammation were tested using Spearman's test. Associations with categorical variables were tested by either Mann-Whitney or analysis of variance tests for selected dependent variables, or unpaired *t-test for independent variables, or a* χ^2 *test.*

Results

Characterization of Psoriasin-Specific Antibody

Multiple S100 proteins are expressed in individual tissues and cells. To specifically distinguish psoriasin expression within archival formalin-fixed and paraffin-embedded tissues we raised a polyclonal antibody in chicken against a synthetic peptide that corresponded to the COOH terminus of psoriasin. This 14-amino acid region was selected on the basis of very low homology to other S100 proteins. Western blot analysis of an MDA-MB-231 breast cell line transfected with a plasmid incorporating psoriasin cDNA under the control of a CMV promotor (and known to express psoriasin mRNA by Northern blot; unpublished data) and breast tumors showed a single band corresponding to a protein of approx 11.7 kd with the chicken IgY antibody (Figure 1A). This signal could be completely inhibited by preincubation of the primary antibody with psoriasin synthetic peptide (data not shown) and was absent from the wild-type and vector-alone transfected MDA-MB-231 control cells. By comparison, a commercial anti-S100 antibody (Sigma), known to detect several S100 proteins in MDA-MB-231 cells,[24] weakly recognized the same 11.7-kd protein in transfected cells as well as several other S100 proteins in most samples (Figure 1B). Both antibodies reacted with additional higher molecular mass bands in tumor samples. However, specificity of the 11.7-kd psoriasin signal was further confirmed by Western blot using another anti-psoriasin polyclonal rabbit antibody previously raised against a recombinant psoriasin protein (data not shown).

Localization of Cellular Expression of Psoriasin

To assess cellular localization of psoriasin we studied paraffin-embedded tissue blocks from breast, skin, and larynx by immunohistochemistry. The breast tumors studied possessed either high (six cases) or low (seven cases) levels of psoriasin mRNA and total protein expression (determined by Western blot and RT-PCR analysis of

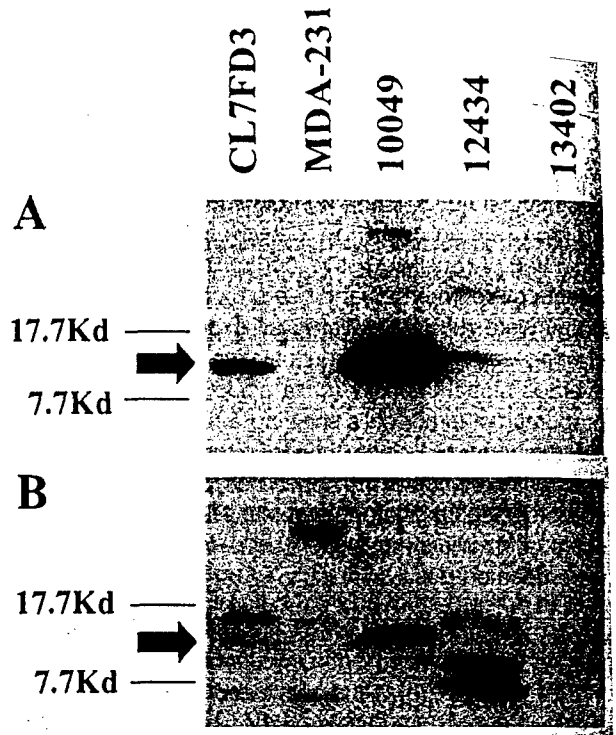

Figure 1. Western blot analysis of cell lines and tumors to demonstrate anti-psoriasin IgY antibody specificity. **A:** A protein band (approx 11.7 kD) detected using a chicken IgY anti-psoriasin antibody in a psoriasin-transfected MDA-MB-231 breast cell line and two tumors (10049, 12434), but absent in tumor 13402 and wild-type MDA-MB-231 cells. **B:** Detection of several S100-like proteins, using a commercial polyclonal S100 antibody applied to the same samples, in addition to weak detection of the same (approx 11.7 kd) protein band seen in **A**.

protein and RNA extracted from sections cut from the adjacent mirror-image frozen tissue blocks). Skin biopsies from the margins of two psoriatic lesions and a squamous carcinoma of larynx were also studied, as psoriasin was originally identified as a highly expressed protein in psoriatic skin and has also been identified as an expressed sequence tag in a cDNA library from laryngeal squamous carcinoma (http://www.ncbi.nlm.nih.gov/UniGene/Hs.112408). All cases were subjected to both immunohistochemistry and *in situ* hybridization on adjacent paraffin sections, and both signals were assessed independently, using a semiquantitative scoring system as described in Materials and Methods.

In breast tumors psoriasin protein was detected predominantly within epithelial tumor cells and was localized within both tumor cell nuclei as well as cytoplasm. Psoriasin was also present within some stromal cells and in some cases also on the luminal aspects of endothelial cells within small vessels (Figure 2). However, *in situ* hybridization demonstrated that mRNA expression was limited to epithelial tumor cells in all cases (Figure 2). The nuclear immunohistochemical staining was completely abolished by competition with the immunizing peptide and was not present in tumors that were negative for psoriasin but showed additional immunoreactive bands on Western blot (eg, see case 13402, Figure 1, and case 8840, Figure 4). Immunohistochemistry and Western blot were concordant in 12/13 cases. In one case Western blot analysis was negative and weak focal staining was

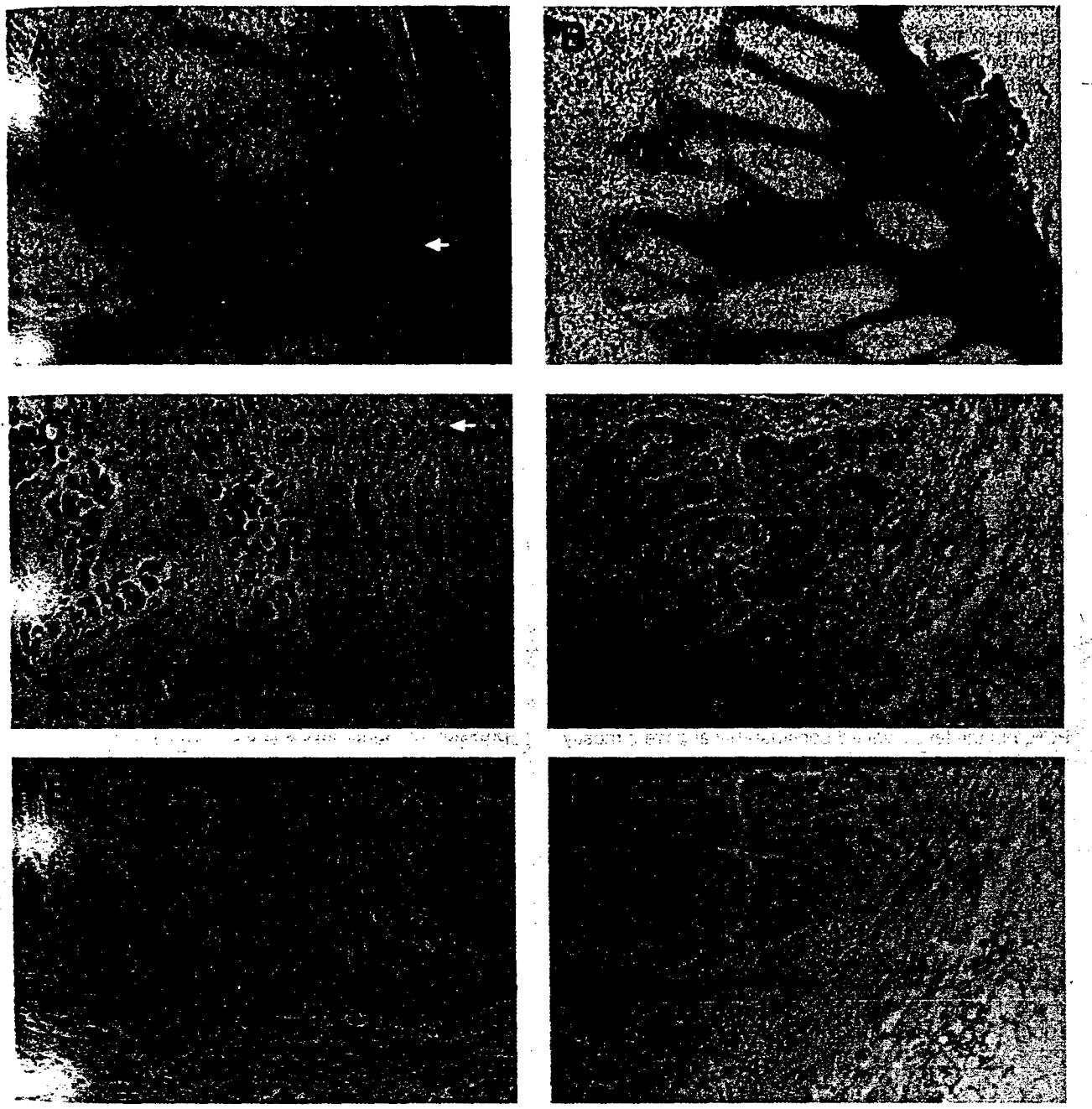

Figure 2. Immunohistochemical and *in situ* hybridization analysis of the cellular distribution and patterns of expression of psoriasin within psoriatic skin and breast carcinoma. Psoriasin protein is localized in hyperplastic epidermis of skin to both nuclei (**A**, **white arrow**) and cytoplasm (**A**, **black arrow**) of keratinocytes. Similar nuclear and cytoplasmic staining is seen in breast epithelial tumor cells (**C**, **black arrow**; case 8965). Psoriasin protein is also detected within occasional stromal inflammatory cells (**C**, **white arrow**). **E:** H&E-stained section from the same region of the tumor shown in **C**. Psoriasin mRNA expression in skin is restricted to epithelial cells in suprabasal layers of epidermis (**B**) and scattered invasive epithelial tumor cells in breast tumors (**D**), detected using antisense probe (**B** and **D**) compared to sense probe (**F**). Original magnification for all panels at the microscope, ×200.

seen by immunohistochemistry. Specificity of the nuclear signal was further confirmed by the fact that the presence of immunohistochemically detected protein expression, assessed on the basis of nuclear staining, was highly concordant (92%) with expression detected by *in situ* hybridization mRNA.

In skin, immunohistochemical staining was localized to keratinocytes within the mid to upper zones of the epidermis of skin showing psoriasiform hyperplasia. These keratinocytes corresponded to the cells that also showed mRNA expression by *in situ* hybridization in adjacent sections (Figure 2). The adjoining normal skin was negative. Occasional positive immunohistochemical staining, but no mRNA signal, was also observed in stromal cells in the dermis underlying the psoriatic lesion. As seen in breast tumor cells, psoriasin protein was localized both to the nucleus and cytoplasm within keratinocytes (Figure 2). The same nuclear and cytoplasmic localization was also detected in a squamous laryngeal carcinoma (data not shown). However, the polyclonal rabbit anti-psoriasin

antibody previously shown to provide immunofluorescent staining in frozen skin sections[13,25] did not detect any signal on paraffin sections from skin or breast. Additional experiments were performed with the chicken IgY anti-psoriasin antibody on skin and breast tumor sections in which immunohistochemical conditions (microwave *versus* protease antigen retrieval) and tissue treatment/fixation conditions (formalin *versus* alcohol *versus* paraformaldehyde *versus* frozen) were varied, and nuclear localization persisted under all conditions (data not shown).

Expression of Psoriasin mRNA in Invasive Breast Tumors

The changes in psoriasin expression previously observed in association with the transition from *in situ* to invasive carcinoma suggested a functional role in the early stages of progression. However, alteration of psoriasin expression in normal skin has also been associated with abnormal keratinocyte differentiation. To examine further the relationship of psoriasin with differentiation and invasiveness, we used RT-PCR and Western blot to examine psoriasin mRNA and protein levels in a cohort of invasive tumors. These tumors included several different tumor types and a range of differentiation, as determined by tumor grade and estrogen receptor status (Table 1).

Psoriasin mRNA was detected in all tumors by RT-PCR, but the levels varied considerably and were mostly low (Figure 3). Within the invasive ductal subgroup there was no significant difference in psoriasin expression with tumor grade. There was also no significant difference between tumor size or type, although there was a trend toward lower levels of expression in both well-differentiated tumor types, tubular and mucinous carcinomas, whereas lobular and medullary carcinomas showed a trend toward higher expression than invasive ductal tumors. However, higher levels of psoriasin mRNA expression showed a significant inverse correlation with both ER and PR levels ($r = -0.66$, $P = 0.0001$; $r = -0.47$, $P = 0.0003$, Spearman) and with ER and PR negative status (ER-ve *vs.* ER+ve; $n = 28$ *vs.* 29, mean (SD) 1.032 (0.7) *vs.* 0.32 (0.36), $P < 0.0001$ Mann-Whitney; PR-ve *vs.* PR+ve, $n = 25$ *vs.* 32, 1.05 (0.72) *vs.* 0.37 (0.40), $P < 0.0001$) in all tumors and within the invasive ductal subgroup. Psoriasin expression was also higher in axillary node-positive cases in all tumors (mean (SD) = 0.86 (0.73) *vs.* 0.59 (0.66), and the difference was statistically significant for the invasive ductal subgroup (mean (SD) = 0.88 (0.79) *vs.* 0.38 (0.28), $P = 0.035$, *t*-test). These relationships with ER, PR, and nodal status (Table 2) were also evident and remained statistically significant after correction of psoriasin levels for the relative tumor cell content, assessed as a percentage within the paraffin sections adjacent to the frozen tissue sections studied.

Psoriasin protein was detected by Western blot analysis in 10 tumors (Table 1 and Figure 4). These tumors (six ductal, two lobular, two medullary) corresponded to those with the highest mRNA levels observed by RT-PCR (above 1.0 arbitrary expression units). Also consistent with RT-PCR analysis, Western blot-positive invasive ductal tumors were also significantly associated with ER-negative ($P < 0.0001$) and PR-negative ($P < 0.0012$) and node-positive ($P = 0.0143$) status (Table 2).

The relationship between psoriasin mRNA and protein expression and host inflammatory response was also examined (Table 2). Psoriasin mRNA showed a significant positive correlation in the entire cohort ($n = 57$, $r = 0.47$, $P = 0.0002$), in the entire cohort excluding the medullary carcinoma subgroup, which includes inflammatory infiltrates as a diagnostic criterion ($n = 52$, $r = 0.42$, $P = 0.0022$), and within the invasive ductal subgroup alone ($n = 34$, $r = 0.39$, $P = 0.023$). Cases with Western blot-detectable psoriasin protein also showed increased inflammatory infiltrates, both in the entire cohort (mean (SD) = 3.6 (1.1) *vs.* 2.3 (1.2), $P = 0.004$) and in the entire cohort excluding the medullary subgroup (mean (SD) = 3.3 (0.89) *vs.* 2.1 (0.98), $P = 0.007$).

Discussion

We have developed a psoriasin-specific antibody and confirmed its specificity as well as its ability to detect the psoriasin protein in formalin-fixed and paraffin-embedded specimens. We have shown that there is a high concordance between psoriasin mRNA and protein levels in invasive tumors, and persistance of psoriasin expression at higher levels is significantly associated with poor prognostic markers, including ER- and PR-negative and lymph node-positive status. Psoriasin expression within breast tumor cells is also associated with inflammatory infiltrates.

Indirect support for a role for S100 genes in breast tumor progression is provided by several observations. Disruption of calcium signaling pathways has been implicated as a central mechanism in tumorigenesis and specifically in the process of invasion and metastasis.[26] Moreover, the chromosomal location of the S100 gene family lies in a region of chromosome 1 that frequently (>50%) shows loss of heterozygosity in invasive tumors.[27] Furthermore, several S100 genes are expressed in breast cell lines and tumors and are known to manifest alteration of their expression in association with tumorigenesis and progression.[11,24] In particular, S100A2 and S100A4 have been identified to be differentially expressed between normal and neoplastic cells[3,28,29] and up-regulated in metastatic as compared to nonmetastatic cells in both mouse and rat mammary tumor cell lines.[5,30] *In vivo* studies of breast tumors have also shown a correlation between high levels of S100A4 expression, nodal metastasis, and ER-negative status.[31] More direct evidence has emerged from modulation of S100A4 expression in transfected cell lines that have shown that overexpression of S100A4 can also induce the metastatic phenotype in mouse, rat, and human cells.[4,6,32] Furthermore, there is evidence that S100A4 may exert its effect on cell cytoskeleton[8,9] and motility,[7] and it has also been demonstrated that up-regulation of S100A4 in mouse tumor cell lines can down-regulate expression of E

Table 1. Clinicopathological Parameters, Histological Composition of the Tumor Section, and Psoriasin Expression in 57 Invasive Breast Carcinomas Assessed by RT-PCR and Western Blot

	Clinicopathological parameters							Psoriasin		
TB#	Type	ER	PR	GrSc	Size	NS	Inf	RT-PCR	RT-PCR/Inv%	WB
11549	muc	194	133		3	−	2	0.06	0.15	−
10515	muc	341	176		3	−	1	0.08	0.14	−
9948	muc	46	22		6.5	−	1	0.10	0.16	−
10582	muc	109	62		2.3	na	1	0.14	0.34	−
8832	muc	295	177		4	−	2	1.94	2.77	−
8021	muc	331	328		2.3	−	2	0.11	0.15	−
11387	tub	105	35		3.5	na	2	0.09	0.29	−
9483	tub	56	0		1.2	−	2	0.09	0.91	−
11651	tub	67	24		2.2	−	3	0.23	0.77	−
8814	tub	232	103		2	−	2	0.44	1.45	−
[illegible]	tub	29	73		2	−	1	0.52	5.21	−
12072	tub	8.3	5		2.3	+	3	0.67	1.34	−
13041	med	3.4	9		2	−	5	0.40	0.49	−
13153	med	4.9	2.4		3	na	5	0.61	0.76	−
11867	med	1.4	9		1.6	+	5	1.60	2.67	+
13058	med	4.6	12		2.8	−	5	1.63	2.04	−
12434	med	1	1.3		1.2	−	5	1.63	3.27	+
8639	ilc	52	83		na	−	1	0.20	0.67	−
8799	ilc	111	139		6	+	2	0.31	3.15	−
8993	ilc	142	528		8	+	1	0.52	0.86	−
9801	ilc	2.1	9.8		na	−	3	0.56	1.60	−
8921	ilc	2.3	8.9		8	−	2	2.07	3.77	+
8961	ilc	0.7	3.4		2.5	−	3	2.34	5.84	+
9000	idc	392	596	7	2.5	−	1	0.07	0.09	−
13402	idc	49	35	4	2.8	−	2	0.07	0.17	−
11971	idc	97	25	4	1.5	−	2	0.13	0.42	−
8684	idc	74	43	7	5	+	1	0.14	0.35	−
12853	idc	17.3	83	9	4.8	+	4	0.15	0.22	−
8840	idc	74	68	7	1.8	+	3	0.17	0.37	−
8834	idc	10	147	5	2	−	2	0.17	0.34	−
8674	idc	16.7	4.5	9	na	−	2	0.19	0.35	−
12037	idc	225	144	4	3.5	+	2	0.20	0.40	−
12868	idc	93	141	9	3.5	na	1	0.21	0.28	−
8599	idc	58	81	4	3.5	−	1	0.24	0.79	−
10105	idc	0.9	3.8	9	3	+	4	0.24	0.40	−
7928	idc	33	72	5	3	+	2	0.27	0.67	−
13414	idc	15.5	59	5	4.1	−	2	0.28	0.56	−
11343	idc	78	44	4	na	−	3	0.29	0.73	−
10644	idc	130	4.7	9	3.2	+	2	0.32	0.81	−
10137	idc	42	26	7	1.8	−	1	0.44	0.89	−
10064	idc	0.8	4.6	9	2.5	na	2	0.53	0.88	−
11769	idc	1.1	3.5	7	na	−	3	0.56	0.80	−
8932	idc	114	27	4	2	−	1	0.56	1.13	−
10906	idc	46	6.6	9	4.5	na	5	0.58	0.64	−
8789	idc	0.8	0.4	7	na	na	3	0.66	1.64	−
10150	idc	70	42	7	na	−	1	0.67	1.68	−
11459	idc	3.6	98	5	4.6	+	3	0.67	0.96	−
13191	idc	17.2	9.2	9	3.2	−	2	0.69	0.87	−
10124	idc	1.9	12.9	9	3	−	4	1.00	1.42	−
8830	idc	0.7	8	9	6	+	4	1.06	1.32	+
8790	idc	6	50	5	1.5	+	2	1.07	3.58	−
11118	idc	6.6	11.8	5	8.5	+	2	1.10	2.20	−
12715	idc	1.5	16	7	3	na	3	1.24	2.06	+
9631	idc	0.7	4.5	9	na	+	4	1.32	3.10	+
8965	idc	0.4	9.9	7	na	+	4	1.85	2.64	+
10049	idc	0.8	14	9	3.7	+	4	2.01	5.04	+
8704	idc	0.7	3.5	7	3.5	+	2	2.60	6.50	+

TB, tumor bank case number; type, mucinous (muc), tubular (tub), medullary (med), lobular (ilc), ductal (idc); ER, PR, estrogen/progesterone receptor levels (fmol/mg protein); GrSc, Nottingham grade score; Size, tumor size (cms); NS, nodal status, positive (+), negative (−), not available (na); Inf, estimate of inflammatory infiltrate, low (1) to high (5). RT-PCR, psoriasin mRNA level determined by RT-PCR; RT-PCR/Inv%, psoriasin mRNA level determined by RT-PCR and adjusted for the percentage tumor cell content of the tissue section (as described in Materials and Methods); WB, psoriasin protein level determined by Western blot.

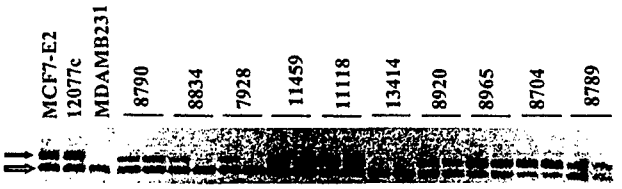

Figure 3. RT-PCR analysis of psoriasin mRNA expression in invasive breast tumors. Psoriasin (**upper black arrow**) and GAPDH (**lower open arrow**) from duplicate PCRs of 10 representative tumors. Control lanes include estradiol-treated MCF7-E2 cells, a tumor control 12077c, and wild-type MDA-MB-231 cells.

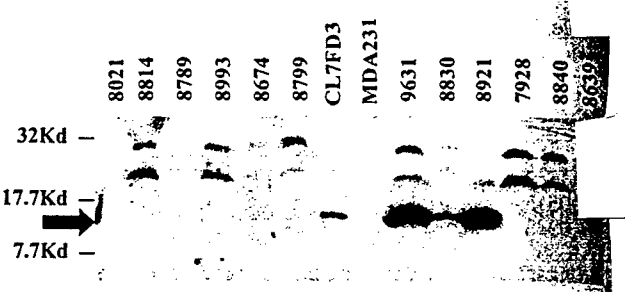

Figure 4. Western blot analysis of psoriasin protein expression in invasive breast tumors. Psoriasin (**black arrow**) is detected in 3/12 representative tumors and within the positive control (CL7FD3).

cadherin and disturb the intracellular distribution of B-catenin.[10]

A possible role for psoriasin (S100A7) in breast cancer first emerged when it was also identified as a cDNA down-regulated in a nodal metastasis relative to a primary breast tumor.[33] Nevertheless, the significance of the initial observation was unclear because of the fact that expression was only detectable in a small proportion of cells within invasive primary tumors studied by *in situ* hybridization and overall could be detected in only 18% of primary tumor specimens assessed by Northern analysis. An explanation for this paradox became apparent when psoriasin was also identified by us as a gene that is particularly highly expressed in the ductal epithelial cells of preinvasive ductal carcinoma *in situ*,[1] which can be present as a significant component with invasive tumor specimens. We have now shown that when higher levels of psoriasin expression persist within invasive tumors, this correlates with indicators of increased metastatic potential. It should be noted that the strong relationship with ER status is compatible with studies of S100A4[31] and the *in vitro* observation[33] (and our unpublished data) that psoriasin is regulated by estradiol in MCF7 cells. Although it is interesting that the nature of this correlation is different between the *in vitro* and *in vivo* situations, similar differences have been found with other genes in breast tumors,[34] suggesting that additional external factors may influence psoriasin regulation *in vivo*.

Although the biological effect of alteration of psoriasin in breast tumors is currently unknown, it is interesting to speculate from this pattern of expression that psoriasin may be important in the invasive phenotype.[16] This role might be mediated through an indirect influence on the effector cells of the host immune response or perhaps through a more direct influence on the epithelial tumor cell. The first hypothesis is supported by the correlation seen here with the degree of host inflammatory cell response within breast tumors and the previous evidence that implicates psoriasin as a chemotactic factor.[14] However, psoriasin protein was only detected in approximately 50% of medullary and ductal tumors with marked inflammatory responses. The second hypothesis is supported by our observation that psoriasin may not only be secreted[13,15] but also can be localized in both nuclear and cytoplasmic compartments in normal skin and breast tumors. Although further studies beyond immunohistochemistry are necessary to confirm this observation, the pattern of expression is consistent between cells in two

Table 2. Relationship between Psoriasin Expression and Prognostic and Tissue Factors

		All				IDC			
		n	Low Ps	High Ps		*n*	Low Ps	High Ps	
ER	−	28	14	4	$P = 0.0001$	19	10	9	$P = 0.0019$
	+	29	28	1		15	15	0	
PR	−	25	13	12	$P = 0.001$	15	8	7	$P = 0.018$
	+	32	29	3		19	17	2	
NS	−	30	24	6	ns ($P = 0.095$)	14	13	1	$P = 0.0002$
	+	19	11	8		15	8	7	
INFL	Low	34	29	5	$P = 0.049$	20	17	3	ns ($P = 0.07$)
	High	18	11	7		14	8	6	
Size	<2	12	9	3		6	5	1	
	2–5	29	22	7	ns	18	14	4	ns
	≥5	7	4	3		3	1	2	
Grade	Low					12	10	2	
	Mod					10	7	3	ns
	High					12	8	4	
Type	idc	34	25	9					
	ilc	6	4	2					
	med	5	2	3	ns				
	muc	6	5	1					
	tub	6	6	0					

ER, PR, estrogen/progesterone receptor status; NS, nodal status; INFL, inflammatory infiltrate; Size, tumor size (cms); Grade, Nottingham grade Type, mucinous (muc), tubular (tub), medullary (med), lobular (ilc), ductal (idc); Low Ps/High Ps, low/high psoriasin mRNA level determined by RT-PCR (cutpoint values used as described in Materials and Methods). *P* values determined by χ^2 or ANOVA tests. ns, not significant.

closely related epithelia, epidermis and breast ductal epithelium, and the detection of nuclear and cytoplasmic signal was unrelated to tissue fixation or immunohistochemistry protocol, which may effect staining with some antibodies.[35,36] Dual localization and alteration of the subcellular localization with disease has also been observed with another S100 related keratinocyte protein, profilaggrin, expressed in the epidermis.[2,37] Similarly, altered cellular distribution of proteins such as BRCA1 and B-catenin are also recognized to be an important aspect of tumor progression.[38–40] Furthermore, other S100 proteins have previously been associated with both extracellular and intracellular actions,[41] and previous studies have also indicated potential interactions for S100A4 with both cytoskeletal[8,9] and nuclear[42] proteins. It has also recently been shown that other secreted S100 proteins can be localized to cytoplasm and nucleus,[43,44] and specifically S100A2 has been found in breast cell nuclei, whereas S100A6 localizes to the cytoplasm[24]; however, the functional significance of these findings remains unknown.

In conclusion, we have shown that expression of psoriasin (S100A7) mRNA and protein correlates with indicators of poor prognosis in invasive breast tumors, including ER, PR, and nodal status, but is not related to differentiation, as manifested by invasive tumor type or grade. The relationship observed between psoriasin and the inflammatory response is also compatible with a role as a chemotactic factor; however, the possibility of additional intracellular functions is raised by the presence of its nuclear localization in both skin and breast tumors. Further studies will be necessary to confirm the latter observation and pursue the biological functions of psoriasin in relation to breast tumor progression.

Acknowledgments

The authors thank Prof. J. E. Celis (University of Aarhus, Aarhus, Denmark) for kindly providing anti-psoriasin antibody and Helmut Dotzlaw and Caroline Cummins-Leygue for assistance with cell transfections. We also thank Bionostics, North York, for assistance with antibody production. The tissues used in this study were provided by the Manitoba Breast Tumor Bank, which is funded by the National Cancer Institute of Canada.

References

1. Leygue E, Snell L, Hiller T, Dotzlaw H, Hole K, Murphy LC, Watson PH: Differential expression of psoriasin messenger RNA between in situ and invasive human breast carcinoma. Cancer Res 1996, 56:4606–4609
2. Schafer BW, Heizmann CW: The S100 family of EF-hand calcium-binding proteins: functions and pathology. Trends Biochem Sci 1996, 21:134–140
3. Lee SW, Tomasetto C, Swisshelm K, Keyomarsi K, Sager R: Down-regulation of a member of the S100 gene family in mammary carcinoma cells and reexpression by azadeoxycytidine treatment. Proc Natl Acad Sci USA 1992, 89:2504–2508
4. Lloyd BH, Platt-Higgins A, Rudland PS, Barraclough R: Human S100A4 (p9Ka) induces the metastatic phenotype upon benign tumour cells. Oncogene 1998, 17:465–473
5. Sherbet GV, Lakshmi MS: S100A4 (MTS1) calcium binding protein in cancer growth, invasion and metastasis. Anticancer Res 1998, 18: 2415–2421
6. Grigorian M, Ambartsumian N, Lykkesfeldt AE, Bastholm L, Elling F, Georgiev G, Lukanidin E: Effect of mts1 (S100A4) expression on the progression of human breast cancer cells. Int J Cancer 1996, 67:831–841
7. Ford HL, Salim MM, Chakravarty R, Aluiddin V, Zain SB: Expression of Mts1, a metastasis-associated gene, increases motility but not invasion of a nonmetastatic mouse mammary adenocarcinoma cell line. Oncogene 1995, 11:2067–2075
8. Bastholm L, Elling F, Georgiev G, Lukanidin EKM, Tarabykina S, Bronstein I, Maitland N, Lomonosov M, Hansen K, Georgiev G, Lukanidin E: Metastasis-associated Mts1 (S100A4) protein modulates protein kinase C phosphorylation of the heavy chain of nonmuscle myosin. J Biol Chem 1998, 273:9852–9856
9. Ford HL, Zain SB: Interaction of metastasis associated Mts1 protein with nonmuscle myosin. Oncogene 1995, 10:1597–1605
10. Keirsebilck A, Bonne S, Bruyneel E, Vermassen P, Lukanidin E, Mareel M, Van Roy F: E-cadherin and metastasin (mts-1/S100A4) expression levels are inversely regulated in two tumor cell families. Cancer Res 1998, 58:4587–4591
11. Borglum AD, Flint T, Madsen P, Celis JE, Kruse TA: Refined mapping of the psoriasin gene S100A7 to chromosome 1cen-q21. Hum Genet 1995, 96:592–596
12. Hoffmann HJ, Olsen E, Etzerodt M, Madsen P, Thogersen HC, Kruse T, Celis JE: Psoriasin binds calcium and is upregulated by calcium to levels that resemble those observed in normal skin. J Invest Dermatol 1994, 103:370–375
13. Madsen P, Rasmussen HH, Leffers H, Honore B, Dejgaard K, Olsen E, Kiil J, Walbum E, Andersen AH, Basse B, et al.: Molecular cloning, occurrence, and expression of a novel partially secreted protein "psoriasin" that is highly up-regulated in psoriatic skin. J Invest Dermatol 1991, 97:701–712
14. Jinquan T, Vorum H, Larsen CG, Madsen P, Rasmussen HH, Gesser B, Etzerodt M, Honore B, Celis JE, Thestrup-Pedersen K: Psoriasin: a novel chemotactic protein. J Invest Dermatol 1996, 107:5–10.
15. Celis JE, Rasmussen HH, Vorum H, Madsen P, Honore B, Wolf H, Orntoft TF: Bladder squamous cell carcinomas express psoriasin and externalize it to the urine. J Urol 1996, 155:2105–2112
16. Watson PH, Leygue ER, Murphy LC: Psoriasin (S100A7). Int J Biochem Cell Biol 1998, 30:567–571
17. Hiller T, Snell L, Watson PH: Microdissection RT-PCR analysis of gene expression in pathologically defined frozen tissue sections. Biotechniques 1996, 21:38–40
18. Ellis IO, Galea M, Broughton N, Locker A, Blamey RW, Elston CW: Pathological prognostic factors in breast cancer. II. Histological type. Relationship with survival in a large study with long-term follow-up. Histopathology 1992, 20:479–489
19. Elston CW, Ellis IO: Pathological prognostic factors in breast cancer. I. The value of histological grade in breast cancer: experience from a large study with long-term follow-up. Histopathology 1991, 19:403–410
20. Leygue ER, Watson PH, Murphy LC: Estrogen receptor variants in normal human mammary tissue. J Natl Cancer Inst 1996, 88:284–290
21. Schagger H, von Jagow G: Tricine-sodium dodecyl sulfate-polyacrylamide gel electrophoresis for the separation of proteins in the range from 1 to 100 kDa. Anal Biochem 1987, 166:368–379
22. Leygue E, Snell L, Dotzlaw H, Hole K, Hiller-Hitchcock T, Roughley PJ, Watson PH, Murphy LC: Expression of lumican in human breast carcinoma. Cancer Res 1998, 58:1348–1352
23. Ercolani L, Florence B, Denaro M, Alexander M: Isolation and complete sequence of a functional human glyceraldehyde-3-phosphate dehydrogenase gene. J Biol Chem 1988, 263:15335–15341
24. Ilg EC, Schafer BW, Heizmann CW: Expression pattern of S100 calcium-binding proteins in human tumors. Int J Cancer 1996, 68: 325–332
25. Ostergaard M, Rasmussen HH, Nielsen HV, Vorum H, Orntoft TF, Wolf H, Celis JE: Proteome profiling of bladder squamous cell carcinomas: identification of markers that define their degree of differentiation. Cancer Res 1997, 57:4111–4117
26. Kohn EC, Liotta LA: Molecular insights into cancer invasion: strategies for prevention and intervention. Cancer Res 1995, 55:1856–1862
27. Munn KE, Walker RA, Varley JM: Frequent alterations of chromosome

1 in ductal carcinoma in situ of the breast. Oncogene 1995, 10:1653–1657
28. Wicki R, Franz C, Scholl FA, Heizmann CW, Schafer BW: Repression of the candidate tumor suppressor gene S100A2 in breast cancer is mediated by site-specific hypermethylation. Cell Calcium 1997, 22: 243–254
29. Ebralidze A, Tulchinsky E, Grigorian M, Afanasyeva A, Senin V, Revazova E, Lukanidin E: Isolation and characterization of a gene specifically expressed in different metastatic cells and whose deduced gene product has a high degree of homology to a Ca^{2+}-binding protein family. Genes Dev 1989, 3:1086–1093
30. Barraclough R, Rudland PS: The S-100-related calcium-binding protein, p9Ka, and metastasis in rodent and human mammary cells. Eur J Cancer 1994, 30A:1570–1576
31. Albertazzi E, Cajone F, Leone BE, Naguib RN, Lakshmi MS, Sherbet GV: Expression of metastasis-associated genes h-mts1 (S100A4) and nm23 in carcinoma of breast is related to disease progression. DNA Cell Biol 1998, 17:335–342
32. Grigorian MS, Tulchinsky EM, Zain S, Ebralidze AK, Kramerov DA, Kriajevska MV, Georgiev GP, Lukanidin EM: The mts1 gene and control of tumor metastasis. Gene 1993, 135:229–238
33. Moog-Lutz C, Bouillet P, Regnier CH, Tomasetto C, Mattei MG, Chenard MP, Anglard P, Rio MC, Basset P: Comparative expression of the psoriasin (S100A7) and S100C genes in breast carcinoma and co-localization to human chromosome 1q21–q22. Int J Cancer 1995, 63:297–303
34. Yarden RI, Lauber AH, El Ashry D, Chrysogelos SA: Bimodal regulation of epidermal growth factor receptor by estrogen in breast cancer cells. Endocrinology 1996, 137:2739–2747
35. Scully R, Ganesan S, Brown M, De Caprio JA, Cannistra SA, Feunteun J, Schnitt S, Livingston DM: Location of BRCA1 in human breast and ovarian cancer cells (technical comments). Science 1996, 272:123–124.
36. Chen Y, Chen P-L, Riley DJ, Lee W-H, Allred DC, Osborne CK: Location of BRCA1 in human breast and ovarian cancer cells (technical comments). Science 1996, 272:125–126
37. Ishida-Yamamoto A, Takahashi H, Presland RB, Dale BA, Iizuka H: Translocation of profilaggrin N-terminal domain into keratinocyte nuclei with fragmented DNA in normal human skin and loricrin keratoderma. Lab Invest 1998, 78:1245–1253
38. Wilson CA, Ramos L, Villasenor MR, Anders KH, Press MF, Clarke K, Karlan B, Chen JJ, Scully R, Livingston D, Zuch RH, Kanter MH, Cohen S, Calzone FJ, Slamon DJ: Localization of human BRCA1 and its loss in high-grade, non-inherited breast carcinomas. Nature Genet 1999, 21:236–240
39. Chen Y, Chen CF, Riley DJ, Allred DC, Chen PL, Von Hoff D, Osborne CK, Lee WH: Aberrant subcellular localization of BRCA1 in breast cancer. Science 1995, 270:789–791
40. Sheng H, Shao J, Williams CS, Pereira MA, Taketo MM, Oshima M, Reynolds AB, Washington MK, DuBois RN, Beauchamp RD: Nuclear translocation of beta-catenin in hereditary and carcinogen-induced intestinal adenomas. Carcinogenesis 1998, 19:543–549
41. Hessian PA, Edgeworth J, Hogg N: MRP-8 and MRP-14, two abundant Ca(2+)-binding proteins of neutrophils and monocytes. J Leukoc Biol 1993, 53:197–204
42. Albertazzi E, Cajone F, Lakshmi MS, Sherbet GV: Heat shock modulates the expression of the metastasis associated gene MTS1 and proliferation of murine and human cancer cells. DNA Cell Biol 1998, 17:1–7
43. Yang Q, O'Hanlon D, Heizmann CW, Marks A: Demonstration of heterodimer formation between S100B and S100A6 in the yeast two-hybrid system and human melanoma. Exp Cell Res 1999, 246:501–509
44. Mandinova A, Atar D, Schafer BW, Spiess M, Aebi U, Heizmann CW: Distinct subcellular localization of calcium binding S100 proteins in human smooth muscle cells and their relocation in response to rises in intracellular calcium. J Cell Sci 1998, 111:2043–2054

Journal of Pathology
J Pathol 2000; **192**: 313–320.

Original Paper

Lumican and decorin are differentially expressed in human breast carcinoma

Etienne Leygue[1], Linda Snell[2], Helmut Dotzlaw[1], Sandra Troup[2], Tamara Hiller-Hitchcock[2], Leigh C. Murphy[1], Peter J. Roughley[3] and Peter H. Watson[2]*

[1] *Department of Biochemistry and Molecular Biology, University of Manitoba, Faculty of Medicine, Winnipeg, Manitoba, Canada, R3E OW3*
[2] *Department of Pathology, University of Manitoba, Faculty of Medicine, Winnipeg, Manitoba, Canada, R3E OW3*
[3] *Genetics Unit, Shriners Hospital for Children, Montreal, Quebec, Canada, H3G 1A6*

*Correspondence to:
Dr P. H. Watson, Department of Pathology, D212-770 Bannatyne Ave, University of Manitoba, Winnipeg, Manitoba R3E OW3, Canada.
E-mail:
pwatson@cc.umanitoba.ca

Received: 22 June 1999
Revised: 1 February 2000
Accepted: 17 April 2000

Abstract

Previous studies have shown that lumican is expressed and increased in the stroma of breast tumours. Lumican expression has now been examined relative to other members of the small leucine-rich proteoglycan gene family in normal and neoplastic breast tissues, to begin to determine its role in breast tumour progression. Western blot study showed that lumican protein is highly abundant relative to decorin, while biglycan and fibromodulin are only detected occasionally in breast tissues ($n=15$ cases). Further analysis of lumican and decorin expression performed in matched normal and tumour tissues by *in situ* hybridization showed that both mRNAs were expressed by similar fibroblast-like cells adjacent to epithelium. However, lumican mRNA expression was significantly increased in tumours ($n=34$, $p<0.0001$), while decorin mRNA was decreased ($p=0.0002$) in neoplastic relative to adjacent normal stroma. This was accompanied by a significant increase in lumican protein ($n=12$, $p=0.0122$), but not decorin. Further evidence of altered lumican expression in breast cancer was manifested by discordance between lumican mRNA and protein localization in some regions of tumours but not in adjacent morphologically normal tissues. It is concluded that lumican is the most abundant of these proteoglycans in breast tumours and that lumican and decorin are inversely regulated in association with breast tumourigenesis.

Keywords: **lumican; decorin; small leucine-rich proteoglycan; breast cancer; tumour progression**

Introduction

The development and progression of breast carcinoma are caused by alterations in the expression of multiple genes, most of which are responsible for normal physiological pathways and the necessary cellular interactions to support these functions within the mammary gland. These include alterations in the interactions between the epithelial and stromal cells, which are manifested in tumours by well-recognized morphological changes known as the stromal reaction [1]. Such alterations in stromal–epithelial interactions may influence the risk of transformation of the breast epithelial cell and may contribute to the very early steps in tumourigenesis, as has recently been proposed in other systems [2]. However, the net effect of these alterations in the stroma on the later stages of tumour progression is unresolved [3].

Resolution of this issue is complicated by the recognition that the stroma is a highly complex tissue that includes a variety of different types of fibroblasts [4] and a range of proteins, glycoproteins, and proteoglycans which may play a role in tumour biology. We have recently extended this list by identifying lumican, a member of the small leucine-rich proteoglycans (SLRPs) as an mRNA that is expressed in the stroma of normal breast tissues and is overexpressed in invasive carcinomas [5]. Members of this family of proteoglycans have been implicated principally in matrix assembly and structure [6], but also more recently in the control of cell growth [7]. While studies of decorin have shown altered expression in neoplastic stroma [3], lumican has previously been studied only in the context of connective tissue and corneal disease [8,9], and the role of SLRPs in human breast cancer is relatively unexplored. To explore further the potential role of lumican and related genes in breast tumour progression, we have now examined the expression of lumican relative to that of other members of the SLRP family, decorin, biglycan and fibromodulin, at both mRNA and protein level, in normal and neoplastic breast tissues.

Materials and methods

Human breast tissues

All breast tumour cases used for this study were selected from the NCIC-Manitoba Breast Tumor Bank (Winnipeg, Manitoba, Canada). As has been previously described [10], tissues are accrued to the bank from cases at multiple centres within Manitoba, rapidly collected, and processed to create matched formalin-fixed, paraffin-embedded, and frozen tissue

blocks with the mirror image surfaces orientated by coloured inks. The histology and cellular composition of every sample in the bank are interpreted in haematoxylin and eosin (H&E)-stained sections from the face of the former tissue block.

For the initial study to compare broadly the expression of different members of the SLRP gene family, a mixed pilot cohort was selected from the Tumor Bank to include nine different invasive carcinomas, three normal tissue samples from patients with cancer, and three normal tissues from normal patients without cancer. The invasive tumours included different tumour types (five ductal, three lobular, and one tubular carcinoma), grades (four high, one moderate, four low Nottingham grades), and oestrogen receptor (ER) levels (three ER < 10 fmol/mg, three ER 10–20, three ER 39–169), and total stromal fractions ranging from 50 to 95% of the cross-sectional area. The mean patient ages were 62, 70, and 28 years for each subgroup, respectively (tumour tissues, normal tissues adjacent to tumours, and normal tissues).

For the subsequent studies to compare lumican and decorin expression, a second more defined and homogeneous cohort of 46 cases was selected to provide matching primary tumour tissues and adjacent normal tissue. This cohort included only invasive ductal carcinomas and was primarily selected to ensure availability of histologically confirmed and distinct regions comprising morphologically normal and tumour tissue elements in different blocks (12 cases, for western blot studies) or the same block (34 cases, for *in situ* hybridization studies). The subset used for western blot studies was also selected to possess equivalent cross-sectional areas [mean section area$^{(SD)}$ in tumour tissues $= 0.86^{(0.44)}$ cm^2, adjacent normal tissues $= 0.85^{(0.35)}$ cm^2] and stromal content [mean stromal area$^{(SD)}$ in tumour tissues $= 68^{(10)}$%, adjacent normal tissues $= 89^{(6)}$%] between the matching blocks and to incorporate cancer cases from both post-menopausal (six cases mean$^{(SD)}$ $= 76^{(7)}$ years) and pre-menopausal patients (six cases mean$^{(SD)}$ $= 44^{(3)}$ years).

Sodium dodecyl sulphate/polyacrylamide gel electrophoresis (SDS/PAGE) and immunoblotting

Total proteins were extracted from frozen tissue sections. These were cut from the face of frozen tissue blocks immediately adjacent to the face of a matching paraffin block [11] from which paraffin sections had been previously cut for pathological assessment and for *in situ* hybridization. For the first cohort of cases, an average of 20 20 μm tissue sections were cut from each typical tissue block (0.5×1.0 cm^2 cross-sectional area) and used for extraction; however, the number of tissue sections was varied for each case according to the measured area of the tissue within individual blocks, to ensure that equivalent volumes of tissue were used for the extraction, which was done as described previously [12]. For the second cohort of matching tissue samples, the same number of frozen sections (20×20 μm) was cut from the measured surface of each tissue block together with a single section from the adjacent paraffin block. This was used as a reference for composition and protein extraction was then performed on the frozen sections with equivalent volumes of extraction buffer. Proteins present in equivalent volumes of extracts were analysed by SDS/PAGE and immunoblotting, using anti-peptide antibodies specific for the carboxyl-terminal regions of the core proteins of lumican, decorin, fibromodulin, and biglycan [12–14]. The specificity of all antibodies was verified by peptide absorption and SLRP cross-reactivity analysis. Protein signals were detected by chemiluminescence and photographed prior to quantitation by video-image analysis and densitometry using an MCID M4 system and software (Imaging Research, St Catherines, Ontario, Canada). All signals were then adjusted with reference to control cartilage samples run with each blot. For the second cohort of matched tissue samples, signals were also adjusted with reference to the measured cross-sectional area and the stromal content of the tissue block to control for equivalent loading. Additional analysis was performed on all signals after further adjustment for relative stromal content of the tissue sections assessed in adjacent H&E sections.

Immunohistochemistry

Immunohistochemistry was performed on paraffin sections using the same antibody to lumican as used for immunoblotting [9,12]. Sections (5 μm thick) were obtained from paraffin-embedded tissue blocks matching the frozen tissue blocks of those cases used for reverse transcription-polymerase chain (RT-PCR) and protein analysis. After deparaffinizing, clearing, and hydrating in TBS buffer (Tris buffered saline, pH 7.6) the sections were pretreated with 3% hydrogen peroxide for 10 min to remove endogenous peroxidases and non-specific binding was blocked with normal swine serum, 1:10 (Vector Laboratories S-4000). TBS was used between steps to rinse and as a diluent. Primary antibody to lumican was applied at a 1:400 dilution overnight at 4°C, followed by biotinylated secondary swine anti-rabbit IgG, 1:200 (DAKO) for 1 h at room temperature. Tissue sections were incubated 45 min at room temperature with an avidin/biotin horseradish peroxidase system (Vectastain ABC Elite, Vector Lab.) followed by detection with DAB (diaminobenzidine), counterstaining with 2% methyl green, and mounting. A positive tissue control (colonic mucosa) and a negative reagent control (no primary antibody) were run in parallel. Immunostaining patterns and intensity were assessed by light microscopic visualization.

In situ hybridization

Paraffin-embedded 5 μm sections of breast tissues were analysed by *in situ* hybridization according to a previously described protocol [5]. For lumican, the plasmid Lumi-398, which consisted of pGEM-T plasmid (Pharmacia Biotech), containing a 398 bp portion of

lumican cDNA between bases 1332 and 1729, was used as a template to generate UTP^{S35} labelled sense and antisense riboprobes using Riboprobe Systems (Promega, Madison, WI, USA) and either the T7 or SP6 promotor at the 5′ or 3′ end of the lumican sequence according to the manufacturer's instructions. For decorin, the plasmid Dec-322 was used as a template. This consisted of pGEM-T plasmid containing a decorin insert with a comparable length (322 bp) to the lumican probe generated by PCR amplification from the decorin cDNA [12] using primers that corresponded to decorin (sense 5′-AAATGCCCAAAACTCTTCAG-3′ and antisense 5′-AAACTCAATCCCAACTTAGCC-3′) [15]. All PCR cDNAs and plasmid inserts were sequenced to confirm their identity. Levels of lumican and decorin expression were assessed in normal and tumour regions by microscopic examination at low magnification and with reference to the negative sense and positive control tumour sections. This was done as previously described [5] by scoring the estimated average signal intensity (on a scale of 0–3) and the proportion of stromal cells showing a positive signal (0, none; 0.1, less than one-tenth; 0.5, less than one-half; 1.0, greater than one-half). The intensity and proportion scores were then multiplied to give an overall score. Regions with a score lower than 1.0 were deemed negative or weakly positive.

Microdissection and protein extraction analysis

To assess protein localization within regions of tumours, two cases were selected that showed marked and well-defined regions within the same tissue section with discrepancies between mRNA and protein expression. This was determined by *in situ* hybridization and immunohistochemistry in adjacent serial sections from paraffin tissue blocks. The mirror image frozen tissue blocks to these paraffin blocks were used for microdissection as previously described [11] and protein was extracted from these histologically defined regions as described above. Briefly, thin 5 μm frozen sections were cut from the faces of the frozen tissue blocks and stained by H&E, and the relevant histological regions of approximately 1–2 mm^2 distinguished and confirmed by reference to the paraffin sections already studied. Multiple thick frozen sections (20 × 20 μm) were then cut, rapidly stained, and microdissected at room temperature from each section in turn, and the microdissected tissue fragments were frozen again prior to protein extraction.

Results

Identification of lumican as the most abundant SLRP in normal and neoplastic breast tissues

To determine the relative importance of altered lumican expression in breast tumourigenesis, the expression of lumican protein was compared with that of three other members of the SLRP family, decorin, fibromodulin and biglycan, by western blot in a heterogeneous panel of nine breast tumours and six normal tissues.

Lumican was highly abundant in all samples and in both neoplastic and normal tissues (Figure 1). A significant increase was seen in the mean level of lumican protein between normal and tumour [$mean^{(SD)}$ tissue adjusted optical density units, normal $= 0.43^{(0.08)}$, tumour $= 0.56^{(0.15)}$, $p = 0.026$, Mann–Whitney test]. Although an apparent difference in the level of lumican between normal samples from normal patients and normal samples adjacent to tumours was seen, this difference did not persist when the different stromal content of these samples was taken into account. Similarly, there was no difference in the levels in tumour tissues on comparing pre- and post-menopausal patients. Nevertheless, an increase in the overall molecular weight and polydiversity was noted between normal tissues and morphologically normal tissue adjacent to tumours, which might be attributable to either different age or association with tumour in the adjacent breast.

In comparison, decorin, although also present in most samples examined by western blot, was much less abundant relative to the cartilage control (Figure 1). It should be noted that the decorin (in common with biglycan and fibromodulin) signals shown in Figure 1 also required a three-fold longer chemiluminescent exposure time (9 s) than that for lumican (3 s). How-

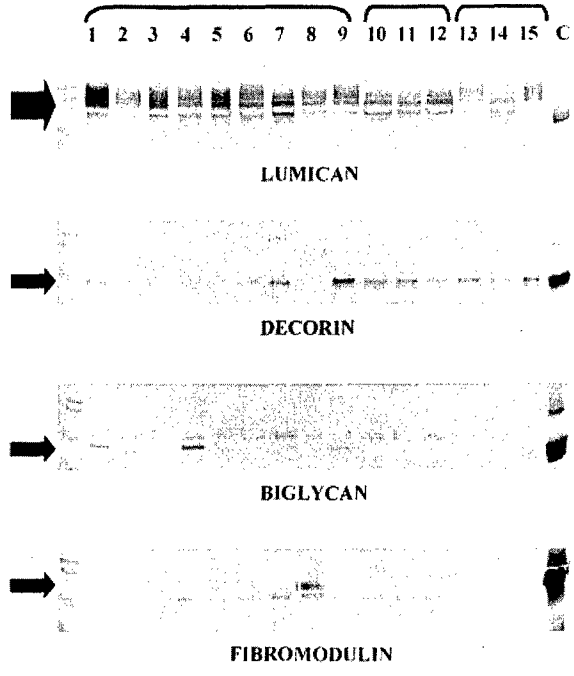

Figure 1. Immunoblotting study of lumican, decorin, biglycan, and fibromodulin protein expression in human breast tumours (lanes 1–9); normal tissues from normal patients (lanes 10–12); and normal tissues adjacent to carcinomas (lanes 13–15). All protein samples were extracted from sets of frozen tissue sections bracketed by sections assessed by H&E stain and light microscopy to confirm content. Chemiluminescent signals for decorin, biglycan, and fibromodulin required three-fold longer exposure times than that for lumican. Molecular markers (left) and cartilage control sample (right) are present in all panels

ever, in contrast to lumican, there was a marked decrease in decorin between normal and tumour samples [mean$^{(SD)}$ optical density units; normal = $0.21^{(0.06)}$, tumour = $0.13^{(0.14)}$, $p = 0.066$, Mann–Whitney test]. No difference was seen in the signals between normal samples from normal and cancer patients.

Fibromodulin expression was not detected in normal tissues and at only low levels in 3/9 tumours, where the presence of fibromodulin correlated with those tumours with the highest content of epithelial tumour cells. Biglycan was also only detected at low levels in 2/6 normal tissues and 3/9 tumours, where in contrast to fibromodulin, its presence correlated directly with those tumours with the highest content of collagenous stroma.

Lumican and decorin are differentially expressed between normal and neoplastic tissues

In order to examine further the distinct alterations in the expression of lumican and decorin, the mRNA and protein expression of both genes was examined in 46 cases by *in situ* hybridization (34 cases) and western blot (12 cases) from the second cohort of cases, comprising matched normal and tumour samples.

As previously shown, prominent lumican mRNA expression was detected, using an antisense probe, in stromal fibroblast-like cells within the tumour and immediately adjacent to invasive tumour cells. Assessment of mRNA levels using a semi-quantitative approach, as detailed in the Materials and methods section, also confirmed our previous observations [5] made on a different set of tumours, and lumican mRNA was found to be significantly elevated in the majority of tumours when levels were compared with those present in adjacent normal stroma ($p < 0.0001$, Wilcoxon test, Figures 2 and 3B). Higher levels of lumican (≥ 1) were present in tumour than in normal tissue in 26/34 cases. At the same time, decorin levels also showed a consistent and significant difference, with lower levels seen in stroma associated with tumour, relative to stroma associated with adjacent normal tissue components ($p < 0.0002$, Wilcoxon test, Figures 2 and 3C), with lower levels of decorin (≥ 1) present in tumour than in normal tissue in 22/34 cases. The pattern of expression of decorin was also identical in sections from the same cases studied with a different *in situ* hybridization riboprobe (data not shown). Although we have previously noted a relationship between lumican and poor prognostic factors, these associations were not found in the present series.

In keeping with the pattern of mRNA expression, the mean lumican protein signal assessed by western blot was also higher in 9/12 tumours relative to normal tissues [mean$^{(SD)}$ optical density units, normal = $0.22^{(0.15)}$, tumour = $0.43^{(0.19)}$, $p = 0.0122$ Wilcoxon test]. Once again, in contrast to this, decorin

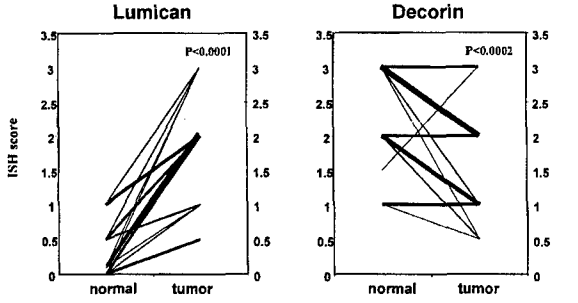

Figure 2. Lumican and decorin mRNA levels in matched normal and tumour tissues, assessed by *in situ* hybridization and semi-quantitative scoring as described in the Materials and methods section. The thickness of each line (on a scale of 1–9) corresponds to the number of cases showing the same differences in scores ($n = 34$ cases)

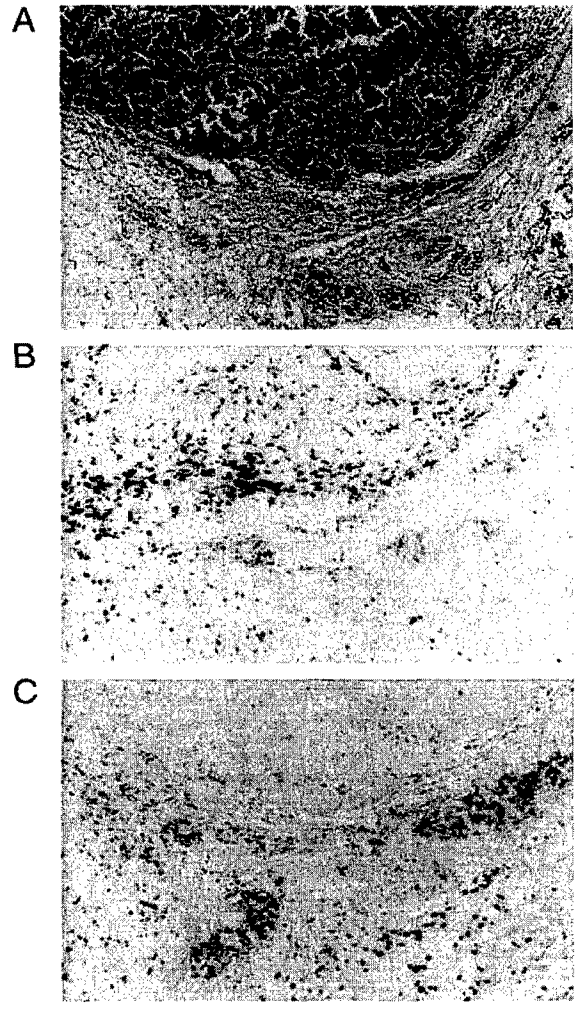

Figure 3. Lumican and decorin mRNA expression detected by *in situ* hybridization within a breast tumour section. Panel A (H&E section) shows the histology including the invasive tumour (upper area), the tumour margin (middle), and adjacent normal tissue including lobular-ductal units (lower area). Lumican expression (B) is high within the tumour and tumour margin and lower in the normal fat and collagenous stroma adjacent to the normal lobules. Decorin (C) shows high expression in the normal stroma adjacent to normal lobules and reduced expression in the tumour. ×340

protein was lower in 7/12 tumours relative to normal tissues, but in this case the differences were not statistically significant [mean$^{(SD)}$ optical density units, normal = $0.22^{(0.19)}$, tumour = $0.17^{(0.2)}$, p = ns (not significant), Wilcoxon test]. These contrasting patterns of lumican and decorin expression also persisted after standardization of western blot signals for relative stromal content (data not shown).

Lumican mRNA and protein expression can occur in different regions within breast tumours

Immunohistochemical study of the lumican distribution within the same tissues that had already been examined by *in situ* hybridization was performed using the same antibody [9,12] that had been employed for western blot analysis (Figure 4). This showed that lumican was abundant throughout the collagenous stroma of both normal and tumour sections, with prominent deposition around small vessels, breast duct, and lobular structures. There was increased deposition within the collagenous stroma of tumours, in particular at the invasive margins and in areas of dense collagen within central regions of some tumours, compared with adjacent normal tissues. However, in some cases there were distinct regions, up to 2 mm in area within the tumour sections, containing loose stroma in which there was a complete absence of lumican detectable by immunohistochemistry (Figures 4C and 4D); but the same regions showed high expression when examined for lumican mRNA by *in situ* hybridization in adjacent sections (Figures 4A and 4B). Similarly, other areas showed strong staining for lumican protein, but low levels of mRNA.

To explore the possibility that the absence of lumican expression detected by immunohistochemistry might be due to the conformation of the native protein or the binding of lumican to other proteins, resulting in the masking of the carboxy-terminal epitope, specific areas measuring approximately 1 mm^2 each were microdissected from frozen sections of two tumours and lumican protein was assessed under denaturing conditions by SDS/PAGE and western blot. In both cases, those regions with high mRNA expression and negative by immunohistochemistry were also negative by western blot, while areas showing very low mRNA expression but strong staining by immunohistochemistry were positive by western blot (Figure 5).

Discussion

We have shown that lumican is the most abundant proteoglycan in comparison with several other members of the family of small leucine-rich proteoglycans (SLRPs) in breast cancer. We have also extended our previous observations [5], based on the detection of lumican mRNA, in showing that the total lumican protein is also increased in breast tumours relative to adjacent normal tissues. Our results also demonstrate that this pattern of up-regulation of lumican in relation to breast tumourigenesis is distinct from that of the closely related decorin gene, which is inversely regulated and reduced at mRNA and to a lesser extent at protein levels, in tumour relative to adjacent normal tissue. Finally, we have shown that lumican expression in tumours may also be associated with an abnormal distribution within the stroma, manifested by discordance between mRNA and protein deposition within subregions of breast tumours.

The family of SLRPs share several common features, including a central region of leucine-rich repeats bounded by flanking cysteine residues, and localization in the extracellular matrix. The SLRPs can be separated into three subgroups that include decorin and biglycan, lumican and fibromodulin, and epiphycan and osteoglycin, which are distinguishable by amino acid homologies and also by gene structure [16]. Decorin, probably the best studied of these genes, is known to interact with a variety of extracellular matrix molecules and has been shown to be capable of influencing collagen fibril growth and assembly both *in vitro* and *in vivo* [6,7]. Decorin may also influence tumour cell growth through indirect effects on the availability of growth factors from the extracellular matrix, or directly through activation of the EGF receptor and induction of the p21 cell-cycle inhibitor [18]. In contrast, less is known about lumican and other SLRPs. However, *in vitro* and *in vivo* data indicate that lumican is also important in the regulation of collagen fibril assembly [19]. This view is supported by recent observations based on mice with homozygous deletion of the lumican gene, where loss of corneal transparency and increased skin fragility are associated with disorganized and loosely packed collagen fibres related to increased and irregular fibril size, and interfibrillar spacing, as viewed by light and electron microscopy [8].

The observation that lumican is highly abundant compared with other SLRPs in breast tumours cannot be interpreted to mean that it is necessarily the most important. This is underscored by the recent demonstration that although decorin is apparently more abundant than versican in prostate cancer tissue, only an increase in the larger chondroitin sulphate proteoglycan versican correlates with grade, and inversely with progression-free survival, in prostate cancer [20]. Similarly, the increase in lumican as seen here in association with breast tumourigenesis may be less important than the parallel decrease in decorin. It should also be noted that while the present study was focused primarily on examining the relative expression of SLRPs between matched normal and tumour tissues and was not necessarily designed to compare levels between cases, we did not observe any significant relationship between lumican or decorin and prognostic factors within this tumour cohort, as previously noted [5]. While this leaves open the question of a role for these SLRPs in later tumour progression, the implication of altered expression for the earlier stages of tumourigenesis remains intriguing. It is possible to

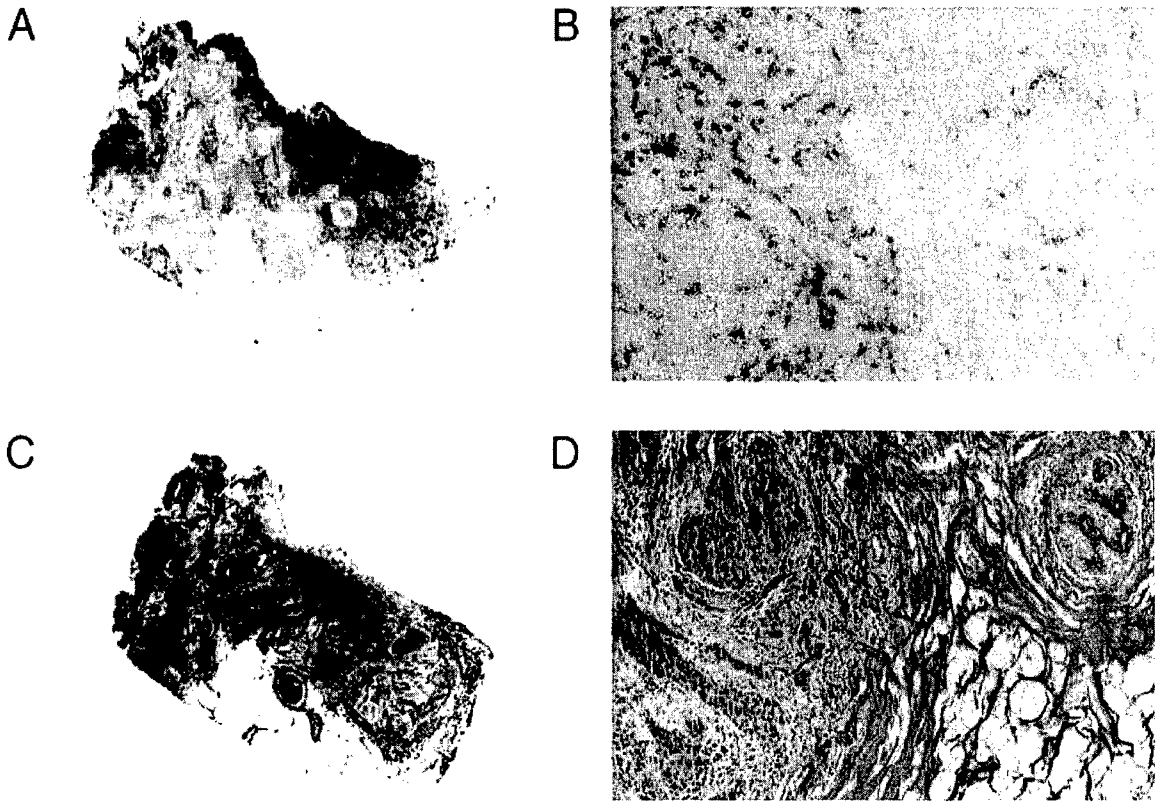

Figure 4. *In situ* hybridization and immunohistochemical study showing regional discordance in lumican mRNA (A, B) and protein expression (C, D) displayed in adjacent sections in breast tumours. Panels A and C show the overall pattern of mRNA (A, black signal) and protein (C, brown staining) within a tissue section (0.4 × 0.8 cm in size) that includes regions of *in situ* and invasive tumour (upper left and upper middle) and adjacent normal tissue (lower left and lower right). Panels B and D show a detailed microscopic view (× 400) of the cellular localization of mRNA and protein within a small region at the invasive edge within the same section (tumour component at left, normal component at right)

speculate that both induction of lumican and decrease in decorin in stromal fibroblasts within the invasive tumour may represent a positive host response, to abrogate the disorganization of collagen within the tumour stroma, encourage macrophage localization [21], and inhibit the growth of epithelial cancer cells, through the increased availability of growth factors inhibitory to breast epithelial cell growth [22]. Alternatively, these alterations may represent a negative host response contributing to early tumour development. Increased lumican mRNA expression may reflect a response to locally increased proteolysis or altered deposition of the lumican protein that is the cause of the disorganization of the collagenous stroma, which in turn facilitates tumour cell invasion. Similarly, a decrease in decorin may remove an inhibitory effect on epithelial tumour cell growth through repression of p21 [7]. A role for and the distinction between these opposing potential effects will clearly require further study.

The differences in lumican levels between normal and tumour tissues observed by both immunohistochemistry and western blot are not as marked as those seen at the level of mRNA expression. While differences in the assays may account for some of this discrepancy, it is clear that it may also be attributable to the discordance that can exist between lumican mRNA and protein expression detected by *in situ* and immunohistochemical techniques respectively, within the same regions of breast tumour stroma. A similar discordance between mRNA and protein expression has been previously observed in the course of studies on lumican and other large and small proteoglycans in different tissues. For example, in corneal development in the chicken, the mRNA levels for lumican and decorin do not always reflect the rate of synthesis of the corresponding proteins and the efficiency of translation of lumican varies over time [23]. Similar discordance between aggrecan and versican mRNA and protein has been seen in normal tendon [24], between decorin and biglycan mRNA and protein localization in normal and reactive gastric mucosa [25], and in regions of cartilage matrix around vascular channels and the growth plates of long bones in normal cartilage [26]. In this latter instance, the discordance was attributed to a high rate of breakdown and removal at these sites. This conclusion is supported by studies on endothelial cells which show that growth factors such as bFGF can increase not only both biglycan transcription and protein synthesis,

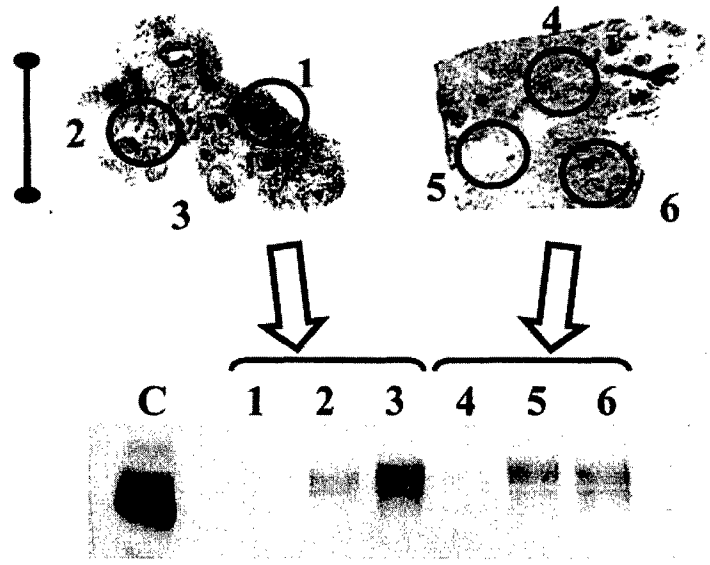

Figure 5. Lumican protein expression detected by immunohistochemistry (upper panel) and western blot (lower panel) demonstrating concordance in the assessment of protein levels in microdissected subregions within two breast tumour sections. The upper panels show IHC sections (tumour A, left; tumour B, right; scale bar = 5 mm). The mRNA and protein signals were detected by *in situ* hybridization (ISH) and immunohistochemistry (IHC) in each region in adjacent sections and ISH/IHC levels were assessed semi-quantitatively (negative, weak +, strong + +) as follows: tumour A: region 1 = + +/−, region 2 = −/+ +, region 3 (remainder of section) = +/+ +; tumour B: region 4 = +/−, region 5 = −/+ +, region 6 = + +/+ +. The lower panel shows the western blot (C = cartilage control; lanes 1–6 correspond to regions assessed and microdissected above)

but also the corresponding rate of proteolysis [27]. The absence of protein could also reflect masking of the epitope by conformational changes in the native protein, by changes in post-translational modification, or by binding to another protein. Alternatively, this could reflect reduced translation, increased breakdown, or failure to bind within the immediate stroma and rapid translocation of the protein to adjacent areas of the tissue. Our microdissection experiments, applied to small regions where lumican mRNA is highly expressed, suggest that the corresponding protein is truly absent in these areas and that epitope masking due to conformation or binding proteins is an unlikely explanation for the observation. However, it could also be the case that the necessary binding sites are not available in the immature stroma associated with rapid growth of tumours and that this allows translocation of newly synthesized lumican to binding sites in adjacent tissue.

The reciprocal nature of the changes in the expression of lumican and decorin is intriguing. Although definitive characterization of the stromal cell types awaits primary culture studies, direct comparison of *in situ* hybridization performed on serial sections suggests that expression of both genes apparently occurs in the same fibroblast-like cells in breast tissue stroma. While lumican has not previously been studied in human tumours, the expression of decorin mRNA and proteoglycans incorporating chondroitin sulphate epitopes has been shown to be increased in colon, prostate, and basal cell carcinomas [28–30], but a more recent study of multiple stromal genes in breast tumours found no difference in the levels of decorin mRNA between tumour and normal tissue, although noting increased expression in the stroma immediately adjacent to *in situ* components [31]. However, the normal tissue examined was selected to be well away from the primary tumour and this, together with differences in the method of quantitation, the definition of tumour regions, and the focus on matched samples, limits a full comparison with our observations. For example, morphologically normal tissue immediately adjacent to carcinomas may be influenced by paracrine growth factors derived from the tumour and may also harbour molecular alterations [32] that might influence local gene expression. However, similar immunohistochemical studies of breast tumours using monoclonal antibodies raised against chondroitin sulphate and dermatan sulphate small proteoglycan have shown reduced decorin expression within invasive as compared with surrounding normal stroma, consistent with our findings [33]. Decorin and other SLRPs are known to be independently regulated and mutually exclusive [26] and compensatory changes in the expression between different SLRPs have been observed [34]. However, this appears to be usually manifested by genes within subgroups of the SLRP family. At the same time, reciprocal changes in the expression between lumican and decorin have not been described in lumican or decorin 'knockout' mice [8,17]. The factors that influence altered expression of these genes in breast tumour stroma remain to be elucidated.

In summary, we have shown that lumican is highly abundant relative to decorin, biglycan, and fibro-

modulin in normal and neoplastic breast tissues. We have also shown that increased lumican protein expression and altered regional localization occur in breast tumours and that different and reciprocal alterations in expression occur between lumican and decorin. The functional significance and the role of alterations in these stromal proteoglycans in breast tumourigenesis and progression remain to be determined.

Acknowledgements

This work was supported by grants from the Medical Research Council of Canada (MRC) and the US Army Medical Research and Materiel Command (USAMRMC). The Manitoba Breast Tumor Bank is supported by funding from the National Cancer Institute of Canada (NCIC). PHW is an MRC Scientist; LCM is an MRC Scientist; and EL is a recipient of a USAMRMC Postdoctoral Fellowship. TH-H is a recipient of an MRC studentship award.

References

1. Peyrol S, Raccurt M, Gerard F, Gleyzal C, Grimaud JA, Sommer P. Lysyl oxidase gene expression in the stromal reaction to *in situ* and invasive ductal breast carcinoma. *Am J Pathol* 1997; **150**: 497–507.
2. Kinzler KW, Vogelstein B. Landscaping the cancer terrain [comment]. *Science* 1998; **280**: 1036–1037.
3. Iozzo RV. Tumor stroma as a regulator of neoplastic behavior. Agonistic and antagonistic elements embedded in the same connective tissue [editorial]. *Lab Invest* 1995; **73**: 157–160.
4. Spanakis E, Brouty-Boye D. Discrimination of fibroblast subtypes by multivariate analysis of gene expression. *Int J Cancer* 1997; **71**: 402–409.
5. Leygue E, Snell L, Dotzlaw H, *et al.* Expression of lumican in human breast carcinoma. *Cancer Res* 1998; **58**: 1348–1352.
6. Iozzo RV. The family of the small leucine-rich proteoglycans: key regulators of matrix assembly and cellular growth. *Crit Rev Biochem Mol Biol* 1997; **32**: 141–174.
7. Santra M, Mann DM, Mercer EW, Skorski T, Calabretta B, Iozzo RV. Ectopic expression of decorin protein core causes a generalized growth suppression in neoplastic cells of various histogenetic origin and requires endogenous p21, an inhibitor of cyclin-dependent kinases. *J Clin Invest* 1997; **100**: 149–157.
8. Chakravarti S, Magnuson T, Lass JH, Jepsen KJ, LaMantia C, Carroll H. Lumican regulates collagen fibril assembly: skin fragility and corneal opacity in the absence of lumican. *J Cell Biol* 1998; **141**: 1277–1286.
9. Cs-Szabo G, Melching LI, Roughley PJ, Glant TT. Changes in messenger RNA and protein levels of proteoglycans and link protein in human osteoarthritic cartilage samples. *Arthritis Rheum* 1997; **40**: 1037–1045.
10. Watson PH, Snell L, Parisien M. The NCIC-Manitoba Breast Tumor Bank: a resource for applied cancer research. *Cmaj* 1996; **155**: 281–283.
11. Hiller T, Snell L, Watson PH. Microdissection RT-PCR analysis of gene expression in pathologically defined frozen tissue sections. *Biotechniques* 1996; **21**: 38–40.
12. Grover J, Chen XN, Korenberg JR, Roughley PJ. The human lumican gene. Organization, chromosomal location, and expression in articular cartilage. *J Biol Chem* 1995; **270**: 21942–21949.
13. Roughley PJ, White RJ, Cs-Szabo G, Mort JS. Changes with age in the structure of fibromodulin in human articular cartilage. *Osteoarthritis Cart* 1996; **4**: 153–161.
14. Roughley PJ, White RJ, Magny M-C, Liu J, Pearce RH, Mort JS. Non-proteoglycan forms of biglycan increase with age in human articular cartilage. *Biochem J* 1993; **295**: 421–426.
15. Vetter U, Vogel W, Just W, Young MF, Fisher LW. Human decorin gene: intron–exon junctions and chromosomal localization. *Genomics* 1993; **15**: 161–168.
16. Hocking AM, Shinomura T, McQuillan DJ. Leucine-rich repeat glycoproteins of the extracellular matrix. *Matrix Biol* 1998; **17**: 1–19.
17. Danielson KG, Baribault H, Holmes DF, Graham H, Kadler KE, Iozzo RV. Targeted disruption of decorin leads to abnormal collagen fibril morphology and skin fragility. *J Cell Biol* 1997; **136**: 729–743.
18. Moscatello DK, Santra M, Mann DM, McQuillan DJ, Wong AJ, Iozzo RV. Decorin suppresses tumor cell growth by activating the epidermal growth factor receptor. *J Clin Invest* 1998; **101**: 406–412.
19. Ying S, Shiraishi A, Kao CW, *et al.* Characterization and expression of the mouse lumican gene. *J Biol Chem* 1997; **272**: 30306–30313.
20. Ricciardelli C, Mayne K, Sykes PJ, *et al.* Elevated levels of versican but not decorin predict disease progression in early-stage prostate cancer. *Clin Cancer Res* 1998; **4**: 963–971.
21. Funderburgh JL, Mitschler RR, Funderburgh ML, Roth MR, Chapes SK, Conrad GW. Macrophage receptors for lumican. A corneal keratan sulfate proteoglycan. *Invest Ophthalmol Vis Sci* 1997; **38**: 1159–1167.
22. Santra M, Skorski T, Calabretta B, Lattime EC, Iozzo RV. *De novo* decorin gene expression suppresses the malignant phenotype in human colon cancer cells. *Proc Natl Acad Sci U S A* 1995; **92**: 7016–7020.
23. Cornuet PK, Blochberger TC, Hassell JR. Molecular polymorphism of lumican during corneal development. *Invest Ophthalmol Vis Sci* 1994; **35**: 870–877.
24. Waggett AD, Ralphs JR, Kwan AP, Woodnutt D, Benjamin M. Characterization of collagens and proteoglycans at he insertion of the human Achilles tendon. *Matrix Biol* 1998; **16**: 457–470.
25. Schonherr E, Lugering N, Stoll R, Domschke W, Kresse H. Differences in decorin and biglycan expression in patients with gastric ulcer healing. *Scand J Gastroenterol* 1997; **32**: 785–790.
26. Bianco P, Fisher LW, Young MF, Termine JD, Robey PG. Expression and localization of the two small proteoglycans biglycan and decorin in developing human skeletal and non-skeletal tissues. *J Histochem Cytochem* 1990; **38**: 1549–1563.
27. Kinsella MG, Tsoi CK, Jarvelainen HT, Wight TN. Selective expression and processing of biglycan during migration of bovine aortic endothelial cells. The role of endogenous basic fibroblast growth factor. *J Biol Chem* 1997; **272**: 318–325.
28. Adany R, Heimer R, Caterson B, Sorrell JM, Iozzo RV. Altered expression of chondroitin sulfate proteoglycan in the stroma of human colon carcinoma. Hypomethylation of PG-40 gene correlates with increased PG-40 content and mRNA levels. *J Biol Chem* 1990; **265**: 11389–11396.
29. Hunzelmann N, Schonherr E, Bonnekoh B, Hartmann C, Kresse H, Krieg T. Altered immunohistochemical expression of small proteoglycans in the tumor tissue and stroma of basal cell carcinoma. *J Invest Dermatol* 1995; **104**: 509–513.
30. Iozzo RV, Cohen I. Altered proteoglycan gene expression and the tumor stroma. *Experientia* 1993; **49**: 447–455.
31. Brown LF, Guidi AJ, Schnitt SJ, *et al.* Vascular stroma formation in carcinoma *in situ*, invasive carcinoma, and metastatic carcinoma of the breast. *Clin Cancer Res* 1999; **5**: 1041–1056.
32. Deng G, Lu Y, Zlotnikov G, Thor AD, Smith HS. Loss of heterozygosity in normal tissue adjacent to breast carcinomas. *Science* 1996; **274**: 2057–2059.
33. Nara Y, Kato Y, Torii Y, *et al.* Immunohistochemical localization of extracellular matrix components in human breast tumours with special reference to PG-M/versican. *Histochem J* 1997; **29**: 21–30.
34. Nelimarkka L, Kainulainen V, Schonherr E, *et al.* Expression of small extracellular chondroitin/dermatan sulfate proteoglycans is differentially regulated in human endothelial cells. *J Biol Chem* 1997; **272**: 12730–12737.

Angio-Associated Migratory Cell Protein (AAMP) mRNA is associated with necrosis and is differentially expressed between High-grade and Low-grade Ductal Carcinoma *In Situ* (DCIS) of the Breast

Adewale Adeyinka, Ethan Emberley, Yulian Niu, Linda Snell, Leigh C. Murphy, Heidi Sowter, Charlie Wykoff, Adrian Harris, and Peter H. Watson.

Affiliations of authors: Department of Pathology (AA, EE, YN, LS, PHW.) and Department of Biochemistry and Molecular Biology (LCM), University of Manitoba, Faculty of Medicine, Winnipeg, Manitoba, Canada, R3E OW3 and Imperial Cancer Research Fund Molecular Oncology Laboratory (HS, CW, ALH), University of Oxford, Institute of Molecular Medicine, John Radcliffe Hospital, Oxford, OX3 9DU, UK

Running title: DCIS and AAMP expression in breast cancer.

Footnotes:
1 This work was supported in part by grants from the Canadian Institutes of Health (CIHR), the Canadian Breast Cacner Research Initiative, and the U.S. Army Medical Research and Materiel Command (USAMRMC). The Manitoba Breast Tumor Bank is supported by funding from the National Cancer Institute of Canada (NCIC). E .E. is supported by a USAMRMC predoctoral award. A. A. is supported by a USAMRMC postdoctoral award. P. H. W. is supported by a CIHR Scientist award and by a USAMRMC Academic Award.
2 Address requests for reprints to Dr. Peter Watson at Department of Pathology, D212-770 Bannatyne Ave, University of Manitoba, Winnipeg, MB. R3E OW3, Canada. Phone: (204) 789 3435; Fax: (204) 789 3931; E-mail: pwatson@cc.umanitoba.ca.
3 The abbreviations used are: AAMP, angio associated migratory protein; RT-PCR, reverse transcription-polymerase chain reaction; H&E, Hematoxylin/Eosin; ER, estrogen receptor; PR, progesterone receptor.

Abstract
The risk of recurrence and progression of ductal carcinoma in-situ (DCIS) of the breast is best designated by morphological indicators including nuclear grade and presence of necrosis. To identify molecular alterations underlying these morphological features we have compared gene expression within a cohort of 10 cases of DCIS (6 high-grade or intermediate-grade DCIS with necrosis and 4 low-grade DCIS) using microdissection and cDNA microarray. A set of 42 cDNAs, from a group of 1,500, was identified that were consistently differentially expressed and whose expression profile clustered with DCIS grade. Amongst this set, the angio-associated migratory protein (AAMP) was identified as an mRNA that is consistently higher in high-grade DCIS (p= 0.0095) and that is also induced by hypoxia in the T47D breast cancer cell line. Differential expression was confirmed by quantitative reverse transcriptase polymerase chain reaction (RT-PCR) and *in situ* hybridization analysis of 37 DCIS. AAMP mRNA tended to be associated with high and intermediate-grade DCIS and DCIS with necrosis. However, no relationship was observed between AAMP and angiogenesis, and its functional role in tumorigenesis and breast cancer progression remains to be determined.

Introduction
In recent years there has been an increase in the numbers of ductal carcinoma in-situ (DCIS) and other pre-invasive breast lesions diagnosed.[1, 2] As a result, these lesions have become an increasingly significant problem in the evaluation and management of patients with breast disease. To predict the relative risk of recurrence and/or the progression of DCIS to invasive tumors, different classifications have been proposed[3]. These are based on a combination of morphological features such as nuclear grade, presence of necrosis, margin width and tumor size and reflect a recognition that DCIS is in fact a spectrum of disease with different morphological characteristics as well as biological and clinical behavior. However, useful as these classifications may be, discordance is common in their use[4] underscoring the need for better predictors of outcome and progression of DCIS.

As already noted, intraductal necrosis is a distinctive morphological feature of some types of high risk DCIS[5] and is believed to be attributable to the presence of severe hypoxia that can arise within the duct through an imbalance between metabolic requirements and blood supply.[5] Thus although comparatively little is known about the genetic and molecular events that are responsible for the progression of some DCIS to invasive breast carcinoma, alterations in the molecular mechanisms associated with the hypoxia response or activation of the normal response to less severe hypoxia may therefore offer potential indicators of risk of progression in DCIS lesions.

cDNA microarray analysis is a useful technique for the molecular profiling of the gene expression pattern of cells representing the various stages of malignant transformation.[6] Microdissection techniques, including manual and laser capture microdissection (LCM) have recently emerged as effective tools to isolate well defined population of cells from heterogeneous tissue sections as is often encountered in breast cancer.[7, 8] Combining microdissection and microarray analysis we investigated the differences between the gene expression patterns of low-grade DCIS and high-grade DCIS in order to identify differentially expressed genes that may be associated with the known different risks of recurrence and progression of these tumor types. It is anticipated that some of the products of the genes identified may serve as molecular biomarkers for assessing the risk of progression of DCIS or provide targets for new therapies.

Materials and Methods

Human breast tumor samples

Human DCIS samples were obtained from the NCIC-Manitoba Breast Tumor Bank (Department of Pathology, University of Manitoba, Winnipeg, Canada).[9] All cases in the bank have been rapidly frozen at 70 ^{0}C after surgical removal and subsequently processed to create formalin-fixed paraffin-embedded tissue blocks and matched frozen tissue blocks with mirror image surfaces corresponding to the formalin-fixed tissue blocks. Histological interpretation and assessment of every sample in the Bank is done on hematoxylin/eosin (H&E)-stained sections from the paraffin tissue by a pathologist.

Two cohorts of tumors were selected. The first cohort of 10 tumors comprised DCIS lesions with homogenous nuclear grade within each lesion. These included 4 high grade and 2 intermediate grade (all with >10% of ducts containing necrosis), and 4 low-grade DCIS cases and were used as the primary microdissection series. The second cohort comprised 28 DCIS specimens used to confirm the differential expression observed in the microdissected cases. Tumor classification and the evaluation of intraductal necrosis were done on high quality hematoxylin and eosin stained slides derived from the formalin fixed and paraffin embedded blocks by 2 pathologists (AA and PHW), independent of the array or subsequent gene expression analysis. The classification of DCIS into histological grades was done according to the Van Nuys grading system.[3, 10] and tumors were assigned to the highest histological grade present in the tissue section studied. Both cohorts combined (38 tumors) included 6 low-grade DCIS, 11 intermediate-grade DCIS and 21 high-grade DCIS. Twenty-seven tumors were estrogen receptor (ER)-positive, 11 were ER-negative, 25 were progesterone receptor (PR)-positive and 13 were PR-negative (Table 1). Steroid receptor status was determined by ligand-binding assay. A positive ER status and positive PR status were defined as more than 3 fmol/mg protein and more than 15 fmol/mg protein, respectively.

Microdissection

Tumor samples were microdissected by two methods, depending on the size and the geographical complexity of the DCIS lesions. A manual dissection-microscope method previously established in our laboratory[7] was used where possible as it is rapid and reliable, however a laser-capture microdissection method using an Arcturus Pixell II instrument (Arcturus Engineering, Inc. Mountain View, CA) was used for two cases with a heavy inflammatory cell infiltrate of the stroma around the ducts and to obtain epithelial cells from a normal breast sample. For the manual microdissection, tumor cells were dissected from 6-10 20-μm frozen sections of tumors mounted on agarose gel dropped onto a plain glass slide and stained briefly with H&E, as previously described [7]. For laser microdissection, tumor cells were microdissected from 14-17 10-μm frozen sections mounted onto plain glass slides and stained with H&E according to the Arcturus Engineering protocol.[11]

Tissue RNA extraction

Total RNA was extracted with Trizol Reagent (Life Technologies, Inc.) from tumor cells obtained from all 10 microdissected DCIS using a small scale RNA extraction protocol.[7] Total RNA was similarly extracted from six 20-μm frozen sections from each of the 28 DCIS tumors constituting the second cohort.

Cell line culture and RNA extraction

The T47D human breast cancer cell line was obtained from the Imperial Cancer Research Fund (ICRF) cell service, and grown in DMEM , RPMI or Hams F-12 supplemented with 10% fetal calf serum (Globepharm), L-glutamine (2 μM), penicillin (50 IU/ml) and streptomycin sulphate (50 μg/ml). Parallel incubations were performed on flasks of cells approaching confluence in normoxia (humidified air with 5% CO_2) or hypoxia. Hypoxic conditions were generated in a Napco 7001 incubator (Precision Scientific) with 0.1% O_2, 5% CO_2 and balance N_2. Total RNA was prepared according to Chomczynski and Sacchi[12] and the quality assessed by absorbance at 260/280nm as well as by electrophoresis in 1% agarose gels by staining of the 28S rRNA with ethidium bromide.

Microarray cDNA membranes

Human GF-200 cDNA Microarray membranes and the Pathways 2.01 analysis software were purchased from Research Genetics, Inc. Reverse transcription, ^{33}P-labeling and hybridization of RNA to array membranes were done according manufacturer's instructions. Briefly, for each sample, 1μg of total RNA was reverse transcribed in the presence of 10 μl [^{33}P]dCTP at a concentration of 10 mCi/ml, dATP, dGTP, dTTP at 20 mM, 500ng of Oligo-dT and 200 units of SuperScript II RT (Life Technologies, Inc.), all in a 30 μl volume. The labeled cDNA was purified by passing through a Bio-Spin 6 Chromatography column (Bio-Rad), denatured and hybridized to human GF-200 cDNA microarray membranes. Membranes were pre-hybridized at 42 ^{0}C for at least 2 hours in 5 ml microhyb solution (Research Genetics, Inc) in the presence of 1.0 μg/ml poly-dA and 1.0 μg/ml Cot 1 DNA. After an overnight (20hr) hybridization with labeled cDNA, membranes were washed, exposed to Imaging screen-K (Bio-Rad) and scanned in a phosphorimager (Bio-Rad). The tiff images (Figure 2) obtained from the phosphorimager were imported into the Pathways 2.01 analysis software (Research Genetics, Inc.) for analysis and comparison between different membranes from different tumors. Membranes to which ^{33}P-labeled reverse transcribed RNA from high-grade or intermediate–grade DCIS was hybridized were compared with membranes to which ^{33}P-labeled reverse transcribed RNA from low-grade DCIS was hybridized. To compare two membranes, an all-data-point method of normalization was used and cDNA showing expression levels lower than 10X background were masked from comparison. A 1.8 fold or greater differential expression was considered significant. Each

cDNA spot on the Pathways pseudo-color membrane showing >= 1.8 fold differential expression was examined by direct vizualization to eliminate those that might be false positives — spots judged to be not properly centered or spots influenced by 'bleed-over' from adjacent spots. A similar approach was used to compare profiles of gene expression between normoxic and hypoxic T47D breast cells.

Real time quantitative RT-PCR

Total RNA from the 10 microdissected samples used for the GeneFilter hybridization and the 28 DCIS samples of the second cohort were reverse transcribed in a total volume of 20 µl as described previously.[7] For each sample, 2 µl of 0.1 µg/µl of total RNA was added to an 18 µl RT mix (4 µl of 5X RT buffer; 1 µl each of dATP, dCTP, dGTP, and dTTP, all at a concentration of 2.5 mM; 2 µl of 0.1% bovine serum albumin (BSA); 2 µl of 100 mM dithiothreitol (DTT); 2 µl of dimethyl sulfoxide (DMSO); 2 µl of 50 µM Oligo-dT primer, and 2 µl of 200 units/µl of Moloney murine leukemia virus reverse transcriptase) and incubated at 37°C for 1.5 hrs. The resulting cDNA was diluted with 20 µl of sterile water and used as template for the quantitative RT-PCR.

The mRNA sequences of the genes identified using the array membranes and corresponding Research Genetics information were determined by using the blast module of National Center for Biotechnology Information database. Primers that specifically detect these sequences were designed and employed for the RT-PCR reaction using the LightCycler Instrument (Roche Molecular Biochemicals) and the LightCycler-DNA Master SYBR Green I reaction mix for PCR (Roche Molecular Biochemicals), containing the SYBR Green I dye as detection format. For each sample, triplicate reactions were set up in capillaries with the following reaction mix: 0.33 µl DNA template; 0.2 µl each of 50 mM sense and antisense primers; 1.6 µl of 25 mM $MgCl_2$; 2 µl LightCycler-DNA Master SYBR Green I reaction mix, and 16 µl sterile water. For each batch of reactions controls included RT-negative and RNA-negative controls, and serial dilutions (1 ng, 0.01 ng and 0.0001 ng) of plasmid DNA as standards for linear regression analysis of unknown samples. The denaturation, amplification, melting curve analysis, and cooling programs of the LightCycler instrument were set according to manufacturer's specifications. The annealing temperature and elongation time, however, were set depending on primers and product length, respectively. PCR products were run on a 1.5% agarose gel to confirm the PCR specificity. The expression of Cyclophilin 33A, a house keeping gene, was used to normalize for variances in RNA and cDNA input. The AAMP primers were sense, 5'–CGC CTG CTT ACT GAC TAC C–3' and antisense, 5'-GTA TCT CTT CCT CCT TTC CAC-3', with annealing temperature of 57°C and elongation time of 20 seconds. The cyclophilin 33A primers were sense, 5'-GCT GCG TTC ATT CCT TTT G-3' and antisense 5'-CTC CTG GGT CTC TGC TTT G -3', with annealing temperature of 60°C and elongation time of 10 seconds.

In situ hybridization

Paraffin embedded 5 µm breast tumor sections were analyzed for AAMP mRNA expression by in situ hybridization, according to a previously described protocol[13]. The plasmid pT7T3D-pac containing a 460-bp insert of the human AAMP cDNA (IMAGE consortium clone Id 789011, GenBank accession no. AA452988) was used as a template to generate sense and antisense probes. UTP ^{35}S-labelled riboprobes were synthesized using Riboprobe Systems (Promega, Madison, WI) according to manufacturer's instructions. Sense probes were used as controls. In situ hybridization and washing conditions were as described previously.[13] Sections were developed, after 5 weeks, using Kodak NTB-2 photographic emulsion and counterstained with Lee's stain.[13]

Levels of AAMP mRNA expression were assessed in the sections by microscopic examination using a semiquantitative approach.[13] Scores were obtained by estimating the average signal (on a scale of 0-3) and the proportion of ductal cells showing a positive signal (0, none; 0.1, less than 10%; 0.5, less than 50%; 1.0, greater than 50%). The intensity and proportion score were then multiplied to give an overall score

Immunohistochemistry

To assess the vascular pattern and vessel density in each of the DCIS samples, tumor sections were stained for CD34 antigen using a mouse anti-human monoclonal antibody to CD34 (Novo Castra Laboratories) and DAKO EnVision™ System, Peroxidase (DAKO Diagnositics Canada Inc.). 5µm thick sections were cut, mounted on Superfrost/Plus (Fisherbrand) slides, dried overnight at 37 °C, dewaxed in xylene (4 min) and rehydrated in graded alcohol. Blocking steps included peroxidase blocking reagent (0.03% hydrogen peroxide containing sodium azide) for 5 min to block endogenous peroxidase and Universal Blocker (DAKO Diagnostics Canada Inc.) for 15min to prevent non-specific staining. Tissue sections were incubated overnight at 4 °C with the primary antibody (1:50 dilution in Antibody Diluting Buffer) (DAKO Diagnositics Canada Inc.) after an initial incubation, with the same antibody, at 37 °C for 30mins. Following the overnight incubation, slides were treated with labeled Polymer (goat anti-rabbit and goat anti-mouse immunoglobulin in Tris-HCl buffer containing carrier protein and anti-microbial agent) for 30 min at RT. Finally, slides were incubated for 10 min with Substrate AEC Chromogen (3-amno-9-ethylcarbazole). Each incubation step was followed by 2 min. TBS wash x2. The slides were counterstained with hematoxylin, immersed in a bath of ammonia water and a cover slip was applied. Vascular endothelial cells were used as a positive internal control. Tumors were classified into stromal or rim type angiogenic patterns according to established criteria.[14] Microvascular density was assessed by comparing the density of vessels in the tumor area with that of adjacent normal tissue, where available, in each tumor section.

Statistics

The Mann-Whitney U test, the Fisher's exact test, and Spearman's correlation coefficient were used as appropriate. To determine the reproducibility of hybridization results with the GF-200 membrane, the normalized intensity values of all the 5,568 gene spots from duplicate hybridizations of the same RNA from

the hypoxic T47D cells were compared by linear regression and correlation analyses. For all tests, statistical significance was considered to be at the $p<0.05$ level (Graphpad prism, Graphpad Software, San Diego, CA.).

Results

Microdissection and microarray cDNA filters

The manual and laser assisted microdissection techniques proved to be equally effective in isolating ductal carcinoma cells from our DCIS specimens (Figure 1). We were able to isolate approximately 2 μg of total RNA from 14-17 10-μm frozen sections of the two tumors and the normal sample subjected to the laser assisted method of dissection, whereas the manual dissection method yielded approximately2-4 μg of total RNA from 6-10 20-μm frozen sections of tumor samples. The quality of hybridization signals produced by the labeled reverse transcribed total RNA obtained by both dissection techniques were also comparable as assessed by the exposure time needed to obtain equivalent signal intensities for analysis.

For the purpose of analysis, the six DCIS tumors with high or intermediate grade nuclear morphology and necrosis were grouped together and signals from each hybridized cDNA microarray membrane was compared with that for each of the four low-grade tumors (Figure 2A-C) giving 24 pairs of comparisons. After masking those transcripts showing expression levels lower than 10X background, we were left with approximately 1,500 cDNAs for our comparison analysis. The level of consistency of the array hybridization was examined in duplicate hybridizations of RNA from the T47D cell line to the GF-200 membrane, which demonstrated that a high level of consistency could be obtained (r^2 =0.88, data not shown). Nevertheless, to exclude the transcripts that might be differentially expressed due to individual differences between the tumors or due to variations in hybridization conditions between each experiment, we have included in our list of differentially expressed transcripts only those that were differentially expressed in at least 9 pairs of comparison (Table 2). This ensures only the inclusion of transcripts that were differentially expressed in at least three different high-grade/intermediate-grade DCIS compared with the low-grade DCIS samples. Using this selection criterion, 14 transcripts (7 named genes and 7 ESTs) were overexpressed in the low-grade DCIS compared with high-grade/intermediate grade DCIS, whereas 28 transcripts (18 named genes and 10 ESTs) were overexpressed in high-grade/intermediate-grade DCIS compared with the low-grade DCIS lesions.

To assess the relationship between patterns of gene expression and DCIS histology, a two-way pairwise average linkage cluster analysis was applied (with the Cluster program),[15] to organize the 42 consistently differentially expressed genes and tumors such that genes and tumors with similar expression patterns are clustered together and adjacent to one another.[15] Normalized gene expression data were logarithmically transformed and average linkage hierarchical clustering was performed using an uncentered correlation for both array and gene-clustering dimensions. The resulting phylogenetic tree (visualized with the Treeview program)[15] showed that, apart from one high-grade tumor, all the high- and intermediate-grade DCIS were more closely related to each other than they were to the low- grade DCIS lesions, which in turn were more related to a normal breast sample (Figure 2D). To identify genes that were both differentially expressed and that also might be associated with hypoxia, we compared the set of 28 cDNAs consistently overexpressed in high grade DCIS with 31 cDNAs found to be overexpressed in the T47D cell line subjected to hypoxia, and analyzed in parallel with the DCIS lesions using the same microarray filter. The AAMP gene was found to be common to both sets of differentially expressed genes and was assessed further. The mRNA for AAMP was differentially overexpressed in 11 pairs of tumor comparisons (mean 2.1 fold across two high-grade DCIS and one intermediate-grade DCIS compared with the low-grade DCIS lesions). AAMP was similarly overexpressed in T47D cells analyzed by array (mean 2.5 fold) subjected to hypoxic as compared to normoxic conditions (Figure 3A).

Real time quantitative RT-PCR for AAMP mRNA

AAMP mRNA expression was then assessed by RT-PCR in the 10 original microdissected tumors and subsequently in 28 additional non-microdissected DCIS samples. RT-PCR assay in one sample from the second DCIS cohort failed to yield a product with the control. AAMP expression in the microdissected ductal epithelium from the initial 10 DCIS tumors was higher in high- and intermediate-grade DCIS ($P=0.0095$, Mann Whitney) compared with the low-grade DCIS (Figure 3B). Among the 27 non-microdissected DCIS series, total AAMP expression within the tumor section tended to be associated with higher grade and necrosis. ($P=0.0427$, one-tailed, Mann Whitney) (Figure 3C). The overall expression level of AAMP in these 27 tumors did not show any association with either the progesterone receptor ($p=0.55$, Mann Whitney) or estrogen receptor ($p=0.37$, Mann Whitney) status of the tumors.

In situ hybridization (ISH)

AAMP mRNA expression was also assessed by *in situ* hybridization in all 37 tumors. The AAMP antisense probe showed stronger signals for AAMP mRNA in high-grade DCIS ducts and DCIS ducts with necrosis as compared with low-grade ducts, with variation from duct to duct in individual tumors. However there was no marked gradation in expression from luminal to stromal aspect of ducts with central necrosis. Expression was also observed in blood vessels in the stroma around the ducts (Figure 4). The *in situ* hybridization intensity score assigned to each tumor was based on an average of the epithelial expression assessed from all the ducts in the sections examined. AAMP expression detected by ISH showed some relationship to grade and necrosis, though this association was at best of borderline significance. AAMP ISH scores were higher in intermediate/high grade DCIS ($p=0.05$, Fisher's exact test) and in tumors with necrosis ($p=0.09$, Fisher's exact test) compared with low grade and those without necrosis, respectively. There was no association between the levels of AAMP detected by ISH and the estrogen receptor ($p=0.2$, Fisher's exact test) or progesterone receptor ($p= 0.5$, Fisher's exact test) status of tumors.

Immunohistochemistry

The two vascular patterns associated with DCIS lesions[14] were demonstrated among our samples using the CD34 antibody.

CD34 immunostaining data was available for 31 of the 37 tumors — two were not evaluated due to background staining and paraffin-embedded blocks had been exhausted for the remaining four. Eight of the 31 tumors (25.8%) for which CD34 immunostaining data was available had the stromal pattern of angiogenesis, whereas 17 (54.8%) had the rim type pattern and the remaining 6 tumors (19.4%) had a mixed stromal and rim pattern. Both the stromal and rim type angiogenic patterns were detected in high-grade tumors showing high levels of AAMP mRNA expression (Figure 4E and F). The circumference of ducts surrounded by microvessels in tumors with the rim pattern varied between 5% and 100%. Twenty-three of the 31 tumors that were assessable for CD34 immunostaining had a higher vascular density compared with adjacent normal tissue. No significant association was observed between the level of AAMP expression and vascular density or either of the angiogenic patterns observed.

Discussion

We have shown that while levels of gene expression are mostly similar between morphologically different DCIS, consistent differences in expression of a subset of genes can be identified between low-grade and high-grade DCIS. Amongst these differentially expressed genes the angio-associated-migratory protein (AAMP) was found to be expressed at a higher level by most high-grade DCIS and DCIS with necrosis and is also overexpressed in a breast cancer cell line subjected to hypoxia.

The two microdissection techniques employed in the present study were effective in isolating ductal cells from our samples. The laser-assisted microdissection, however, limits the thickness of sections for dissection to a maximum of 10 μm hence the need to dissect more sections in order to obtain a reasonable yield of RNA for hybridization. An alternate approach would be to dissect a minimum number of cells to obtain enough RNA that could serve as a template for transcriptional-based RNA amplification.[8] Our approach of dissecting cells from several sections, though seemingly burdensome, avoids the technical difficulties associated with RNA amplification.

cDNA microarray analysis is a powerful tool for the simultaneous analysis of large sets of genes and for the profiling of different tissue types. Studies have, however, shown that any single microarray output is subject to some variability and that pooling of data from replicates can provide a more reliable classification of gene expression.[16] In the present study, the small amount of RNA available from some of our microdissected samples precluded us from carrying out replicate array experiments on the same sample. We have, however, attempted to address the issue of variability by pooling data from multiple comparisons of different tumors and selecting only those transcripts that are consistently differentially expressed in our comparisons. This we believe may be more stringent than replicate experiments on the same sample.

Aside from the present study, there exists no gene expression profiling data comparing different grades of DCIS. However, similar to our findings, loss of heterozygosity (LOH)/allelic imbalance studies as well as comparative genomic hybridization (CGH) studies have shown that there are distinct genetic changes associated with the level of differentiation/grade and morphology of DCIS of the breast.[17, 18, 19] For example, LOH studies have shown that allelic imbalances on 16q and 17p are associated with low-grade or non–comedo DCIS, whereas allelic imbalances on 11q and 17q are associated with high-grade DCIS and/or the presence of comedo necrosis.[17, 18] In addition, these genetic changes were independent of the steroid receptor status of the tumors studied.[18] CGH studies also have demonstrated that losses of 16q material were seen most exclusively in well- and intermediately-differentiated DCIS, gains of 1q and losses of 11q material were seen in intermediately differentiated DCIS, whereas a higher frequency of amplifications of 17q12 and 11q13 were observed in poorly-differentiated DCIS.[19] Nevertheless, our present approach of using gene expression profiling has the advantage of identifying specific genes that may be important in the differentiation and progression of DCIS, whereas LOH and CGH studies can only identify larger genomic areas harboring several genes.

The hierarchical cluster algorithm operating on a very small set of samples (10 tumors and 1 normal breast sample) and expression data (42 genes and ESTs), was, apart from one high-grade tumor, able to group the DCIS lesions based on morphological classification. The high/intermediate tumors clustered together, whereas the low-grade and normal tissue clustered together (Figure 2D). The two low-grade tumors on the same limb of the phylogenetic tree as the higher-grade tumors separated from them further down the limb to cluster together. The genes and ESTs more highly expressed in the low grade-tumors all clustered together (cluster 1, figure 2D) and showed expression in the normal tissue sample, indicating that these transcripts were probably downregulated in the higher grade tumors showing low levels of expression. On the other hand, the transcripts showing a high level of expression in the higher grade tumors (clusters 2 and 3, figure 2D) all showed low levels of expression in the normal tissue as well as in the low-grade tumors (especially cluster 2), an indication that these transcripts were upregulated in these higher grade tumors.

Of interest among the cluster 1 genes are syndecan 4 (*SDC4*), metalloproteinase inhibitor 1, and *N-RAS*. In addition to the antiangiogenic function of metalloproteinase inhibitor 1, it shares with *SDC4* a role in cell-extracellular matrix interaction to inhibit invasion.[20] *N-RAS*, though able to induce anchorage independent growth, is unable to induce an invasive phenotype in breast cancer cells.[21] In addition, matrix metalloproteinases are known to play an important role in RAS-mediated invasiveness of human epithelial cells.[21]

Cluster 2 transcripts were of low expression in the low grade-tumors, whereas cluster 3 transcripts showed a moderate level of expression in the two low-grade tumors on the same limb of the phylogenetic tree as the higher grade tumors. Among the cluster 2 (figure 2D) genes, the kinases, *NDR* and *SGK*, and the phosphatase *PPP6C*, are serine/threonine specific in their catalytic activities and they have been implicated in cell cycle regulation.[22, 23, 24, 25] In addition, *NDR* and *PPP6C* regulate cell morphology,[23, 24] whereas SGK is able to prevent the fork head transcription factor (FKHRL1) induced apoptosis.[25] *UBE2I*, the human homolog of the yeast *UBC9* that mediates the transition from G1 to S-phase of the cell cycle[26], is known to interact with *RAD51* and *RAD52*, which are part of the *BRCA1* pathway,[27, 28] as well as with *TP53*.[27] *PRCC*, the translocation gene in papillary renal cell

carcinoma is speculated to function in the signaling cascade because it possesses a proline-rich domain.[29] Its recent association with graft-versus-host reaction[30] raises the possibility that it might play a role in inflammatory response that is frequently associated with high-grade comedo type DCIS. Up-regulation of desmocollin 2 (an intracellular desmosome junction protein) mRNA in some of the high-grade DCIS leaves room for one to speculate that loss of this gene may be important for the transition of DCIS to invasive tumor since a member of the desmocollin subfamily of the cadherin superfamily, desmocollin 3, has been reported to be downregulated in invasive breast cancer.[31]

Carbonic anhydrase II (*CA II*), a cytosolic carbonic anhydrase (CA) isoenzyme is highly expressed in several tumor types including gastric, colorectal, and pancreatic carcinomas[32, 33, 34] as well as malignant brain tumors.[35] and its expression has been shown to correlate with biological aggressiveness of rectal cancer.[34] Furthermore we have recently found that altered expression of other carbonic anhydrases, *CA IX and CAXII,* is a frequent occurrence between low and high grade DCIS [36]. The expression of these transmembrane isoenzymes is influenced by hypoxia and differentiation and they are expressed on different aspects of the breast cell membrane where they may act to influence the local extracellular pH surrounding the cancer cells thereby possibly creating a microenvironment conducive for tumor growth and spread.[37] In preliminary experiments we have not be able to demonstrate hypoxia regulation of *CA II* in breast cell lines (data not shown) and a similar role for the intracellular *CA II* in the progression of breast cancer remains to be determined. However, higher levels of the intracellular *CA II* in high grade DCIS may be part of coordinated changes in pH regulation, and by causing an increased generation of intracellular CO_2, *CA II* may facilitate the actions of the extracellular CA isoenzymes.[38]

The cluster 3 gene (figure 2D), human neutral amino acid transporter B (*SLC1A5*) was reported to show elevated levels of expression in multicellular hepatoma spheroids displaying central necrosis, similar to that seen in high grade DCIS, when compared with single cell suspension. This elevated level of *SLC1A5* mRNA paralleled changes in glutamine uptake by tumor cells in this model, suggesting that a hypoxic tumor microenvironment impacts on the uptake of specific nutrients.[39] *SMARCD2* is a component of the SWI/SNF complex that enhances transcriptional activation by the estrogen receptor and the retinoic acid receptor.[40] *CRABP2* (cluster 2, figure 2D) is another gene that is associated with the retinoic acid receptor. It regulates the access of retinoic acid to retinoic acid receptors in the nucleus and exerts a regulatory feed back control on the effect of retinoic acid on cell differentiation. Overexpression of *CRABP2* by DCIS would seem to suggest that retinoids might have a role to play in preventing DCIS progression. However, the effect of retinoid on cancer cells is dependent on dose and the expression of nuclear retinoid receptors.[41, 42, 43] The role of *CRABP2* and *SMARCD2* in the evolution of DCIS of the breast will require further investigation. One important goal of expression profiling is to develop a molecular based classification system for tumors.[44, 45] However, further expression-profiling studies of a larger series of DCIS of the breast as well as proper identification of the genes represented by the ESTs we have identified is necessary to give insight into how the clustering we have observed may be useful in developing a molecular signature for DCIS of the breast.

AAMP was first isolated from a human melanoma cell line as a motility-associated cell protein and was found to be expressed strongly in endothelial cells, cytotrophoblast, and poorly differentiated colon adenocarcinoma cells found in lymphatics.[46] The AAMP protein has two immunoglobulin domains and six WD40 repeat domains, suggesting possible membership in both the immunoglobulin superfamily and the WD40 repeat family of proteins.[46, 47] Immunoglobulin superfamily members are binding proteins that function extracellularly as adhesion proteins.[47, 48] The WD40 repeat proteins — so named because they are characterized by a cluster of repeated sequences, each repeating around 40 amino acids in length and usually ending in tryptophan-aspartate (WD) — regulate cellular functions such as cell fate determination, gene transcription, mRNA modification, transmembrane signaling, vesicle fusion, and cell division.[49, 50] The presence of both the immunoglobulin type domains and WD40 repeats sequence motifs in AAMP implies a multifunctional role for this protein.[47] Experimental evidence to date suggests that AAMP may play a role in cell motility and angiogenesis. This has been examined and demonstrated in endothelial cells.[51] However, we and others have shown that AAMP is expressed by other cells and this property, which may be related to the fact that it shares a common epitope with α-actinin and a fast twitch skeletal muscle fiber protein,[47] is not necessarily restricted to endothelial cells and angiogenesis.[52] Of possible interest is another related WD40 repeat protein, the MAPK activator with WD repeats (MAWD) protein, that has been implicated in breast tumor progression.[53]

There is ample evidence that the switch of a tumor to an angiogenic phenotype is crucial for progression and metastasis, therefore, increased angiogenesis in DCIS could precede the switch to an invasive phenotype and be a marker of poor prognosis.[14, 54] We attempted — based on the hypothesis that DCIS cells expressing a high level of AAMP mRNA, and subsequently the protein, are likely to have a dense rim of microvessels around them — to correlate the different angiogenic patterns within DCIS with the level of expression of AAMP mRNA. Although our analysis did not show any association between the level of expression of AAMP mRNA and any of the angiogenic patterns associated with DCIS of the breast, this does not completely exclude the fact that AAMP may play a role in endothelial cell migration and angiogenesis in DCIS. Several reasons may account for our inability to demonstrate a relationship between AAMP mRNA expression within the neoplastic ductal epithelium of DCIS and angiogenic pattern. First is the small number of DCIS tumors, especially low-grade tumors available for this study. Second is the complexity of the angiogenic process itself; other angiogenic factors induced by hypoxia, for example, VEGF and Endothelin1 may also come into play making it difficult to correlate only one factor with the angiogenic pattern. Indeed, previous attempts to correlate angiogenic patterns in DCIS with known angiogenic factors have resulted in conflicting reports; for example, both the stromal and rim angiogenic patterns have been correlated with thymidine phosphorylase expression in DCIS in different reports.[55, 56] A third factor is that AAMP mRNA expression levels may not necessarily correlate with the level of AAMP protein and this is

compounded by the additional source of expression of AAMP by endothelial cells in the stroma. This extra-epithelial source of AAMP probably accounts for the inability to fully reproduce the AAMP-grade/necrosis association demonstrated in our microdissected series in the non-microdissected cohort and may play an important role in determining the pattern of angiogenesis. This, however, underscores the usefulness of microdissection techniques in profiling ubiquitously expressed genes from specific cell types in a heterogeneous tissue environment.

Necrosis is believed to represent the extreme manifestation of hypoxia in tissues.[57] The finding that AAMP is induced in-vitro in a breast cell line subjected to hypoxia and also in-vivo in DCIS associated with necrosis, suggest that AAMP may be a hypoxia regulated gene that may influence growth and survival of DCIS. However, necrosis may be attributable to other causes and alternative stresses may influence gene expression in cells subjected to hypoxia.[58] Regulation by hypoxia in-vitro may also not be the only or dominant factor in the complex in-vivo environment.[36] Further work will be required to establish if AAMP expression is directly regulated by mediators of hypoxia response and to confirm the observation here that expression in-vivo may be indicative of hypoxia.

In summary, we have shown that high grade DCIS can be distinguished from low grade DCIS by the pattern of gene expression and that upregulation of AAMP, a hypoxia regulated gene in a breast cell line that has previously been associated with angiogenesis and tumor progression, is also associated with necrosis in DCIS. The previous observation that AAMP can also be expressed in metastatic adenocarcinoma[46] coupled with the present findings indicate that AAMP may be involved in more than one stage of tumor progression.

References

1. Ernster VL, Barclay J: Increase in ductal carcinoma *in situ* (DCIS) of breast in relation to mammography: a dilemma. J Natl Cancer Inst Monogr 1997, 22:151-156
2. Elston CW, Ellis IO, Pinder SE: Prognostic factors in invasive carcinoma of the breast. Clin Oncol 1998, 10:14-17
3. Silverstein MJ, Lagios MD, Craig PH, Waisman JR, Lewinsky BS, Colburn WJ, Poller DN: A prognostic index for ductal carcinoma in situ of the breast. Cancer 1996, 77:2267-2274
4. Sneige N, Lagios MD, Schwarting R, Colburn W, Atkinson E, Weber D, Sahin A, Kemp B, Hoque A, Risin S, Sabichi A, Boone C, Dhingra K, Kelloff G, Lippman S: Interobserver reproducibility of the Lagios nuclear grading system for ductal carcinoma *in situ*. Human Pathol 1999, 30:257-262
5. Fisher ER, Dignam J, Tan-Chiu E, Costantino J, Fisher B, Paik S, Wolmark N: Pathologic findings from the National Surgical Adjuvant Breast Project (NSABP) eight-year update of Protocol B-17: intraductal carcinoma. Cancer 1999, 86:429-438
6. Sgroi DC, Teng S, Robinson G, LeVangie R, Hudson JR, Elkaloun AG: In vivo gene expression profile analysis of human breast cancer progression. Cancer Res 1999, 59:5656-5661
7. Hiller T, Snell L, Watson PH: An approach for microdissection/RT-PCR analysis of gene expression in pathologically defined frozen tissue sections. Biotechniques 1996, 21:38-42
8. Luzzi V, Holtschlag V, Watson MA: Expression profiling of ductal carcinoma *in situ* by laser capture microdissection and high-density oligonucleotide arrays. Am J Pathol 2001, 158:2005-2010
9. Watson P, Snell L, Parisien M: The role of a tumor bank in translational research. Canadian Medical Association Journal 1996, 15:281-283
10. Silverstein MJ, Poller DN, Waisman JR, Colburn WJ, Barth A, Gierson ED, Lewinsky B, Gamagani P, Slamon DJ: Prognostic classification of breast ductal carcinoma-in-situ. Lancet 1995, 345:1154-1157
11. Arcturus Engineering, Inc: http://www.arctur.com/technology/protocols.html
12. Chomczynski P, Sacchi N: Single-step method of RNA isolation by acid guanidinium thiocyanate-phenol-chloroform extraction. Anal Biochem 1987, 162:156-159
13. Leygue E, Snell L, Dotzlaw H, Hole K, Troup S, Hiller-Hitchcock T, Murphy LC, Watson PH: Mammoglobin, a potential marker of breast cancer nodal metastasis. J Pathol 1999, 189:28-33
14. Engels K, Fox SB, Whitehouse RM, Gatter KC, Harris AL: Distinct angiogenic patterns are associated with high-grade *in situ* ductal carcinomas of the breast. J Pathol 1997, 181:207-212
15. Eisen MB, Spellman PT, Brown PO, Botstein D: Cluster analysis and display of genome-wide expression patterns. Proc Natl Acad Sci U S A 1998, 95:14863-14868
16. Lee MLT, Kuo FC, Whitmore GA, Sklar J: Importance of replication in microarray gene expression studies: statistical methods and evidence from repetitive cDNA hybridizations. Proc Natl Acad Sci U S A 2000, 97:9834-9839
17. O'Connell P, Pekkel V, Fuqua SAW, Osborne K, Clark G, Allred DC: Analysis of loss of heterozygosity in 399 premalignant breast lesions at 15 genetic loci. J Natl Cancer Inst 1998, 90:697-703
18. Ando Y, Iwase H, Ichihara S, Toyoshima S, Nakamura T, Yamashita H, Toyama T, Omoto Y, Karamatsu S, Mitsuyama S, Fujii Y, Kobayashi S: Loss of heterozygosity and microsatellite

instability in ductal carcinoma in situ of the breast. Cancer Lett 2000, 156:207-214
19. Buerger H, OtterbachF, Simon R, Poremba C, Diallo R, Decker T, Riethdorf L, Brinkschmidt C, Dockhorn-Dworniczak B, Boecker W: Comparative genomic hybridization of ductal carcinoma in situ of the breast-evidence of multiple genetic pathways. J Pathol 1999, 187:396-402
20. Sanderson RD: Heparan sulfate proteoglycans in invasion and metastasis. Semin Cell Dev Biol 2001, 12:89-98
21. Moon A, Kim MS, Kim TG, Kim SH, Kim HE, Chen YQ, Kim HR: H-ras, but not N-ras, induces an invasive phenotype in human breast epithelial cells: a role for MMP-2 in the H-ras-induced invasive phenotype. Int J Cancer 2000, 85:176-181
22. Millward T, Cron P, Hemmings BA: Molecular cloning and characterization of a conserved nuclear serine(threonine) protein kinase. Proc Natl Acad Sci U S A 1995, 92:5022-5026
23. Millward TA, Hess D, Hemmings BA: Ndr protein kinase is regulated by phosphorylation on two conserved sequence motifs. J Biol Chem 1999, 274:33847-33850
24. Bastians H, Ponstingl H: The novel human protein serine/threonine phosphatase 6 is a functional homologue of budding yeast Sit4p and fission yeast ppe1, which are involved in cell cycle regulation. J Cell Sci 1996, 109:2865-2874
25. Brunet A, Park J, Tran H, Hu LS, Hemmings BA, Greenberg ME: Protein kinase SGK mediates survival signals by phosphorylating the forkhead transcription factor FKHRL1 (FOXO3a). Mol Cell Biol 2001, 21: 952-965
26. Watanabe TK, Fujiwara T, Kawai A, Shimizu F, Takami S, Hirano H, Okuno S, Ozaki K, Takeda S, Shimada Y, Nagata M, Takaichi A, Takahashi E, Nakamura Y, Shin S: Cloning, expression, and mapping of UBE2I, a novel gene encoding a human homologue of yeast ubiquitin-conjugating enzymes which are critical for regulating the cell cycle. Cytogenet Cell Genet 1996, 72:86-89
27. Shen Z, Pardington-Purtymun PE, Comeaux JC, Moyzis RK, Chen DJ: Associations of UBE2I with RAD52, UBL1, p53, and RAD51 proteins in a yeast two-hybrid system. Genomics 1996, 37:183-186
28. Welcsh PL, Owens KN, King MC: Insights into the functions of BRCA1 and BRCA2. Trends Genet 2000, 16:69-74
29. Weterman MJ, van Groningen JJ, Jansen A, van Kessel AG: Nuclear localization and transactivating capacities of the papillary renal cell carcinoma-associated TFE3 and PRCC (fusion) proteins. Oncogene 2000, 19:69-74
30. Wakui M, Yamaguchi A, Sakurai D, Ogasawara K, Yokochi T, Tsuchiya N, Ikeda Y, Tokunaga K: Genes highly expressed in the early phase of murine graft-versus-host reaction. Biochem Biophys Res Commun 2001, 282:200-206
31. Klus GT, Rokaeus N, Bittner ML, Chen Y, Korz DM, Sukumar S, Schick A, Szallasi Z: Down-regulation of the desmosomal cadherin desmocollin 3 in human breast cancer. Int J Oncol 2001, 19:169-174
32. Parkkila S, Parkkila AK, Juvonen T, Lehto VP, Rajaniemi H: Immunohistochemical demonstration of the carbonic anhydrase isoenzymes I and II in pancreatic tumours. Histochem J 1995, 27:133-138
33. Pastorekova S, Parkkila S, Parkkila AK, Opavsky R, Zelnik V, Saarnio J, Pastorek J: Carbonic anhydrase IX, MN/CA IX: analysis of stomach complementary DNA sequence and expression in human and rat alimentary tracts. Gastroenterology 1997, 112:398-408
34. Bekku S, Mochizuki H, Yamamoto T, Ueno H, Takayama E, Tadakuma T: Expression of carbonic anhydrase I or II and correlation to clinical aspects of colorectal cancer. Hepatogastroenterology 2000, 47:998-1001
35. Parkkila AK, Herva R, Parkkila S, Rajaniemi H: Immunohistochemical demonstration of human carbonic anhydrase isoenzyme II in brain tumours. Histochem J 1995, 27:974-982
36. Wykoff CC, Beasley N, Watson PH, Campo L, Chia SK, English R, Pastorek J, Sly WS, Ratcliffe P, Harris AL: Expression of hypoxia-inducible and tumor-associated carbonic anhydrase in ductal carcinoma in situ of the breast. Am J Pathol 2001, 158:1011-1019
37. Ivanov SV, Kuzmin I, Wei MH, Pack S, Geil L, Johnson BE, Stanbridge EJ, Lerman MI: Down-regulation of transmembrane carbonic anhydrases in renal cell carcinoma cell lines by wild-type von Hippel-Lindau transgenes. Proc Natl Acad Sci U S A 1998, 95:12596-12601
38. Parkkila S, Rajaniemi H, Parkkila AK, Kivela J, Waheed A, Pastorekova S, Pastorek J, Sly WS: Carbonic anhydrase inhibitor suppresses invasion of renal cancer cells in vitro. Proc Natl Acad Sci U S A 2000, 97:2220-2224
39. Pawlik TM, Souba WW, Sweeney TJ, Bode BP: Amino acid uptake and regulation in multicellular hepatoma spheroids. J Surg Res 2000, 9:15-25
40. Chiba H, Muramatsu M, Nomoto A, Kato H: Two human homologues of Saccharomyces cerevisiae SWI2/SNF2 and Drosophila brahma are transcriptional coactivators cooperating with the estrogen receptor and the retinoic acid receptor. Nucleic Acids Res 1994, 22:1815-1820

41. Lotan R: Retinoids and chemoprevention of aerodigestive tract cancers. Cancer Metastasis Rev 1997, 16:349-356
42. Wan H, Oridate N, Lotan D, Hong WK, Lotan R: Overexpression of retinoic acid receptor beta in head and neck squamous cell carcinoma cells increases their sensitivity to retinoid-induced suppression of squamous differentiation by retinoids. Cancer Res 1999, 59:3518-3526
43. Uchida D, Kawamata H, Nakashiro K, Omotehara F, Hino S, Hoque MO, Begum NM, Yoshida H, Sato M, Fujimori T: Low-dose retinoic acid enhances in vitro invasiveness of human oral squamous-cell-carcinoma cell lines. Br J Cancer 2001, 85:122-128
44. Perou CM, Jeffrey SS, van de Rijn M, Rees CA, Eisen MB, Ross DT, Pergamenschikov A, Williams CF, Zhu SX, Lee JC, Lashkari D, Shalon D, Brown PO, Botstein D: Distinctive gene expression patterns in human mammary epithelial cells and breast cancers. Proc Natl Acad Sci USA 1999, 9212-9217
45. Perou CM, Sorlie T, Eisen MB, van de Rijn M, Jeffrey SS, Rees CA, Pollack JR, Ross DT, Johnsen H, Akslen LA, Fluge O, Pergamenschikov A, Williams C, Zhu SX, Lonning PE, Borresen-Dale AL, Brown PO, Botstein D: Molecular portraits of human breast tumours. Nature 2000, 406:747-752
46. Beckner ME, Krutzsch HC, Stracke ML, Williams ST, Gallardo JA, Liotta LA: Identification of a new immunoglobulin superfamily protein expressed in blood vessels with a heparin-binding consensus sequence. Cancer Res 1995, 55:2140-2149
47. Beckner ME, Krutzsch HC, Klipstein S, Williams ST, Maguire JE, Doval M, Liotta LA: AAMP, a newly identified protein, shares a common epitope with α-actinin and a fast skeletal muscle fibre protein. Exp Cell Res 1996, 225:306-314
48. Okagaki T, Wber FE, Fischman DA, Vaughan KT, MikawaT, Reinach FC: The major myosin-binding domain of skeletal muscle MyBP-C (C protein) resides in the COOH-terminal, immunoglobulin C2 motif. J Cell Biol 1993, 123:619-626
49. Van de Voorn L, Ploegh HL: The WD-40 repeat. FEBS Lett 1992, 307:131-134
50. Neer EJ, Schmidt CJ, Namburipad R, Smith FT: The ancient regulatory-protein family of WD-repeat proteins. Nature 1994, 371:297-300
51. Beckner ME, Liotta LA: AAMP, a conserved protein with immunoglobulin and WD40 domains, regulates endothelial tube formation in vitro. Lab Invest 1996, 75:97-107
52. Beckner ME, Peterson VA, Moul DE: Angio-associated migratory protein is expressed as an extracellular protein by blood-vessel-associated mesenchymal cells. Microvasc Res 1999, 57:347-352
53. Matsuda S, Katsumata R, Okuda T, Yamamoto T, Miyazaki K, Senga T, Machida K, Thant AA, Nakatsugawa S, Hamaguchi M: Molecular cloning and characterization of human MAWD, a novel protein containing WD-40 repeats frequently overexpressed in breast cancer. Cancer Res 2000, 60:13-17
54. Folkman J, Watson K, Ingber D, Hanahan D: Induction of angiogenesis during the transition from hyperplasia to neoplasia. Nature 1989, 339:58-61
55. Lee AHS, Dublin EA, Bobrow LG: Angiogenesis and expression of thymidine phosphorylase by inflammatory and carcinoma cells in ductal carcinoma *in situ* of the breast. J Pathol 1999, 187:285-290
56. Engels K, Fox SB, Whitehouse RM, Gatter KC, Harris AL: Up-regulation of thymidine phosphorylase expression is associated with a discrete pattern of angiogenesis in ductal carcinomas *in situ* of the breast. J Pathol 197, 182:414-420
57. Leek RD, Landers RJ, Harris AL, Lewis CE: Necrosis correlates with high vascular density and focal macrophage infiltration in invasive carcinoma of the breast. Br J Cancer 1999, 79:991-995
58. Bos R, Zhong H, Hanrahan CF, Mommers EC, Semenza GL, Pinedo HM, Abeloff MD, Simons JW, van Diest PJ, van der Wall E: Levels of hypoxia-inducible factor-1 alpha during breast carcinogenesis. J Natl Cancer Inst 2001, 93:309-314

Table 1a. Morphology, AAMP expression, and steroid receptor status of 10 microdissected DCIS of the beast

LAB#	Nuclear grade	%Necrosis[1]	AAMP RT-PCR	ER status[2]	PR status[3]
12024	HG	75	0.21	-	-
10046	HG	25	0.13	-	-
13110	HG	20	0.34	+	-
13049	HG	20	0.31	+	+
11970	IG	75	0.31	-	-
11722	IG	50	0.11	+	+
10047	LG	10	0.10	+	+
11161	LG	10	0.09	+	+
9062	LG	0	0.10	+	+
10919	LG	0	0.11	+	+

Table 1b. Morphology, AAMP expression, and steroid receptor status of 27 DCIS of the beast

LAB#	Nuclear grade	%Necrosis[1]	AAMP RT-PCR	ER status[2]	PR status[3]
12340	HG	100	1.30	-	-
13115	HG	100	0.63	-	+
15200	HG	90	1.03	+	-
11972	HG	75	0.53	-	-
12054	HG	75	0.56	-	-
12485	HG	75	0.39	+	-
15242	HG	75	0.37	-	+
11202	HG	75	0.72	+	+
12354	HG	75	0.34	+	+
13523	HG	75	0.39	+	+
13423	HG	50	0.34	+	-
12338	HG	50	1.08	+	+
14815	HG	25	0.58	+	+
15134	HG	25	0.49	+	+
13005	HG	20	0.46	-	-
11442	HG	0	1.33	+	+
15344	IG	75	0.55	+	+
11285	IG	50	0.72	+	-
14902	IG	25	0.74	-	+
15108	IG	25	0.46	+	+
10351	IG	10	0.38	+	+
15439	IG	5	0.32	+	+
12438	IG	0	0.64	-	-
12571	IG	0	0.44	+	+
13686	LG	0	0.44	+	+
15284	LG	0	0.47	+	+
15010	IG	20	1.22	+	+

Table 2a. Classification of genes consistently upregulated in high/intermediate-grade DCIS compared with low-grade DCIS of the breast

Accession Number	Gene name	Gene symbol	Average fold change	S.D.	Fold change range	Number of comparisons[1]
Cell Adhesion/Cell motility						
AA428778	Human T cell leukemia LERK-2 (EPLG2)	*EFNB1*	6.9	5.3	2.1-10.0	12
AA452988	Homo sapiens angio-associated migratory cell protein (AAMP)	*AAMP*	2.1	0.2	1.8-2.4	11
AA074677	Human desmocollin-2	*DSC3*	2.1	0.2	1.9-2.4	10
Cell cycle/Cell proliferation regulator						
H73724	Cyclin-dependent kinase 6	*CDK6*	4.4	2.7	2.1-10.3	12
R25074	Human transmembrane 4 superfamily protein (SAS)	*SAS*	8.1	7.1	2.3-14.0	12
Kinase/Phosphatase						
AA521346	Ndr protein kinase	*NDR*	2.6	0.6	2.0-4.0	13
AA486082	Putative serine/threonine protein kinase	*SGK*	3	0.7	2.0-3.6	12
AA521083	Protein phosphatase 6	*PPP6C*	2.6	0.4	2.1-3.2	12
Transcription factor						
AA488233	H.sapiens mRNA for prcc protein	*PRCC*	2.9	0.4	2.2-3.5	12
AA478436	Human SWI/SNF complex 60 KDa subunit (BAF60b)	*SMARCD2*	2.2	0.3	1.9-2.6	9
Receptors and signal transduction						
W39343	V-ral simian leukemia viral oncogene homolog B (ras related; GTP binding protein)	*RALB*	9.5	2.2	6.5-13.5	12
AA598508	Cellular retinoic acid-binding protein 2	*CRABP2*	2.1	0.3	1.8-2.6	9
Cellular Metabolism						
H23187	Carbonic anhydrase II	*CA2*	2.3	0.2	2.0-2.7	9
AA487197	Ubiquitin-conjugating enzyme E2I (homologous to yeast UBC9)	*UBE2I*	2.3	0.4	1.8-2.9	9
AA070997	Proteasome (prosome, macropain) subunit, beta type, 6	*PSMB6*	2.1	0.2	1.8-2.5	9
Molecule Transporter						
T70098	Human neutral amino acid transporter B	*SLC1A5*	6.6	5.9	1.9-10.6	12
RNA binding and RNA processing						
AA490991	Homo sapiens HnRNP F	*HNRNPF*	2.1	0.2	1.8-2.6	11
HUGE						
H75699	KIAA0297 gene	*KIAA0297*	7	5	2.4-17.8	9

Table 2b. Classification of genes consistently upregulated in low-grade DCIS compared with high/intermediate-grade DCIS of the breast

Accession number	Gene name	Gene symbol	Average fold change	S.D.	Fold change range	Number of comparisons[1]
DNA binding						
N54596	Human Krueppel-related zinc finger protein (H-plk)	*H-PLK*	2.4	0.4	1.9-2.9	12
AA452725	Nucleobindin precursor	*NUCB1*	2	0,2	1.8-2.4	9
Cell surface protein						
AA148736	Syndecan 4 (amphiglycan, ryudocan)	*SDC4*	2.4	0.5	1.8-3.2	11
Translation regulation						
R86304	Eukaryotic translation initiation factor 2B	*EIF2B2*	1.9	0.1	1.8-2.1	9
Cell cycle/Cell proliferation regulator						
AA504682	Neuroblastoma RAS viral (v-ras) oncogene homolog	*NRAS*	2.2	0.3	1.8-2.8	12
R82299	S-adenosylmethionine decarboxylase 1	*AMD1*	2.2	0.2	1.9-2.7	11
Transcription factor						
AA504682	SNF2 (sucrose nonfermenting, yeast, homolog)-like 1	*SMARCA1*	2.3	0.4	1.8-3.0	12

Table & Figure Legends

Table 1

[1]Percentage of ducts with necrosis

[2]ER less than 3.0 fmol/mg protein = -; ER more than 3.0 fmol/mg protein = +ve

[3]PR less than 15.0 fmol/mg protein = - ; PR more than 15.0 fmol/mg protein = +ve

Table 2

[1]Numbers of comparisons (maximum number 24) between pairs of DCIS that show differential expression for a particular gene (i.e., comparisons between each of 6 intermediate/high-grade DCIS with each of 4 low-grade DCIS).

Figure 1. Laser-capture microdissection of duct cells from H&E stained frozen section (10 μm) of a high-grade DCIS of the breast. (A) Three ducts (1, 2 and 3) identified for dissection (B) Ducts after dissection (C) Cells from duct successfully captured and transferred.

Figure 2. A-C, Differential gene expression analysis employing the GF200 cDNA array membrane and the Pathways 2.01 analysis software. Hybridization of ^{33}P-labeled reverse transcribed RNA from a high grade DCIS (A) and a low grade DCIS (B) to Human GF200 cDNA array membranes. (C) Portion of synfilter generated by the Pathways 2.01 analysis software from membranes A and B. Yellow spots show genes expressed equally by both samples, green spots; genes differentially expressed by high grade tumor and red spots; genes differentially expressed by low grade tumor. AAMP is represented by green spot sorrounded by blue rectangle. D, Cluster map and phylogenetic tree resulting from an average-linkage cluster analysis of the 42 differentially expressed genes identified in our series of DCIS. Each color patch represents the expression level of the associated gene in that tissue sample with a continuum of expression from bright green (lowest) to bright red (highest). N50 is a normal breast sample, HG, high-grade DCIS; LG, low-grade DCIS; IG, intermediate grade DCIS; 1, cluster of genes and ESTs differentially expressed in low-grade DCIS; 2 and 3, cluster of genes and ESTs differentially expressed in intermediate/high-grade DCIS.

Figure 3. A, comparative ratio analysis of AAMP by real-time quantitative RT-PCR and cDNA array hybridization of hypoxic and normoxic T47D cell line. The PCR data is an average of triplicate reactions, and the array is an average of duplicate hybridization comparison. B, AAMP mRNA expression detected by RT-PCR shown relative to grade and necrosis in 10 microdissected DCIS samples. (necrosis +ve, high-grade DCIS or DCIS with >10% necrosis. n=6; necrosis –ve, non-high-grade DCIS with <10% necrosis. n=4. C, AAMP mRNA expression detected by RT-PCR shown relative to grade and necrosis in 27 DCIS of the breast. (necrosis +ve, high-grade DCIS or DCIS with >10% necrosis. n=21; necrosis –ve, non-high-grade DCIS with <10% necrosis. n=6.

Figure 4. In situ hybridization with ^{35}S-labeled antisense probe for AAMP, showing strong signals for AAMP in high-grade ducts with necrosis (A and B) and weaker signals in low-grade DCIS (D). There were no signals with the sense probe (C), x 40. Immunohistochemistry with antibody against the CD34 antigen showing the rim (arrows, E) and stromal (F) patterns of angiogenesis in tumors A and B, respectively, X 100.

Figure 1

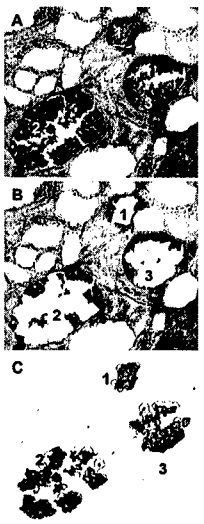

Figure 2

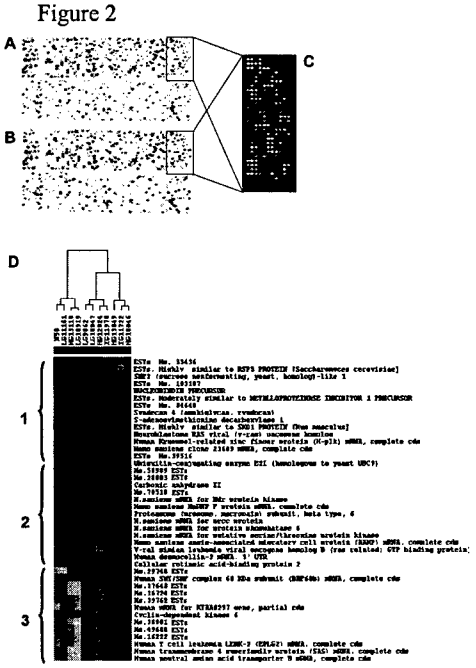

Figure 3

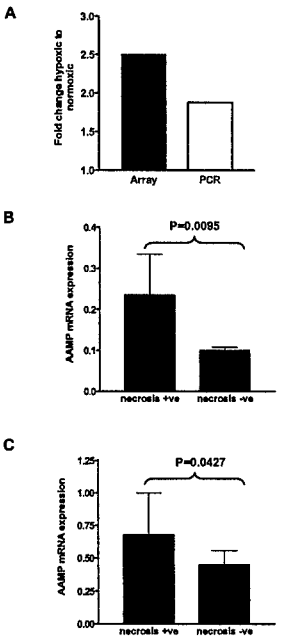

Figure 4

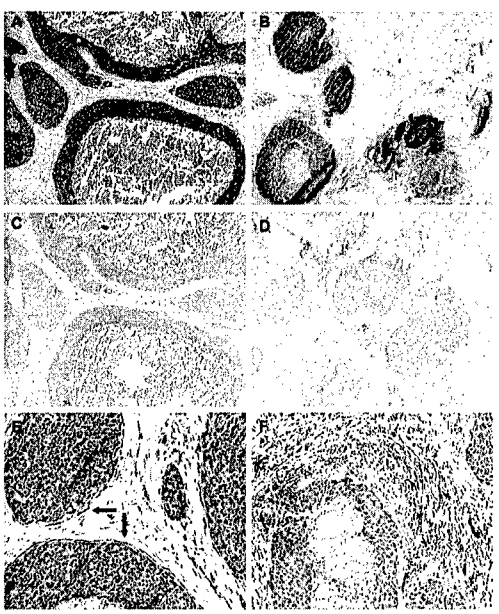

PERGAMON

The International Journal of Biochemistry & Cell Biology 30 (1998) 567–571

The International Journal of Biochemistry & Cell Biology

Molecules in focus

Psoriasin (S100A7)

Peter H. Watson[a,*], Etienne R. Leygue[a], Leigh C. Murphy[b]

[a]Department of Pathology, University of Manitoba, Winnipeg, Manitoba, R3E OW3, Canada
[b]Department of Biochemistry and Molecular Biology, University of Manitoba, Winnipeg, Manitoba, R3E OW3, Canada

Received 6 February 1997; accepted 9 June 1997

Abstract

Psoriasin (S100A7) is a relatively new member of the S100 gene family that is located within the S100 gene cluster on chromosome 1q21 and shares the typical calcium binding domains that define this family of proteins. It was first identified as a 11.4 kDa cytoplasmic and secreted protein isolated from skin involved by psoriasis, which can be induced in cultured squamous epithelial cells. It is now known to be expressed by both normal cultured and malignant keratinocytes and malignant breast epithelial cells within ductal carcinoma *in situ*, suggesting an association with abnormal pathways of differentiation. Current evidence supports a role in the pathogenesis of inflammatory skin disease, as a chemotactic factor for hematopoietic cells, and a role in early stages of breast tumor progression in association with the development of the invasive phenotype. While therapeutic potential as a target for modulation of the inflammatory response in psoriasis awaits further studies, potential clinical applications already include a role as a detection marker for squamous cell carcinoma and a diagnostic marker to distinguish *in situ* from invasive breast cancer cells.

Keywords: Psoriasin; S100; Chemotaxis; Invasion; Breast cancer; Bladder cancer

1. Introduction

Psoriasin is a relatively new member of the S100 gene family that was first identified by [9] as a 11.4 kDa protein induced in squamous epithelial cells of the epidermis isolated from skin involved by psoriasis. Psoriasin shares homology and chromosomal proximity with other members of the S100 gene family, justifying classification as S100A7. The S100 genes encode small cytoplasmic and secreted proteins that share EF-hand helix-loop-helix domains that are important for their function as calcium binding proteins [14]. Broad roles have been proposed for these genes in cell growth, differentiation and determination of cell shape.

2. Structure

The Psoriasin gene maps to chromosome 1q21.2-q22, within a region that encompasses at least 12 of the S100 gene family (see Fig. 1) and several other epidermal differentiation genes [1, 13]. Although the gene has not been sequenced it is likely that it conforms to the organization of adjacent S100 genes. In most

* Corresponding author.

1357-2725/98/$19.00
PII: S1357-2725(97)00066-6

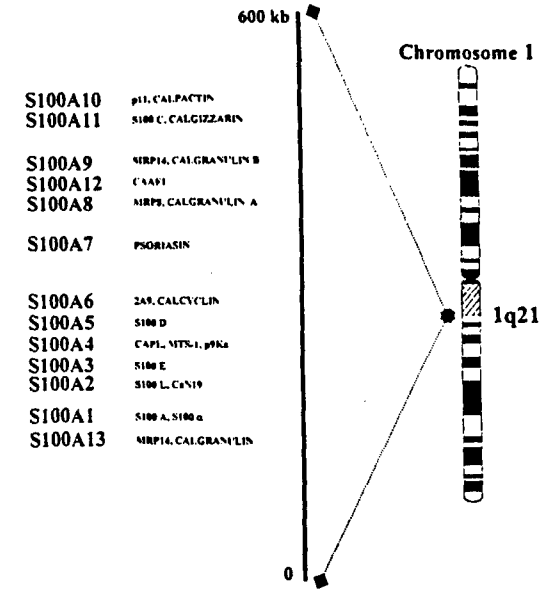

Fig. 1. Diagram of physical map of the S100 gene cluster on chromosome 1q21. Current nomenclature and previous names/synonyms are given on the right and genes are ordered by approximate relative locations.

cases, these possess a simple three exon/two intron structure, with the first exon contributing most of the 5′ untranslated region to the mRNA and the second and third exons covering the coding sequences and contributing one of the two EF-hand-like calcium binding motifs that characterize these proteins. The Psoriasin protein includes an *N*-terminal calcium binding signature that lacks the spacing provided by an additional three amino acids when compared to other S100 genes and a canonical *C*-terminal EF-hand motif. It shares closest overall homologies at the amino acid level to two newly described S100 genes [4], bovine CAAF2 (77%) and CAAF1/S100A12 (63%), as well as recognizable association with MRP8/S100A8 (32%) and p11/S100A10 (23%).

3. Biological function

Psoriasin expression is restricted to keratinocytes and breast epithelial cells, in contrast to the overlapping pattern of the related subgroup of S100 genes A8, A9 and A12, which are also expressed in hematopoietic cells of myeloid lineage. It is known to be both a cytoplasmic and secreted protein that is upregulated in keratinocytes in response to calcium and retinoic acid and during abnormal pathways of differentiation in culture, where Psoriasin is amongst the most highly induced proteins [5]. While the normal function of this protein is unclear it might be deduced from its close relatives. The S100 proteins are believed to influence calcium mediated signal transduction and cellular events through direct target protein interactions, as opposed to a function as mere storage buffers. In this capacity, targets for related S100 proteins include intermediate filaments (S100A8) and annexin (S100A10), implying a role in modulation of cell shape/cytoskeletal architecture or intracellular signal transduction [14]. Heterodimers of the S100A8 and A9 proteins may also have an intracellular activity (as a calcium regulator and/or inhibitor of casein kinase activity) in addition to a complex extracellular activity, both as a migration inhibition factor and a chemotactic factor for monocytes and granulocytes under different circumstances [3]. In the case of Psoriasin, the association with psoriasiform hyperplasia of the skin and its known regulation suggests a role in keratinocyte differentiation. However, Psoriasin may also act as a chemotactic agent [6] to stimulate the neutrophil and $CD4^+$ T lymphocyte infiltration of the epidermis that characterizes psoriasis. These putative functions are summarized in Fig. 2.

4. Role in pathology

The monogram Psoriasin endorses its association with psoriasis and high levels of expression in psoriasiform epidermal hyperplasia adjacent to traumatic skin ulcers have also been observed. However, the gene is clearly also expressed under conditions of abnormal epithelial differentiation and is secreted by neoplastic keratinocytes in carcinoma of the bladder [2]. More recently, Psoriasin and the related S100 A8 and A9 pro-

teins have also been found in other abnormal epithelia, including neoplastic breast ductal epithelium and bronchial epithelium in individuals with cystic fibrosis.

5. Role in breast cancer

Disruption of calcium signalling pathways has been implicated as a central mechanism in tumor-

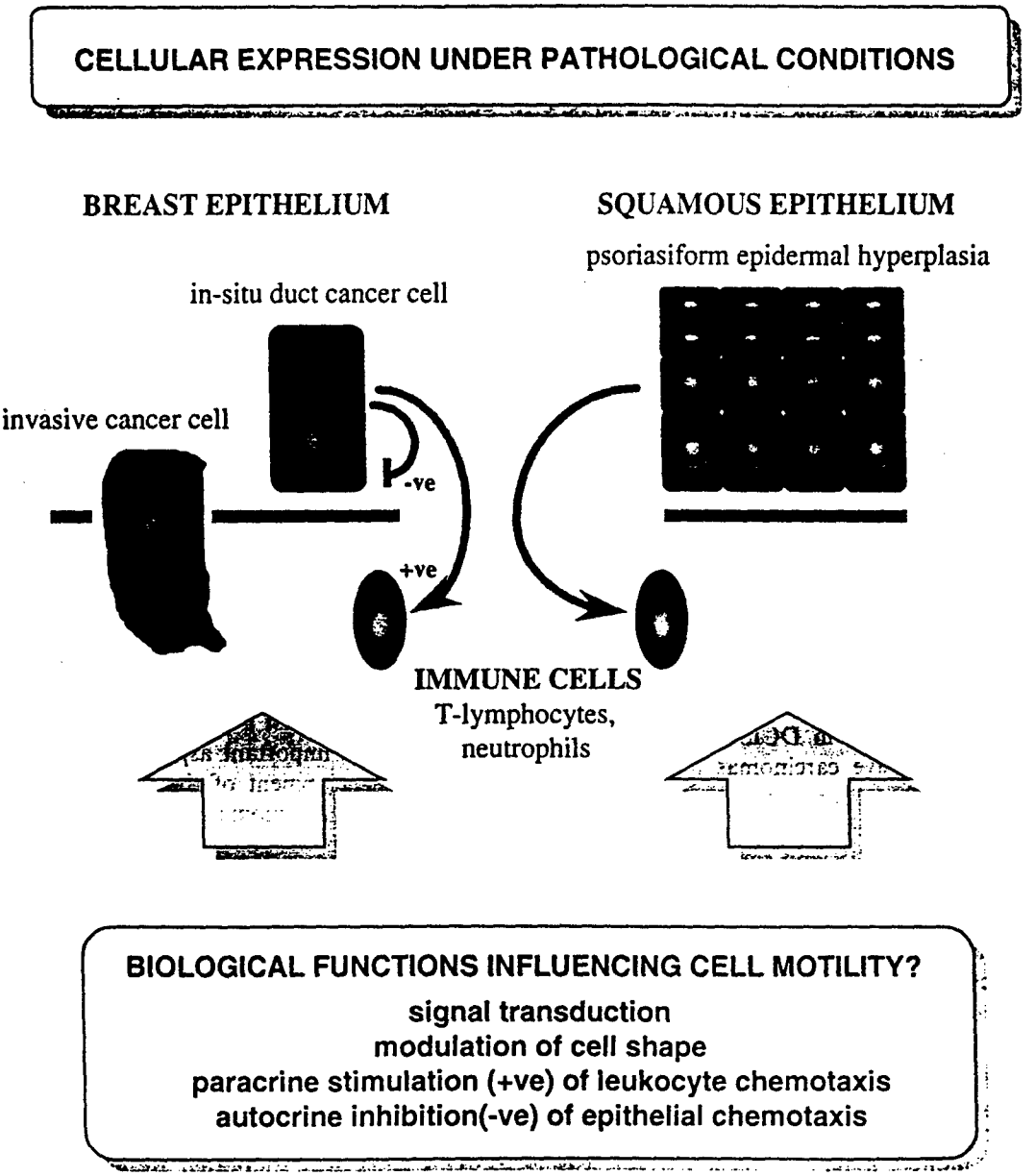

Fig. 2. A schematic representation to illustrate the possible influence of altered psoriasin expression on motility of immune and epithelial cells by intracellular actions (cell signalling and shape) and extracellular actions (chemotaxis) to mediate its role in the pathogenesis of psoriasis in skin and invasion in breast cancer.

igenesis and specifically in the process of invasion and metastasis [7]. One important component of the intracellular calcium signalling system is the S100 family of genes, which are known to be frequently expressed in breast cancer cell lines and tissues [12], but with often intriguingly different patterns of regulation that illustrate the cell type and stage-specific regulation of expression that is characteristic of the S100 family.

A possible role for Psoriasin in breast cancer first emerged when it was identified as a cDNA downregulated in a nodal metastasis relative to a primary invasive breast tumor [10]. Nevertheless, this initial observation contrasted with the fact that expression was only detectable in scattered invasive primary tumor cells by *in situ* hybridization and overall could be detected in less than 18% of primary invasive carcinomas by Northern analysis. The explanation for this paradox most probably lies in the composition of the cases studied. This has become apparent since Psoriasin was later identified as a gene highly expressed in the ductal epithelial cells of pre-invasive ductal carcinoma *in situ* (DCIS), which can be present as a significant component within invasive tumor tissue. Furthermore, study of Psoriasin mRNA expression at different stages of breast tumorigenesis has shown it to be relatively low or undetectable in normal, benign and atypical hyperplastic proliferative ductal lesions, but often highly expressed in DCIS and low or undetectable in invasive carcinomas [8]. This pattern suggests that Psoriasin overexpression is associated with altered differentiation in glandular epithelium of DCIS and may have a role in early breast tumor progression. Additional support for involvement in breast tumor progression is provided by its chromosomal location in a region of chromosome 1 that frequently (>50%) shows loss of heterozygosity in invasive tumors [11].

It is therefore interesting to speculate that Psoriasin is important in the development of the invasive phenotype. This might be mediated through an indirect influence on the effector cells of the host immune response or through a more direct influence on epithelial cell motility (as illustrated in Fig. 2). While no chemotactic effect on epithelial cells has been demonstrated as yet, it is clear that the closely related S100 proteins A8 and A9 and their heterodimeric form can exert inhibitory or stimulatory chemotactic effects on different cell types under different conditions [3]. It is also known that other epithelial-derived proteins can be chemotactic for both macrophages and keratinocytes [15]. Thus, Psoriasin might exert an epithelial migration inhibitory function in *in situ* breast carcinoma cells that once lost could contribute to the onset of successful invasion.

6. In the future

It is now important to identify the receptor and/or cellular targets of a protein that is so highly expressed under certain conditions and stages of epithelial differention, in order to understand its biological function in inflammatory skin disease as well as in neoplasia. Such knowledge might on the one hand become useful in the development of new strategies to block the local epidermal inflammatory response that characterizes psoriasis, and on the other hand for the application of a clinical marker for squamous cell carcinoma of the bladder. In breast cancer, current data suggest a potential role as a clinical marker of an important aspect of cancer pathology, the development of the invasive phenotype from ductal carcinoma *in situ*. Detection of Psoriasin might distinguish *in situ* from invasive cancer in fine needle aspirates where this distinction is not always easy. This potential, as well as determination of any direct role in the process of invasion, remains to be pursued.

Acknowledgements

This work was supported by grants from the Canadian Breast Cancer Research Initiative (CBCRI) and the U.S. Army Medical Research and Material Command (USAMRMC).

References

[1] A.D. Boglum, T. Flint, P. Madsen, J. Celis, T.A. Kruse, Refined mapping of the *psoriasin* gene S100A7 to chromosome 1cen-q21, Hum Genet. 96 (1995) 592–596.

[2] J.E. Celis, H.H. Rasmussen, H. Vorum, P. Madsen, B. Wolf, H. Wolf, T.F. Orntoft, Bladder squamous cell carcinomas express psoriasin and externalise it to the urine, J. Urol. 155 (1996) 2105–2112.

[3] P.A. Hesian, J. Edgeworth, N. Hogg, MRP8 and MRP14, two abundant Ca(2+) binding proteins of neutrophils and monocytes, J. Leucoc.-Biol. 53 (1993) 197–204.

[4] J. Hitomi, K. Maruyama, Y. Kikuchi, K. Nagasaki, K. Yamaguchi, Characterisation of a new calcium binding protein abundant in amniotic fluid, CAAF2, which is produced by fetal epidermal keratinocytes during embryogenesis, Biochem. Biophys. Res. Commun. 228 (1996) 757–763.

[5] H.J. Hoffman, E. Olsen, M. Etzerodt, P. Madsen, H.C. Kruse, T. Kruse, J.E. Celis, *Psoriasin* binds calcium and is upregulated by calcium to levels that resemble those in normal skin, J. Invest. Dermatol. 103 (1994) 370–375.

[6] T. Jinquan, H. Vorum, C.G. Larsen, P. Madsen, H.H. Gesser, B. Gesser, M. Etzerodt, B. Honore, J.E. Celis, K. Thestrup-Pedersen, Psoriasin: a novel chemotactic protein, J. Invest. Dermatol. 107 (1996) 5–10.

[7] E.C. Kohn, L. Liotta, Molecular insights into cancer invasion: strategies for prevention and intervention, Cancer Res. 55 (1995) 1856–1862.

[8] E. Leygue, T. Hiller, L. Snell, K. Hole, H. Dotzlaw, L. Watson, P. Watson, Differential expression of *Psoriasin* (S100A7) mRNA between *in-situ* and invasive human breast cancer, Cancer Res. 56 (1996) 4606–4609.

[9] P. Madsen, H.H. Rasmussen, H. Leffers, B. Honore, K. Olsen, E. Olsen, J. Kiil, E. Walbum, A.H. Andersen, B. Basse et al, Molecular cloning, occurrence, and expression of a novel partially secreted protein "*psoriasin*" that is highly upregulated in psoriatic skin, J. Invest. Dermatol. 97 (1991) 701–712.

[10] C. Moog-Lutz, P. Bouillet, C.H. Regnier, C. Tomasetto, M.-G. Mattei, M.-P. Chenard, P. Anglard, P. Basset, Comparative expression of the *psoriasin* (S100A7) and S100C genes in breast carcinoma and co-localisation to human chromosome 1q21-q22, Int. J. Cancer 63 (1995) 297–303.

[11] K.E. Munn, R.A. Walker, J.M. Varley, Frequent alterations of chromosome 1q in ductal carcinoma *in situ* of the breast, Oncogene 10 (1995) 1653–1657.

[12] M. Pedrocchi, B.W. Schafer, H. Mueller, U. Heizmann, C.W. Heizmann, Expression of calcium binding proteins of the S100 family in malignant human breast cancer cell lines and biopsy samples, Int. J. Cancer 57 (1994) 684–690.

[13] B.W. Schafer, R. Wicki, D. Engelkamp, M.-G. Mattei, C.W. Heizmann, Isolation of a YAC clone covering a cluster of nine S100 genes on human chromosome 1q21: rationale for a new nomenclature of the S100 calcium binding protein family, Genomics 25 (1995) 638–643.

[14] B.W. Schafer, C.W. Heizmann, The S100 family of EF-hand calcium binding proteins: functions and pathology, Trends Biochem. 21 (1996) 134–140.

[15] M.H. Wang, A.A. Dlugosz, Y. Sun, A. Skeel, E.J. Leonard, Macrophage-stimulating protein induces proliferation and migration of murine keratinocytes, Exp. Cell Res. 226 (1996) 39–46.

BioTechniques®
BOOKS

UPDATE SERIES

Selected Papers from BioTechniques with Updates 1997

The PCR Technique: RT-PCR

Edited by

Paul Siebert

Eaton
PUBLISHING

The BioTechniques® Update Series

The PCR Technique: DNA Sequencing
Edited by J. Ellingboe and U. Gyllensten

The PCR Technique: DNA Sequencing II
Edited by U. Gyllensten and J. Ellingboe

The PCR Technique: Quantitative PCR
Edited by J. Larrick

The PCR Technique: RT-PCR
Edited by P. Siebert

Microdissection RT-PCR Analysis of Gene Expression in Pathologically Defined Frozen Tissue Sections

Tamara Hiller, Linda Snell and Peter H. Watson

University of Manitoba, Winnipeg, MB, Canada

Molecular studies of mRNA gene expression in human solid tumors are critically dependent on the ability to apply sensitive assays to tumor tissue that is of the highest quality with respect to pathological definition and cellular preservation. In particular, the interpretation of any analysis must recognize the problems that are posed by variability in cellular composition.

Although the level of mRNA can be assessed by a variety of techniques, many such as Northern blot and RNase protection assay are not sensitive enough to allow the study of small tumor samples that are usually available for research. Alternatively, in situ hybridization allows the assessment of individual cell expression. However, sensitivity, accurate quantitation and determination of mRNA structure can sometimes be a significant limitation. The reverse transcription polymerase chain reaction (RT-PCR) assay offers a sensitive alternative that can allow accurate measurement of both structure and level of mRNA based on very small samples.

We and others have previously demonstrated the feasibility of extracting DNA from microdissected regions within archival formalin-fixed and paraffin-embedded tissue sections to assess alterations in gene structure by PCR (4,10,11). Several groups have also reported RNA extraction from paraffin sections (1,6–9). However, this can require specialized approaches to tissue fixation (6), and our experience is that this allows the amplification of only relatively stable and abundant RNA species, such as "housekeeping genes" (3,8). Alternatively, RNA can be extracted from frozen tissues; however, this has the limitation of suboptimal histological detail for the assessment of tumor parameters and precise cellular composition. In this report, we describe an approach to facilitate microdissection of small pathologically defined regions from frozen tumor sections to provide mRNA for the analysis of gene expression by RT-PCR.

Fresh tissue samples from breast cancer cases are obtained through a standardized and timed collection protocol instituted by the National Cancer

(Reprinted from BioTechniques 21:38-44, July 1996)

Institute of Canada-Manitoba Breast Tumor Bank. Portions of these tissues (typically 0.5 cm^3) are then rapidly bisected, orientated on the external and cut surfaces with different colored dyes (black india ink, alcian blue and mercurochrome) and one-half placed in 10% neutral buffered formalin, and the other is snap-frozen in liquid nitrogen within a cryovial. The fixed-tissue blocks are then processed routinely to produce matching and "mirror image" formalin-fixed, paraffin-embedded and frozen tissue blocks. Thin (5 μm) hematoxylin and eosin (H&E)-stained sections are then prepared from the paraffin blocks to allow interpretation of the detailed histology and tumor composition by light microscopy. The corresponding frozen blocks can then be sectioned in a cryostat to provide thin 5- to 20-μm sections when required, in which the distinction of tumor grade, mitotic rate, in situ tumor vs. florid ductal hyperplasia and other subtle features can be determined by direct comparison with the adjacent high-quality paraffin section.

High-quality total RNA is extractable from whole 20-μm frozen tumor sections using a small scale extraction protocol (TRI Reagent™; Molecular Research Center, Cincinnati, OH, USA) to provide an average yield of 4 $\mu g/cm^2$/20-μm tumor section (consistently optical density $[OD]_{260/280} > 1.8$ as quantitated by spectrophotometer in a 50-μL microcuvette). Although this varies with the tumor cellularity, a typical tumor section measuring 0.25 cm^2 yields 1 μg of total RNA, which is sufficient to be used as a substrate for multiple RT-PCR assays. We have used this approach to reliably amplify a range of gene products such as c-*myc*, *pS2* and *CD44*. We have also examined the effect of reuse and storage on the yield and quality of RNA that can be extracted from frozen tissue sections. Glyceraldehyde-3-phosphate dehydrogenase (GAPDH) and estrogen receptor (ER) gene expression were assessed by RT-PCR using RNA extracted from frozen tissue sections, obtained from four different tumor cases. These had previously been sectioned for successful RT-PCR analysis and then re-frozen from 1½ to 2½ years previously. We

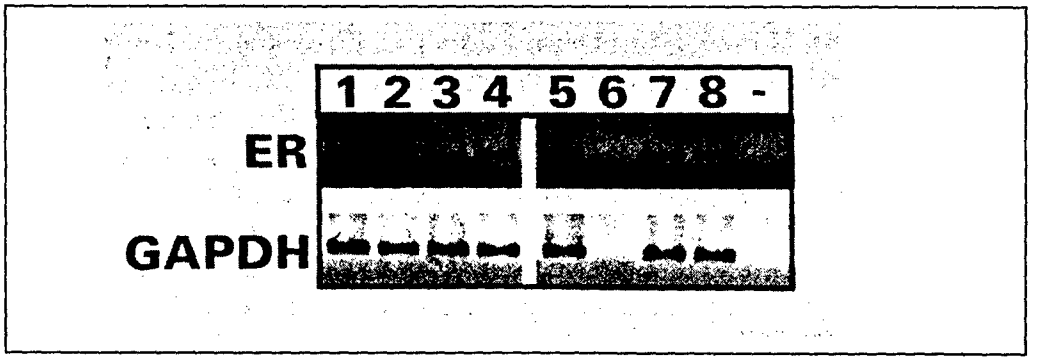

Figure 1. RT-PCR analysis of ER and GAPDH expression within frozen sections from resectioned tumor blocks. RNA was extracted from frozen sections obtained from tumor blocks that had been sectioned and successfully used for RNA extraction and RT-PCR up to 2½ years previously. In all four tumors, the expression of ER and GAPDH can be readily detected in the reused blocks (lanes 1–4), and this is similar to the expression seen in the corresponding samples of RNA stored at -70°C since the original extraction (lanes 5–8). Note that the integrity of one stored RNA sample (lane 6) has been lost.

toxylin solution (Mallinckrodt, Winnipeg, MB, Canada) for 2 s at room temperature, rinsed in water for 10 s, immersed into Eosin Y in 95% ethanol (Mallinckrodt) for 2 s, rinsed again in water for 10 s and then placed under a dissection microscope (wild M3C; Leica). Sections can then be oriented and the histological details confirmed with reference to a paraffin H&E-stained section from the matching paraffin block. Using a scalpel blade and fine needle, specific tumor components within histologically defined areas less than 1–2 mm^2 can be rapidly microdissected within 2 min under a 20× objective at room temperature and placed into a precooled microcentrifuge tube on ice. After a brief centrifugation to pellet the dissected material, 10 µL ddH_2O are added, and the material is snap-frozen by immersion in liquid nitrogen to disrupt tissue architecture. RNA can then be extracted and used as a substrate for RT-PCR assay. For a typical 20-mm breast tumor section, which may contain 10^4 cells within a 2-mm region, we obtain yields of between 0.5–1 µg RNA from 4 microdissected serial sections. The brief H&E stain provides essential cellular discrimination without significantly affecting the ability to perform successful RT-PCR.

To demonstrate the feasibility of this approach, a microdissection experiment performed on tissue from an ER- positive carcinoma is shown in Figure 2. The mRNA expression of the GAPDH "housekeeping" gene is detected in the entire unstained frozen tumor section, in the section following brief H&E staining and in both microdissected tumor and stroma regions. Similarly, expression of ER is seen in the entire tumor section and in the region of invasive carcinoma, but as expected, it is absent in the immediately adjacent lymphocyte-rich stroma.

Following microdissection, 100 ng total RNA from each component were reverse-transcribed in a volume of 20 µL of RT mixture (1× RT buffer and 200 U Moloney murine leukemia virus [MMLV] RTase (Life Technologies, Burlington, ON, Canada); 0.5 mM each dGTP, dATP, dTTP, dCTP; 1 mM bovine serum albumin [BSA]; 0.01 M dithiothreitol [DTT]; 1.25 mM oligo(dT) primer; 5% dimethyl sulfoxide [DMSO]) and incubated for 60 min at 37°C. PCR amplification of GAPDH and ER cDNA was then performed in a Model PTC-100™ thermal cycler (MJ Research, Watertown, MA, USA). Each PCR was performed in a 50-µL volume utilizing 2 µL of the completed RT reaction containing cDNA; 1× PCR buffer; 2 µM $MgCl_2$; 1.1 U *Taq* DNA polymerase (Promega, Unionville, ON, Canada); 200 mM each dGTP, dATP, dTTP and dCTP; and 0.5 mM PCR primers. The PCR protocol consisted of 5 min at 94°C; then 40 cycles of 45 s at 93°C, 45 s at 56°C and 90 s at 75°C; followed by 7 min at 72°C. After thermal cycling was completed, 1.5 µL of gel loading buffer were added to 15 µL of the PCR, and samples were electrophoresed on a 2% agarose gel. PCR products were visualized by subsequent ethidium bromide staining and photography under UV light. The primer sequences used were as follows; $GAPDH^{943}$ 5′ ACCCACTCCTCCACCTTTG 3′, $GAPDH^{1102}$ 5′ CTCTTGTGCTCTTGCTGGG 3′, ER^{675} 5′ TGC-

Update to:

Microdissection RT-PCR Analysis of Gene Expression in Pathologically Defined Frozen Tissue Sections

P.H. Watson, T. Hiller, L. Snell, K. Hole, R. Singh, L.C. Murphy, E.T. Leygue, H. Dotzlaw, A. Kossakowska[1] and A. Kulakowski[2]

University of Manitoba, Winnipeg, MB, Canada; [1]Foothills Hospital, Calgary, AB, Canada; [2]Maria Skoldowska-Curie Memorial Cancer Center, Warsaw, Poland

We have used this approach to pursue the specific goal of identification of genes that influence growth and invasiveness in human breast cancer (1,3). Several indirect approaches to the latter problem have been taken by others, including either assessment of known genes that may be important for invasion on the basis of their discovery and their roles in other experimental systems, or the search for DNA loci with genetic damage (loss of heterozygosity) that might indicate alteration of expression of genes involved in invasion. However, through microdissection RT-PCR of pathologically defined in situ and invasive elements within frozen breast tumor sections and examination of RNA for alterations of gene expression, we have been able to take a more direct approach to this problem. In pursuit of this direction we have made the following progress.

To improve our ability to interpret alterations in levels of gene expression in vivo, we have established a tissue collection protocol and studied the effect of tumor collection time on RNA expression in breast tumor specimens. We have used competitive RT-PCR assays to measure the levels of expression of both relatively stable (estrogen receptor [ER]) and unstable (c-*myc*) RNAs expressed in breast tumors collected and frozen over different times. We have found that the level of c-*myc* RNA declines more rapidly than ER, even in tissues collected and maintained on ice, with mean c-*myc* levels falling to 80% of initial level at 24 h as compared to mean ER levels of 94% of initial levels. Therefore, although differences in RNA levels may not be significant with shorter collection periods, our results show that standardization of the method of tissue collection is important as time to collection can influence mRNA levels of some genes which decay faster than others.

We have also examined the ability to apply our approach to tissue processing, microdissection and RT-PCR to tissues obtained from distant sources by examining breast tumor material transported from Poland, in collaboration with the Warsaw Cancer Institute. Morphological tissue quality assessed on a

Chapter in "Expression Genetics: Differential Display". Editors Arthur and Michael McClelland, Eaton Publishing. 1999

Watson P. H., Hiller-Hitchcock T., Snell L., [1] Hole K., Murphy L.C., Leygue E.T., and Dotzlaw H.[2], Roughley P.J. [3]

Department of Pathology [1] and Department of Biochemistry and Molecular Biology [2], University of Manitoba, Winnipeg, Manitoba, R3E OW3, Canada, and Genetics Unit, Shriners Hospital for children, Montreal, Quebec, H3G 1A6. [3]

Update to : Hiller T, Snell L, Watson P. "Microdissection/RT-PCR analysis of gene expression in pathologically defined frozen sections" Biotechniques, 21, 38-44, 1996.

We have continued to utilize this approach in our research program (1) to pursue the specific goal of identification of genes that influence the acquisition of the invasive phenotype in human breast cancer. Assessment of risk of progression to invasive breast cancer has recently become an increasingly recognizable and defined problem in clinical management. This is partly due to the increasing number of patients who present with pre-invasive ductal carcinoma in-situ, (DCIS) (2). More recently, the demonstration that breast cancer can be delayed or inhibited by tamoxifen therapy in women at high risk as defined in the NSABP trial has also provided a new focus and impetus to improve the accuracy of risk determination (3). But although there is clearly a need for better predicators of biological potential and there has also been an impressive growth in the knowledge of genes involved in tumor invasion and metastasis (4), the importance of most of these factors in the development of the invasive phenotype in the complex heterogeneous disease of human breast cancer has been difficult to establish (5,6). This is partly because many of these genes (including cell adhesion molecules, proteases and motility factors) were first identified in tumor cell lines and systems other than epithelial breast carcinoma. This in turn reflects a lack of suitable breast specific models or breast cell lines that are representative of the pre-invasive, in-situ stage of cancer.

To address this critical issue in the biology of early breast tumor progression, many groups have based their studies on human tissues and begun to survey DCIS lesions with microsatellite markers in search of regions of loss of heterozygosity (LOH) that may harbor tumor invasion suppressor genes. This approach has yielded some interesting loci but not specific genes as yet (7). In contrast, our approach as outlined previously, has been to directly study differential gene expression within histologically defined breast tissues, in order to identify potential 'invasion' genes (1).

This approach has been crucially dependent on the design and maturation of the NCIC-Manitoba Breast Tumor Bank resource to allows selection and dissection of histologically defined frozen breast tissues (8). To date we have identified a number of cDNAs that are differentially expressed between DCIS and invasive tumor components. To rapidly determine the potential of this approach we have initially focused on 6 known cDNAs identified in other systems. We have confirmed amongst these, real differential expression (3 cDNA's, see below), differential expression attributable to differences in local regional composition (1 cDNA) and false positives (2 cDNA's) by in-situ hybridization and RT-PCR. Consideration of the patterns of expression amongst the 3 differentially expressed cDNA's has encouraged us to pursue the potential role of two of these, psoriasin (9) and lumican (10) in invasion.

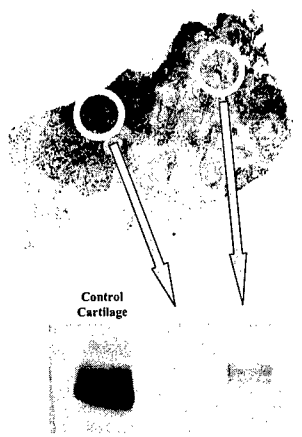

Fig 1. Microdissection and Western blot analysis of lumican protein expression within 1-2mm diameter regions within a frozen breast tumor section that shows discordance with the high (left) and low (right) levels of mRNA expression in eacl region (indicated by density of black grains), as determined by in-situ hybridization applied to a paraffin section of a mirror image block (shown above).

Psoriasin (S100 A7), a member of the S100 calcium binding protein family (11) is differentially expressed in DCIS vs invasive epithelial components. Expression is relatively low or undetectable in normal & proliferative lesions, high in DCIS, but low in invasive carcinomas (9). Furthermore, its potential capability to influence cell motility (12) is compatible with the hypothesis that altered expression may be a marker of invasiveness. Lumican is a small leucine-rich proteoglycan (13), that we have also found overexpressed in the stromal component of invasive breast cancer (14). We have gone on recently to show that it is the most abundant proteoglycan within its

stromal gene family, using an adaptation of our previous techniques to extract protein from microdissected frozen sections. We have also applied microdissection coupled to Western blot to frozen tissue sections to compare lumican protein expression within regions that show different levels of mRNA expression, as determined by in-situ hybridization applied to adjacent mirror image paraffin sections (figure 1). This has clearly shown that altered lumican expression in tumors also involves abnormal protein deposition within subregions of breast tumors. Although not previously studied in tumor progression, its known role in cross linking of collagen (15) supports the hypothesis that such changes in lumican expression may influence invasiveness.

REFERENCES

1. Hiller T., L. Snell L and P. H. Watson. "Microdissection/RT-PCR analysis of gene expression" Biotechniques, 1996, 21, 38-44.
2. Kerlikowske K, Barclay J, Grady D, Sickles EA, Ernster V J Comparison of risk factors for ductal carcinoma in situ and invasive breast cancer. Natl Cancer Inst 1997, 1;89(1):76-82
3. NSABP Website http://www.nsabp.pitt.edu/BCPT_Area.html
4. Dickson, R.B. and Lippman, M.E., Molecular determinants of growth, angiogenesis and metastasis in breast cancer. Semin. Oncol., 1992, 19:286-298
5. Friedrichs K, Franke F, Lisboa BW, Kugler G, Gille I, Terpe HJ, Holzel F, Maass H, Gunthert U. CD44 isoforms correlate with cellular differentiation but not with prognosis in human breast cancer. Cancer Res 1995 15;55(22):5424-5433
6. Hole A, Belkhiri A, Snell L, Watson P. "CD44 variant expression and estrogen receptor status in breast cancer" Breast Cancer Research & Treatment, 1997, 43, 165-173,
7. O'Connell P, Pekkel V, Fuqua SA, Osborne CK, Clark GM, Allred DC Analysis of loss of heterozygosity in 399 premalignant breast lesions at 15 genetic loci. J Natl Cancer Inst 1998 6;90(9):697-703
8. Watson P.H., L. Snell and M. Parisien. "The Role of a Tumor Bank in Translational Research" Canadian Medical Association Journal, 1996,155, 281-283.
9. Leygue E., L. Snell, T. Hiller, H. Dotzlaw, K. Hole, L.C. Murphy and P.H. Watson. "Differential expression of Psoriasin Messenger mRNA between in-situ and invasive human breast carcinoma" Cancer Research, 1996, 56, 4606-4609.
10. Leygue E, Snell L, Dotzlaw H, Hole K, Hiller T, Roughley P, Watson P, Murphy L, "Expression of Lumican in human breast carcinoma" Cancer Research 1998, 58(7): 1348-1352
11. Watson PH, Leygue ER, Murphy LC. Psoriasin (S100A7). Int J Biochem Cell Biol 1998, 30(5):567-571
12. Jinquan T, Vorum H, Larsen CG, Madsen P, Rasmussen HH, Gesser B, Etzerodt M, Honore B, Celis JE, Thestrup-Pedersen K J. Psoriasin: a novel chemotactic protein. Invest Dermatol 1996 , 107(1):5-10
13. Iozzo RV: The family of the small leucine-rich proteoglycans: key regulators of matrix assembly and cellular growth. Crit Rev Biochem Mol Biol 1997, 32: 141-174
14. Chakravarti S, Magnuson T, Lass JH, Jepsen KJ, LaMantia C, Carroll H: Lumican regulates collagen fibril assembly: skin fragility and corneal opacity in the absence of lumican. J Cell Biol 1998, 141: 1277-1286

DEPARTMENT OF THE ARMY
US ARMY MEDICAL RESEARCH AND MATERIEL COMMAND
504 SCOTT STREET
FORT DETRICK, MARYLAND 21702-5012

REPLY TO
ATTENTION OF:

MCMR-RMI-S (70-1y) 8 Jan 2003

MEMORANDUM FOR Administrator, Defense Technical Information Center (DTIC-OCA), 8725 John J. Kingman Road, Fort Belvoir, VA 22060-6218

SUBJECT: Request Change in Distribution Statement

1. The U.S. Army Medical Research and Materiel Command has reexamined the need for the limitation assigned to the enclosed. Request the limited distribution statement for the enclosed be changed to "Approved for public release; distribution unlimited." These reports should be released to the National Technical Information Service.

2. Point of contact for this request is Ms. Judy Pawlus at DSN 343-7322 or by e-mail at judy.pawlus@det.amedd.army.mil.

FOR THE COMMANDER:

Encl

PHYLIS M. RINEHART
Deputy Chief of Staff for
Information Management

ADB265840	ADB266633	ADB282069
ADB279138	ADB251763	ADB265386
ADB264578	ADB281601	ADB282057
ADB281679	ADB258874	ADB258251
ADB281645	ADB281773	ADB264541
ADB261128	ADB281660	ADB241630
ADB261339	ADB259064	ADB281924
ADB273096	ADB266141	ADB281663
ADB281681	ADB281664	ADB281659
ADB259637	ADB258830	
ADB256645	ADB266029	
ADB262441	ADB281668	
ADB281674	ADB259834	
ADB281771	ADB266075	
ADB281612	ADB281661	